PUNCHING SHEAR STRENGTH OF REINFORCED CONCRETE SLAB

by

Xiao-yun Shao

A Thesis

presented to the University of Ottawa

in partial fulfilment of the requirements for the degree of

Master of Applied Science in Civil Engineering

Under supervision of Dr. N. J.Gardner

Department of Civil Engineering

Faculty of Engineering

University of Ottawa

The Master of Civil Engineering Program is a joint program

with Carleton University administered by

the Ottawa-Carleton Institute for Civil Engineering

ABSTRACT

This thesis presents the results of punching shear tests performed on a 2 × 2 bay continuous slab with/and without supplementary supports. On the basis of these tests, the code method of calculating the ultimate strength of interior, edge and corner column connections of flat slab were investigated.

The thickness of the specimen was 140 mm and the spans length were 2743 mm.

The ACI 318-89, BS 8110-85 and CEB-FIP 90 Codes were critically reviewed by comparing with the experiment results and results from the literature. It was found that in general the Code predictions are reasonable but for corner column connections the ACI Code over-estimates the ultimate shear capacity of the slab and BS 8110-85 requirements for edge and corner column connections are simplistic.

The experimental results show that the supplementary supports can increase the ultimate punching shear capacity when the supports are properly located.

Acknowledgements

I would like to express my deepest gratitude to Professor N. J. Gardner, my senior supervisor, for his invaluable guidance and support during preparation of this thesis.

I am thankful to the technical staff of the structure laboratory of the University of Ottawa especially Mr. Mongi Grira.

Many thanks to my family and all my friends who contributed their help and support.

Table of Contents

List of Tables

List of Figures

Notation

A_c	area of failure surface
A_b	cross-section area of steel
A_s	area of steel in chosen section of slab
A_{sp}	area of prestressed reinforcement
A_v	total cross-section area of shear reinforcement
b	side dimension of a square column
B	side length of a square slab
c	diameter of a circular column
d	effective depth of a slab
d'	cover of reinforcing mat
d_a	maximum aggregate size
d_p	effective depth of prestressed concrete
e	eccentricity of a column
e_1	eccentricity of a column in x direction
e_2	eccentricity of a column in y direction
jd	lever arm of the interior resisting moment of a slab
f'_{cc}	cylindrical compressive strength of concrete
f'_{ck}	characteristic compressive strength of concrete
f_{cm}	mean compressive strength of concrete
f_{ct}	tensile strength of concrete

f'_{cu}	cube compressive strength of concrete
f_y	yield stress of non prestressed reinforcing bars
h	overall thickness of the slab
K	dimensionless parameter
K_a	coefficient depends on the type of concrete
K_{sc}	coefficient depends on the geometry of the column
M	applied moment
M_1	applied moment in x direction
M_2	applied moment in y direction
L	shear span length
P_u	theoretical ultimate shear load
P_{ue}	ultimate capacity load at an eccentricity e
P_{ol}	decompression load of a prestressed slab in the longitudinal direction
P_{ot}	decompression load of a prestressed slab in the transverse direction
P_{ul}	longitudinal component of P_u
P_y	yield load
u	length of control perimeter
u_o	perimeter of a column
v_c	ultimate punching shear stress
V	shear force
w	applied uniformly distributed load on the slab
w_t	total applied uniformly distributed load on the slab
w_u	ultimate capacity of the slab (in terms of uniformly distributed load)

θ	angle of failure surface with respect to horizontal
γ_G	load factor
γ_m	material understrength factor
ρ_x, ρ_y	reinforcement ratio in x and y direction respectively

CHAPTER 1

INTRODUCTION

Flat plate structures consist of reinforced concrete slabs supported by columns without drop panels or column capitals. This type of structure is an economical form of high-rise construction because the absence of projecting beams, drop panels and column capitals simplifies formwork and allows the application of interior finishes directly to the soffit of the slab. However, the flat plate is at a disadvantage in comparison to two-way slabs supported by beams or walls because of the risk of brittle punching shear failure at the slab-column connection.

Flat slabs are generally constructed using proprietary flying or table forms and construction is rapid; in extreme cases a new floor can be cast every two or three days. Repetitive use of prefabricated flying forms ensures a consistent high-quality product.

Typical construction procedure involves casting the new slab on formwork (shores) that is supported on a previously cast slab, which in turn is partially supported by reshores to the lower slabs. Loads occurring on the supporting slabs during construction are large and can equal or exceed the supporting slab's service load. The rapid rate of construction causes these loads to be applied to slabs that have not achieved their specified concrete design strength or their modulus of elasticity.

One of the common causes of failure of flat plate structures during construction

is insufficient early-age punching shear capacity under relatively high construction loads. Without an equation to estimate the early-age punching strength of a slab, it is usual to calculate the available early-age shear capacity from the early-age characteristic strength of the concrete and the assumed relationship between the characteristic concrete strength and the shear strength.

The subject of punching shear on reinforced concrete has interested many investigators in the past. Many experiments have been conducted. Empirical and semi-empirical formulas have been developed to relate apparent shearing stresses in the slab, caused by concentrated loads, to the concrete strength. However, most experiments were conducted on isolated slab-column connections which were designed in such a way that the edges of the specimens were at positions representative of lines of contraflexure in continuous slabs. Therefore, the question of whether such experiments can correctly represent continuous slabs in the real structures has to be answered.

The region of a slab in the vicinity of a column could fail in shear by developing a failure surface in the form of a truncated cone or pyramid. This type of failure, called a **punching shear failure**, is usually the source of collapse of flat plate and flat slab buildings.

Punching shear failures are characterised by the deformations prior to failure being smaller than in flexural failures, by the violence of the failure, and a sudden drop in resistance from the peak load which is quite untypical of flexural behaviour. A section sawn through a typical punching failure is shown in Figure 1.1 (Alexander and Simmonds 1991) and Figure 1.2 (Regan 1981) shows load/deflection relationships for a pair of slabs

in which one had shear reinforcement and the other did not.

There exist differences between a true punching failure and a predominantly flexural response. The load-deflection curves of slabs tested under concentrated central load can be used to classify the type of slab failure. According to Marzouk and Hussen (1990), failure modes can be classified into the following three categories: (1) **pure flexural failure**, (2) **pure punching failure**, and (3) **ductile shear failure**. Pure flexural failure takes place in slabs where most of the reinforcement yields before punching occurs and consequently the slab exhibits large deflections prior to failure. Pure shear failure occurs when the slab shows small deflections, with yielding of the tension steel being very localized at the column head. The third type of failure, ductile shear failure, is a transition between the cases of pure punching and pure flexure failures. Figure 1.3, which is from a paper by Criswell (1974), illustrates these types of failures. In this diagram, curves 1 to 3 clearly represent the behaviour of slabs failing by primary punching while curves 6 to 8 show basically flexural behaviour. The slabs represented by curves 4 and 5 attain their yield line strengths but must be regarded as having failed by punching in view of their lack of ductility and 6 to 8 failure to attain the excess strengths of slabs (20% above the yield line load). Such excess strength is expected on account of membrane action and the strain hardening of the reinforcement.

1.1 Existing Problems

However there are many examples of flat plate structures which have failed during construction and clearly demonstrate the disastrous consequences of a punching failure.

In two cases reported by Jirsa (1966), punching shear failure initiated at an interior column and caused a progressive collapse when lower floors failed to support the impact of the material from above. In one case reported by Feld (1964), reinforced concrete flat plate floors of office building, Jackson, Michigan, were 254 mm thick supported on square columns spaced 7.3 m on centres in both directions. First and second floors were several weeks old at the time of the accident and forms and shores had been removed. The third floor concrete was at least 20 days old; forms had been removed and the slab was reshored to the second floor, and was carrying the formwork for the fourth floor. Concrete had been placed in the fourth floor forms. An area about 22 m × 44 m on the second floor dropped first and caused the same area of the first floor dropping all the way to the cellar. Significantly almost all of the columns remained standing full height after the collapse. The cause of the accident was excessive punching shear in the flat plates of the second floor. In another case reported on *Engineering News Report*, July 15, 1971, a four to six bay portion of the twenty-third floor of a high-rise reinforced concrete flat plate structure collapsed during construction and caused progressive failures of the underlying floors. In addition, materials from the collapsing structure dropped on an adjacent flat plate post-tension concrete parking structure resulted in a progressive shear failure at each column in that structure. These cases and failures at slab-column connections in the 1964 Alaska, 1967 Venezuela and the 1971 San Fernando, Calif. earthquakes show the need for caution in calculations of shear at slab-column connections, especially where moments are transferred by the connection.

An alternative construction procedure of using preshores during the stripping of

primary forms and shores has been developed over the past two decades by construction firms in New York [Grossman 1986]. This technique requires that preshores be installed before the form is removed so that the maximum span of unsupported concrete is not greater than 2.5 m to 3 m. This procedure allows fast cycling of reduced sets of primary forms while maintaining full support of the newly placed floors during a stripping operation. By using such a preshoring technique, excessive early-age deflection as well as the creep deflection can be reduced.

Although the preshoring technique has been used for two decades, there is an absence of a theoretical analysis for the slab and reshoring/preshoring system, and little experimental data has been obtained. The question of how supplementary shores affect punching strength and deformation of the slabs is unanswered.

1.2 Scope of Study

The major topic of this thesis is **Punching Shear Strength of Reinforced Concrete Slabs**. In particular attention is focused on the problem of the punching shear strength of slab-column connections with non-prestressed reinforcement and without shear reinforcement. This study is based on loading to failure a 2×2 bay half-scale reinforced concrete slab which contains interior, edge, and corner columns. The experiment was designed in such a way that the capacity of slab-column connections was obtained both with supplementary supports in vicinity of columns and without supplementary supports. The results of this experiment are described and analyzed.

This study also covers the following topics which are related to the punching shear

strength:

(1) Whether the isolated punching test can represent the punching shear behaviour of the slab column system;

(2) The validity of the ACI 318-89, BS 8110-85 and CEB-FIP 90 codes provisions on punching shear.

(3) The behaviour of slab-column connection with moment transfer and without moment transfer;

(4) The effects of supplementary column supports.

This thesis is organized as follows:

Chapter 1: An introduction to punching shear problems and problems during construction, research motivation and the study scope of this thesis.

Chapter 2: An overview of previous punching shear studies and experimental results in both symmetric and non-symmetric punching given by the other researchers.

Chapter 3: A study of ACI 318-89, BS 8110-85 and CEB-FIP 1990 Codes.

Chapter 4: The observation of the behaviour of the slab tested in the University of Ottawa.

Chapter 5: Presentation and discussion of test results.

Chapter 6: Conclusion.

Chapter 7: References.

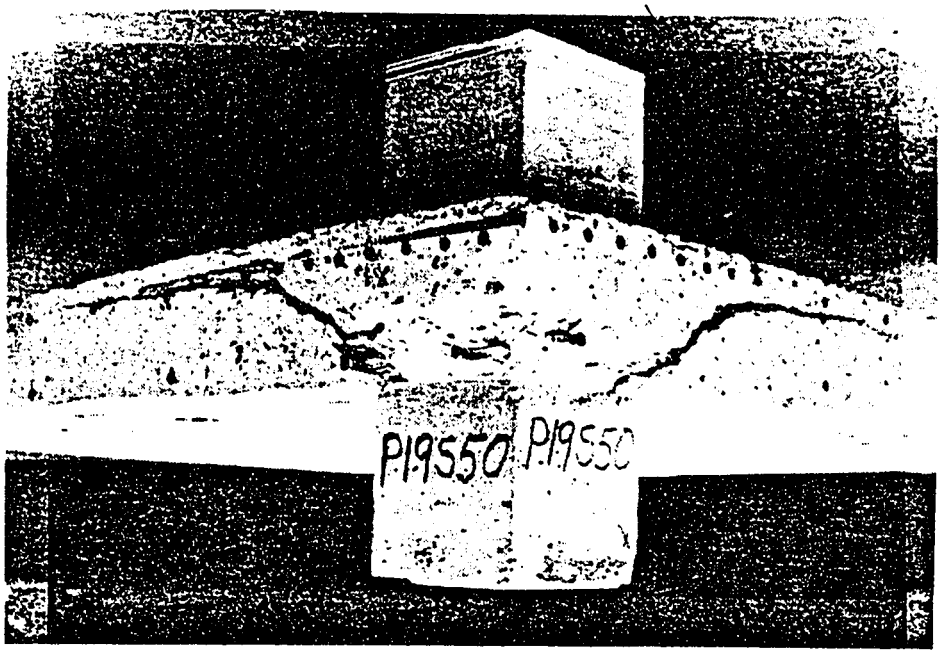

Figure 1.1 Typical Punching Failure

Alexander and Simmonds 1991

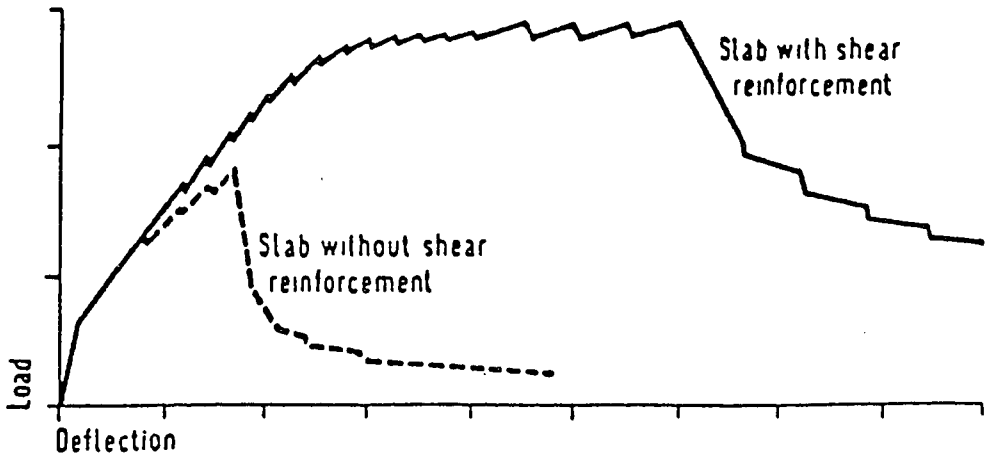

Figure 1.2 Load-deflection Relationships for Slabs with and without Shear Reinforcement (Regan 1981)

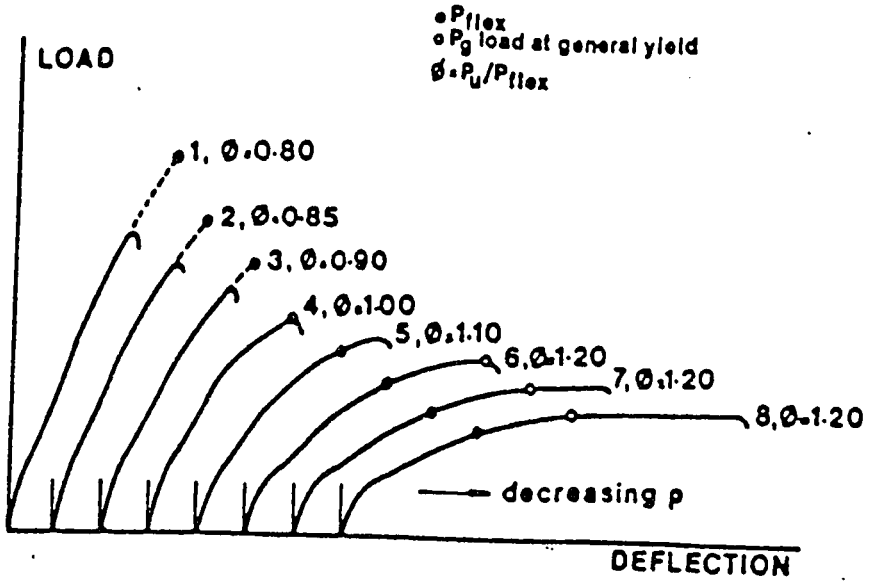

Figure 1.3 The Behaviour of Slabs (Criswell 1974)

CHAPTER 2

AN OVERVIEW OF PUNCHING SHEAR STUDIES

2.1 Introduction

Research on punching shear has yielded a number of methods by which the ultimate shearing strength of slabs can be predicted. In general, the various approaches can be described as either the result of an empirical study, in which a statistical analysis of the available test results was used to establish a relationship between the load or stress at failure and the parameters of the slab, or the result of a rational study, in which the strength of the slab materials and the mechanism of failure are idealized and described mathematically.

The topics of the previous research work can be classified into the following categories:

(1) Symmetric punching shear in which the shear stress is assumed to be uniformly distributed along a control perimeter.

(2) Non-symmetric punching shear in which unbalanced moment distribution is involved in the slab-column connection. Category (2) can be further divided into the following:

(2a) Unbalanced moment at an interior column connection

(2b) Unbalanced moment at edge and corner columns

2.2 Symmetric Punching Shear

By far the greatest number of tests on concentrically loaded interior slab-column connections have been performed on isolated column-slab connection specimens with rotationally unrestrained edges.

2.2.1 Test Arrangement

The main experimental work on punching shear has used specimens intended to represent the negative bending regions around supporting columns or positive moment zones around concentrated loads. The edges of the specimens have thus been at positions representative of lines of contraflexure in continuous slabs. Such test programmes have included:

1. square or circular slabs loaded at their centres through steel plates or stub columns and simply supported around their edges. In the case of square slabs, the corners are generally free to lift.

2. square or circular slabs supported at their centres and loaded around their edges.

3. rectangular slabs supported or loaded at their centres and loaded or supported at two opposite edges.

The first two types are related to flat slab floors while the third has generally been used to model slab bridges.

2.2.2 Observations of Behaviour

Deformation

Depending on the configuration of loads and supports, slabs failing by punching shear may have widely different patterns of flexural cracking prior to failure. Figure 2.1 shows two stages in the development of cracks in a typical two-way ordinary reinforced concrete slab tested by Marti, Pralong and Thurlimann (1977).

It seems that punching failure is preceded by internal diagonal cracking generally occurring at loads of the 1/2 to 2/3 of the ultimate. Evidence of this has been obtained from measurements of changes of slab thickness during loading and from recordings of internal strains. Figure 2.2 shows an interior strain measured by an embedded gauge in one of Regan's (1983) tests. It shows that the interior transverse strain increases rapidly after the load reached 1/2 of the ultimate load. In Grira's (1990) work, a 100 mm thick square slab was sawed across the middle section of the slab after punching shear failure. The cross section in which the diagonal crack run through the slab is shown in Figure 2.3. The behavior after inclined cracking appears to be entirely stable and slabs can be unloaded and reloaded without their ultimate strengths being affected. Figure 2.4 shows changes of slab thickness in a test conducted by Moe (1961).

Rotations in the negative moment regions of slabs on columns are highly concentrated along virtual hinges in the compression zones adjacent to the columns. The deflected profiles of the compressed surface are practically linear while those of the

tension face generally show a slight discontinuity in the region where the shear crack intersects the reinforcement. The discontinuity is more pronounced if the shear crack is not crossed by reinforcement, i.e., if the steel is arranged in rings around the column.

Strains

Strains of the concrete at the compressed surface near a load or support have been measured in many tests. Figure 2.5a, taken from Kinnunen and Nylander (1960), shows radial distributions of strains around a circular column in a slab with ring reinforcement for flexure. It can be seen that the tangential strains were larger than the radial strains and that the latter decreased at loads approaching the ultimate.

Figure 2.5b traces the developments of radial and tangential strains near circular column in two similar tests of slabs with two-way reinforcement by Kinnunen and Nylander (1960). The tangential strains are again larger although the difference between them and the radial deformations are less than those in Figure 2.5a.

Finally, Figure 2.6 shows strains measured by Anis (1970) in a square slab supported at all four edges and loaded through a square column stub. In this case there is a rapid rise in the radial strain very close to the column.

It appears that in symmetrical conditions the tangential strains are considerably greater than the radial strains, except possibly at locations very close to columns.

Concrete strains have been measured in the vertical direction on the faces of columns at levels just below the slab faces. The distribution of these vertical strains give some impression of the variations of shear at column faces. Figure 2.7 shows the results obtained for a small square column in a test by Moe (1961) and it is clear that there is a concentration of strain towards the corners. The concentration generally increases with larger square or rectangular columns but is absent at circular columns as shown in Figure 2.8 from Vanderbilt (1972).

Slab strains have also been measured inside the concrete and Figure 2.9 presents measurements by Shehata (1982) of internal strains at various depths in slabs supported at four edges. It seems that the radial compression zone is larger than the tangential compression zone and that the peak radial strain occurs within the thickness while the maximum tangential strain is at the surface.

By testing high-strength concrete square slabs [Marzouk and Hussein (1991)], a concentration of stress was also evident at the corners of the column stub. It was found that neither the concrete compressive strains in the tangential direction nor those in the radial direction reached a limiting value of 0.0035 for the slabs tested.

As noted by Marzouk and Hussein (1991), the highest steel strain occurred below the stub column. At high reinforcement levels, the yield of tension reinforcement may occur at high loads at the column stub. For lightly reinforced slabs, yielding may initiate at the column stub and gradually progress throughout the whole tension reinforcement.

Cracks

The initial flexural cracks recorded for the test slabs first formed tangentially under the edge of the column stub, followed by radial cracking extending from the column. The first radial cracks were much more pronounced along lines parallel to the reinforcement crossing through the column stub. As the load was increased, the tangential cracks extended outside the circumference of the stub column. These tangential cracks were limited to the column vicinity. The slabs failed with the final shear crack coinciding with, or located outside, these cracks. Final failure is developed by the column punching through the slab as shown in Figure 2.10.

Failure

The punching shear surface on the tension face occurs at a distance of 2 – 3 times the effective slab thickness d from the column face for most of the test slabs. The observed angles of failure surface varied considerably. For normal strength concrete slabs, this angle was found to be between 26^0 and 30^0 by Marzouk and Hussein (1991), in agreement with Regan and Braestrup (1985), while for high-strength concrete slabs the observed angle of failure surface varied between 32^0 and 38^0. A typical failure surface of a high-strength concrete slab is shown in Figure 2.11. If load is applied beyond the initial failure the resistance drops markedly (typically to 20 - 25% of the peak for slabs without shear reinforcement) and the cover in the outer zone of the slab is torn away by the

reinforcement. When the load is removed the inner and outer zones of the slab recover leaving two effectively flat zones separated by the permanent transverse displacement at the failure surface.

2.2.3 Parameter Studies

Much research has been done on the influence of a number of parameters on the ultimate punching shear capacity of reinforced concrete slabs.

The punching load of a slab without shear reinforcement is influenced by: concrete strength, percentage of tension reinforcement, size of column, condition of support, shape of loaded area and distribution of tension reinforcement.

Concrete Strength

A substantial amount of research has been done on the relationship between the concrete strength and the shear strength. Alexander and Simmonds (1987) proposed that punching shear failure could be represented by a truss analogy and that failure is due to the concrete cover failing to contain the out-of-plane component of force between the reinforcement and the concrete compression struts. It was assumed that concrete tensile capacity is related to the square root of the concrete strength. González-vidosa, Kotsovos, and Pavlović (1988) used a nonlinear finite element analysis in which failure is governed by the tensile strength of the concrete, which was assumed to be proportional to the square root of the concrete strength.

Regan (1981) adopted the relationship between punching resistance and concrete strength as:

$$v_c \propto \sqrt[3]{f_{cu}} \tag{2.1}$$

Figure 2.12a shows the above relationship compared with Elstner and Hognestad's test results, where the experimental data from several groups of tests were combined assuming:

$$v_c \propto \sqrt[3]{\frac{100A_s}{bd}} \tag{2.2}$$

The overall agreement seems reasonable.

By using Hadjichristou and Papastavrou's (1980) test results, Regan (1985) plotted graphs of nominal shear stresses v_c calculated for the CEB (1978) perimeter against cylinder strengths f'_c, as shown in Figure 2.12b. The trends of the data are reasonably well represented by :

$v_c \propto (f_{cc})1/3 \quad or \quad v_c \propto (f_{cc})^{1/2}$

While $v_c \propto (f_{cc})^{2/3}$ overestimates the influence of the compressive strengths of these concretes made with natural aggregates and used in reinforced slabs.

Hognestad, Elstner and Hanson's (1964) specimens were the lightweight equivalents of the normal weight slabs tested by Moe (1961). The strengths of the lightweight slabs ranged from 77% to 88% of those in Moe's tests.

Reinforcement

The yield strength f_y of flexural reinforcement does not significantly affect the punching strength and the effect is small enough to be neglected in practice. Two of Moe's series of tests (1961) were similar slabs having steel with a yield strength of 399 N/mm^2 in one set and 482 N/mm^2 in the other, as recorded in Table 2.1. There was no apparent difference between the punching strengths obtained in the similar slabs of the two series.

Tests involving systematic variations of ratios of flexural reinforcement have been reported by Elstner and Hognestad (1956) and by Base (1959) and the results are plotted in Figure 2.13 with variations of concrete strength allowed for assuming P_u proportional to $(fc)^{1/2}$. Satisfactory agreement can be said to exist between the tests on:

$$\tau_u \propto \sqrt[3]{\rho} \tag{2.3}$$

Tests of slabs with reinforcement concentrated toward the column lines have been made by Elstner and Hognested (1956), Moe (1961) and Regan (1981). The data are best interpreted when ρ is determined for the full slab width in negative moment regions. Re-arrangement of reinforcement to a pattern involving concentration is not beneficial. Moe's and Elstner's results show that concentration of tension reinforcement tended to lower somewhat the ultimate shear capacity, rather than increase it. Concentration of tensile reinforcement in the column region is to be encouraged, however, because it optimizes the flexural behaviour of the slab in the service load range.

Kinnunen and Nylander (1960) also tested a number of slabs with ring reinforcement with steel ratios equal to those in other tests with two-way reinforcement. By comparing the results of these two types of slab, it was suggested that ring reinforced slabs were 30% weaker on average than orthogonally reinforced slabs, although their flexural capacities were virtually identical.

Compression Reinforcement has negligible effect on the ultimate shear strength. The ratios of compression steel vary usually from 0.3 to 1 times the ratios of tension steel and the maximum increase of punching resistance is only 12% as reported by Regan (1981). However, as v_{test}/v_{flex} approaches unity an increase in the compression reinforcement ratio increases the ultimate capacity as reported by Neth, de Paive and Long (1981), probably because the tensile in-plane force capacity of the slab is increased.

Slab Depth

Size effect may be taken into account by introducing a coefficient depending upon the slab depth d. Tests of geometrically similar slabs with varying thicknesses have been made by Kinnunen, Nylander and Tolf (1983) and by Regan (1981). The results obtained are shown in Figure 2.14 (Regan and Braestrup 1985) in terms of relative punching strengths plotted against effective depths. The relative strength is the ratio of the ultimate shear stress of the slab, calculated as $P_u / d\,(\sum b + \pi d)$, to the ultimate stress for a slab of the same series with $d = 200$ mm. The tests show a continuous reduction of relative strength with increasing depth throughout the range covered (64 mm $\leq d \leq$ 619 mm). The

line represents v_c proportional to $(1/d)^{1/3}$ and fits the data well. However, BS 8110 uses $(1/d)^{1/4}$ which makes little difference with $(1/d)^{1/3}$ even though it was based upon Regan's work.

The correctness of introducing a size effect has been questioned by some researchers who claim that slenderness (defined as the ratio of the clear distance from the loaded area to the support to effective thickness) and not size is the relevant parameter. The experimental evidence of a size effect is however very strong. The size effect is less pronounced for slabs with shear reinforcement.

Bazant and Cao (1987) tried to use the size-effect law for brittle failures due to distributed cracking to find an improved design formula for punching shear strength. The model used was essentially a modified shear perimeter approach and it was assumed that the shear strength was directly proportional to concrete strength. However, previous test data neither corroborated nor contradicted the applicability of the size-effect law to punching shear.

Column Shape

In general, for the same area of the column, slabs loaded through circular areas are stronger than those loaded through square areas. The limiting shear stress decreases with increasing rectangularity for the loaded area, provided there is marked two-way slab action.

According to Regan (1981), the empirical improvement of correlation with data presently available can be achieved by multiplying the calculated strength by a shape factor:

$$K_{sc}=1.15\sqrt{\frac{4\pi\times(column\ area)}{(column\ perimeter)^2}} \tag{2.4}$$

The basic value $K_{sc} = 1$ corresponds to a square column, and the factor gives a 15% increase of strength for circular columns. For extreme column shapes or virtual line loads, this factor may be excessively conservative.

Lateral Restraint

Taylor and Hayes (1965) tested two types of slabs. In one group of tests lateral expansion was effectively prevented by a massive steel frame, while in the other the slabs were free to expand. The results for three punching sizes are plotted in Figure 2.15 where b is the side length. It can be seen that the lateral restraint increased the ultimate load significantly (up to 60%) for the largest punch size and the lower ratio of reinforcement, but the effect reduced as the punch size decreased or the steel ratio increased, and there was no effect for the smallest punch and the larger ratio of reinforcement.

To simulate plate-column connections in continuous slabs, Vanderbilt (1972) tested specimens consisting of a square plate cast integrally with a surrounding ring beam and

a central column. The span/depth ratio was about 28. He found that the results were not greatly different from those obtained using specimens with simple supports at edges and concluded that the simple specimens appear to be satisfactory for parametric studies. In many real structures there is some resistance to in-plane expansion but it is difficult to assess the degree of restraint in any particular case.

Shear Span Ratio

The test results provided by Regan (1984), Graf (1933), Forsell and Holmberg (1946), indicate that the punching strength is influenced by the clear distance a_v from the loaded area to the support. The punching resistance rises sharply for values of a_v/d (defined as slenderness) less than approximately 1.5. At higher values of the ratio the influence seems to be small or non-existent. This suggests that an empirical method of treating such cases could be based on a multiplying factor $1.5d/a_v$ applied to the shear stress v_c in the part of the perimeter effected by the presence of a support.

Dowel Action

When a punching failure occurs the concrete cover over two-way reinforcement is commonly torn away along the plane of the steel at the outside of its intersection with the inclined failure surface. Thus during the failure the bars act as dowels. There is, however, very little evidence of the significance of dowel action at the maximum load stage.

As mentioned before, Kinnunen and Nylander (1960) tested a number of slabs with ring reinforcement giving steel ratios equal to those in other tests with two-way reinforcement. The results show that the ratio of shear strength with ring reinforcement to two-way reinforcement is 0.66. In a very simplistic way these results could be said to suggest that 34% of the total punching resistance of slabs with two-way reinforcement is attributable to dowel action. However this would ignore differences between the two types of reinforcement other than the absence of dowel action with ring steel. Once a shear crack forms, ring bars between the crack and the column become ineffectual, while two-way steel does not. Also the anchorage of rings outside the crack is total dependent on stresses in the concrete at the steel level between the bars and the crack while two-way reinforcement is anchored in the exterior of the slab.

Rate of Loading

Data on the effects of the loading rate are meagre. Moe (19) found no unfavourable effects for a slab placed under a sustained load equal to three-quarters of its ultimate capacity for 3 months as was shown in Figure 2.4. Criswell (1974) found that for rapid loading in which the maximum load was reached in 20 msec to 40 msec the shear strength increased by 26%, whereas flexural strength increased by only 18%, compared to the strengths for similar specimens in the customary static type test.

2.2.4 Equations of Punching Shear Strength

The earliest attempt on determining punching shear strength was made by Richart (1948) who performed a systematic study of the resistance of foundation footings to shear failure. He observed that the shear failure was accompanied by high tensile stresses in the reinforcement and extensive cracking of concrete and reported that the shear stress v_u computed at a section taken at a distance equal to the effective depth of the slab d from the column face, varied between two limiting values. These values were expressed as a function of the compressive strength of concrete f_{cc} with calculated shear stress v varying between $0.005f_{cc}$ and $0.009f_{cc}$.

The results of these tests have been used to derive slab shear design procedures even though the footing slabs tested were very thick. For this reason, the extrapolation of the results was questioned by many researchers.

In 1956, Elstner and Hognestad (1956) carried out shear tests of 39 reinforced concrete flat slabs in order to extend the ranges of slab variables of previous test programs. The following equation was proposed for slabs without shear reinforcement:

$$v_u = \frac{0.046}{\phi_u} f_{cc} + 333 \qquad (2.5)$$

where ϕ_u is the ratio of the ultimate shearing capacity of the slab to the ultimate flexural capacity of the slab if it had not failed in shear. The ultimate flexural capacity of the slab was calculated using yield line theory.

It was also reported that a concentration of tensile reinforcement directly beneath the loaded area or the presence of compression reinforcement had a negligible effect on the ultimate shear strength of the tested slabs.

In order to study the mechanism of punching failure, Moe (1961) carried out tests of 43 square slabs, (1.8m × 1.8m × 150mm) of which 15 possessed holes at various locations of the slab, 8 were designed to study the effect of varying the concentration of reinforcement through the pyramid of rupture, 6 were used to study the influence of shear reinforcement, 2 were utilized for an investigation into exterior column.

Moe suggested that the critical section to compute the nominal shearing stresses should be taken along the perimeter of loaded area. After a statistical analysis of tests of Richart, Elstner and Hognestad and his tests, Moe proposed the following equation for shear stress:

$$v_u=[15(1-0.075\frac{b}{d})-5.25\phi_u]\sqrt{f_{cc}} \qquad (2.6)$$

Where v_u is in *psi*. The selection of the shear stress to be proportional to the square root of concrete strength was based on the assumption that a shear failure very often is a splitting type failure, similar to the type of failure observed in specimens under tension and the tensile strength is generally assumed to be proportional to $(f_{cc})^{1/2}$.

Yitzhaki (1966) tested 16 circular slabs for punching under circular, square and rectangular load areas, and 12 slabs with diagonal reinforcement. The punching of slabs subjected to concentric loading was explained as being primarily a function of the flexural strength of the slab. By adding flexural reinforcement, the compression force on compression zone increases, hence adding to the frictional resistance to shear.

After reviewing the test results of Elstner and Hognestad, Moe, Kinnunen and Nylander, Yitzhaki proposed the following equation:

$$P_u = 8(1-\frac{w}{2})d^2(149.3+0.164\rho f_y)(1+0.5\frac{c}{d}) \quad (lbs) \tag{2.7}$$

where w is the reinforcing index $(\rho f_y/f_{cc})$ and c is the column size. This equation permits the calculation of punching strength of a slab without reference to a fictitious shear stress. It was shown also that yield line theory is capable of closely predicting the punching strength of many of the tests reported in literature, with slightly higher test strength, the result of strain hardening of the reinforcement.

Long (1975) derived empirical formulas for predicting the punching capacity of slabs at interior columns by simplifying previously reported analytical procedures, which take into consideration the interaction of flexural and shear effects. He recommended that the punching load for a slab is taken to be the lesser of the two values calculated from the following equations.

$$P_u = \frac{0.8\rho f_y d^2 (1 - 0.59\rho \frac{f_y}{f_{cc}})}{(0.2 - 0.9\frac{b}{L_s})} \quad (Lbs) \tag{2.8}$$

$$P_u = \frac{16(b+d)d(100\rho)^{0.25}\sqrt{f_{cc}}}{0.75 + 4\frac{b}{L_s}} \quad (Lbs) \tag{2.9}$$

Where L_s is the span length between two columns. Equation 2.8 was derived on the basis that the flexural steel reinforcement yields before failure. Whereas in equation 2.9, the failure takes place before the steel reaches the yield point.

Regan (1981) proposed a method for calculating the shear strength of slab-column connections. This method was incorporated in the British code (BS 8110-1985). At an interior column free from any unbalanced moment, the following expression for ultimate shear force was proposed.

$$P_u = K_a K_{sc} (\frac{300}{d})^{0.25} (100\rho f_{cu})^{\frac{1}{3}} \times 2.69(u_0 + 7.85d) \quad (N) \tag{2.10}$$

where: $K_a = 0.13$ for normal dense concrete and 0.105 for lightweight aggregate and $K_{sc} = 1.15\ [(4\pi \times \text{column area}/(\text{column perimeter})^2]^{1/2}$.

The prediction by this equation was compared to the test data taken from his work and references. It was found that equation 2.10 is practically a lower bound to the test results and can be taken as an expression of characteristic strength.

In 1990, Gardner (1990) reviewed Regan, Bazant and Cao, and the code equations on punching shear capacity of reinforced concrete slabs and its relation to concrete strength and steel ratio. He discussed his experimental investigations and concluded that the shear capacity is proportional to the cube root of concrete strength and steel ratio. He endorsed an equation similar to that of BS 8110-85 code:

$$v_u = 0.99(\rho f_{cc})^{\frac{1}{3}}\left(\frac{400}{d}\right)^{\frac{1}{4}} \quad (MPa) \tag{2.11}$$

2.3 Non-symmetric Punching Shear

Most connections in flat slab structures must be designed to transfer moment as well as shear. When a flat slab structure resists lateral forces, every connection transfers moment. Even for gravity loading there is always moment at edge and corner columns, and there can be moment transfer at interior columns due to unequal lengths for adjacent spans, pattern loadings, etc.

2.3.1 Interior Column

Theoretical Considerations

When an eccentric load is transferred from a slab to an interior column, a part of the moment is likely to be provided by an uneven distribution of the vertical shear at perimeters around the column. The remainder must be transmitted by flexure, torsion and horizontal shear. Distributions of the three load effects can be estimated by a variety of methods.

Mast (1970) gave solutions for the effects of a concentrated moment applied to an uncracked elastic plate at an interior column of the model illustrated in Figure 2.16. The distribution of the load effects around any closed perimeter is calculated as independent of the geometry of the column. Variations of the boundary conditions should have little effect on the results obtained, but the approach does have the limitation of neglecting the local influence of the column in question. Figure 2.17 reproduced from Mast's paper shows typical distributions of flexure, torsion and shear, while the Table 2.2 gives representative breakdowns of the total moment between the three types of interior reaction at rectangular perimeters. The two figures in parenthesis at the end of each row indicate the sub-division of the moment due to vertical shear effects into parts due to q_x and q_y respectively.

It is noteworthy that for geometrically similar perimeters (the last three rows of Table 2.2) the subdivision of the moment varies very little with distance from the column, so long as the distance is small in comparison with the span of the slab.

If the average value of q_x is taken as the determining effect in regard to punching strength the following deduction may be drawn from the table. The percentage of the total moment resisted by uneven vertical shear q_x is approximately constant (≈30%). Thus the average shear per unit width due to a transferred moment M is

$$q_x=\frac{0.3M}{xy} \tag{2.12}$$

Where x and y is the length of the perimeter. The average shear due to a vertical force P is $q = P/4(x + y)$. Then writing $M = Pe$ the shear produced by an eccentric load

$$q=\frac{P}{4(x+y)}\left[1+\frac{0.3e(x+y)\times 4}{xy}\right] \tag{2.13}$$

$$q\sim P/4(x+y)[1+2.4e/\sqrt{xy}] \tag{2.14}$$

The model shown in Figure 2.18 was analyzed by Yamazaki (1975) using two finite element methods: a general linear elastic method taking account of shear deformation and a plate bending method taking flexural yielding and anisotropy into account but ignoring shear deformation.

In overall terms the results from the two methods show a good agreement which was taken by Yamazaki to justify the use of the plate bending method for the treatment of inelastic behaviour.

Yamazaki (1975) applied his plate bending analysis to the inelastic phase of behaviour using bi-linear moment/curvature relationship. Some of the results obtained are shown in Figure 2.19 where the following features can be observed.

The shear Q_x remains a substantially linear function of the load while the moment M_x increases only slowly after yield. Both the shear and torsion at the side face near the higher loads increase more rapidly with load after the onset of yield. At the other side face, the torsion rate also increases. Finally, at the back face for loading case 2 there is a marked increase in the rate of negative shear although the force there remains small in absolute terms, and there is also an abrupt growth of the reversed moment at the back of the column, even though the gross moment across the slab there is not reversed. This effect could be significant for design. If adequate bottom steel was not provided, the reversed moment could not be sustained and the resulting redistribution of load effects could cause a premature failure.

It is clear that plate analyses can give theoretical shear distributions and their results are relatively simple provided they are restricted to the elastic range. There are, however, considerable problems involved in their use for the prediction of punching resistances. It is difficult to allow for redistribution of effects following flexural cracking and yielding and no solution to date has considered redistributions due to shear cracking. Flexural analyses do not allow for in-plane force effects and yet it is clear that considerable moments can be transmitted at the front and rear column faces by opposed compressive forces even in the absence of bars through the column as indicated in Figure

2.20. However, the division of load effects into flexure, torsion and shear does not define the actual stresses in the concrete which produce a failure. The width over which shear should be averaged in defining a critical condition is also debatable.

In spite of these difficulties plate analysis can be used to assess the distribution of vertical shear due to an unbalanced moment between a slab and a column, and the shear can be averaged over a chosen width. If the perimeter at which moment effects are considered is the same as that used for pure shear loading, the total nominal shear stress can be expressed as

$$v=\frac{P}{ud}[1+\frac{Ke}{c}] \tag{2.15}$$

where u is the length of the control perimeter

K is a numerical co-efficient

e is the eccentricity M/P of the load

M is the unbalanced moment and

c is a dimension dependent on the column dimensions and the slab thickness

Failure may then be predicted to occur when $v = v_{crip}$ with v_{crit} given the same value as for concentric loading. Thus

$$P_u=(udv_{crit})/(1+Ke/c) \tag{2.16}$$

$$M_u=udv_{crit}[e/(1+Ke/c)] \tag{2.17}$$

or:

$$P_u = udv_{crit} - M_u K/c \qquad (2.18)$$

ie., the interaction between P and M for any particular geometry is predicted to be linear.

An alternative to plate theory and simplification of it is to consider the area of the slab-column junction as a cross of beams in the manner shown in Figure 2.21. Beam analogies have been proposed by a number of authors including Hawkins and Corley (1971). In principle the resistance of each beam to the combined effects of bending, shear and torsion can be estimated by standard methods although the applicability of code approaches to the side face beams with high torsion loads is debatable. In the beam analogy the vertical shear due to torsion is small. Another problem with any beam analogy is the division of the overall loads P and $M = Pe$ between the bending, shear and torsion of the various "beams". Although some guidance is available on this subject, no clear solution is available.

Information from Tests

Test Arrangement

Most tests of slab-interior column connections with eccentric loading have been made on square slabs, with plan dimensions approximating to 0.4 times the spans of prototype floors and with central column stubs. In the majority of cases, the column has been loaded either by an eccentric vertical load or by a concentric vertical load plus a moment produced by horizontal forces above and below the slab. In such cases the

peripheries of the slabs have been simply supported with restraint against either all vertical movements or against movement in only one direction.

Some tests have been made with slabs supported by central columns and loaded near the slab edges so as to produce moments in the columns.

Deformations

Hawkins, Bao and Yamazaki (1990) tested 36 specimens to simulate high unbalanced moment transferring at the interior slab-column connections and low unbalanced moment transferring at the connections. Figure 2.22 is the profile of the specimens, and Figure 2.23 is diagram of the total load transferred to the column versus the deflection at the most heavily loaded edge of the slab (D2 in Figure 2.22). Downward arrows at the ends of curves indicate punching failures, and circles along the curves indicate first yielding of the top reinforcement. For a given series, the high unbalanced moment specimen always deflected more than the low unbalanced moment specimen.

Strains

In Hawkins, Bao and Yamazaki's tests (1990), measurements were made of the concrete strains on the bottom surface of the slab on the line of, and perpendicular to, Face AD (Figure 2.24). Tensile strains extended to a distance of about one slab thickness from the column Faces AB and DC, and then strains became compressive between this location and the slab edge. The magnitude of these compressive strains was consistent with the effects on line AD of the static moment due to the downward loading on the

slab's edge. Obviously, the column imposed only a local restraint on the overall bending of the slab.

Steel strains across the width of typical specimens are shown in Figure 2.24. When reinforcement was not concentrated in the column region, the tension steel passing through the column yielded at 50 to 55 percent of the flexural capacity. Large rotations and crack widths are possible at service loads unless the reinforcement is concentrated. Steel in the immediate vicinity of the column usually yielded. For low moment loadings, the bottom slab steel remained in compression throughout the test. For high moment loadings, however, the bottom steel passing through the column rapidly went into tension after first yielding occurred in the top steel. Further, for the top steel, tension spread across the width of the slab with increased loading, while for the bottom steel only the bars passing through the column developed tension.

Failure

Typical crack patterns in the vicinity of the column are shown in Figure 2.25 in which the punching failure surface is shown by thickened and irregular line. Failure due to punching initiated adjacent to the column corners at higher loading side. For low moment loadings, that punching spread almost immediately, completely around the column, and the slab as a whole moved down the column. For high moment loadings, rigid body rotations dominated. Punching spread to the more heavily loaded face of the column. Specimens with high moment loadings did not fail as abruptly as those with low moment loadings. However, for both loadings, the suddenness of the failure increased

with increasing reinforcement ratios.

The slope of the inclined crack was similar for all faces, evidence of torsional effects was slight, and the concrete between the bars framing into each column face was more intact than at the column corners.

There was marked bond distress with reinforcement closely spaced through the column. In these cases as loading progressed, inclined cracks appeared on the vertical surface of the most heavily loaded slab edge. Those cracks extended down to the outermost bars of the concentrated reinforcement. Simultaneous with the final punching failure at the column, a horizontal crack connected those inclined cracks, and the concentrated reinforcement punched out of the slab along its full length.

Parameters

The parameters that affect the punching shear of a slab with unbalanced moment transferred at slab-column connections are the same as in symmetric punching. The most important parameters are the geometry of the connection, the concrete strength, the reinforcement ratio. Lesser effects attributed to the span length between columns, the compression steel and membrane forces.

Concrete strength and type - The test results of Hawkins, Bao and Yamazaki (1990) show that stiffness increased with increasing concrete strengths but at rate less than the ratio of the $(f'_c)^{1/2}$ values. Ductilities increased slightly with increasing concrete strength. However, the use of high-strength concrete caused no fundamental change in

behaviour and there was little change in stiffness or ductility with concrete type. The main effect of using lightweight concrete was a reduction in the ultimate capacity.

Reinforcement ratio - Within a given series, stiffness increased and ductilities decreased as the reinforcement increased. For a given series and a given reinforcement ratio, there was greater ductility for high moment loading than for low moment loading.

Slab depth - Effect was proportional to the square of the slab's effective depth. The result demonstrates a decrease in ductility with increasing shear effects.

Reinforcement concentration - Concentration of the reinforcement through columns increased the stiffness, but for high unbalanced moment loadings decreased the ultimate capacity and ductility, compared to that for specimens with the same reinforcement concentrated immediately outside the column.

Column aspect ratio - Little difference in response for ratios of 0.5 and 1.0, but showed marked decreases in ductility for ratios of 2 and 3.

Tests of simply supported slabs with restraint against vertical movement in either direction and with range of load eccentricities, including pure moment loading, have been reported by Stamenkovic and Chapman (1972). The results are shown in Figure 2.26 as a graph of P/P_0 plotted against M/M_0 where P and M are the ultimate shear and moment in a test and P_0 and M_0 are the ultimate values for pure punching ($M = 0$) and pure

moment loading. The experimental values have been corrected to allow for the fairly small variations of concrete strength. Although there is some scatter in the data, the results can be seen as reasonable support for the linear interaction predicted from both plate bending theory and the simplified methods of codes. Test results reported by Hawkin, Cao and Yamazaki agree with Stamenkovic and Chapman (1972).

In Moe's study (1961), as mentioned before, an unbalanced moment transferred to the column was studied. Moe assumed the variation of shear stressed around the column perimeter to be linear and that the maximum shear stress would be the same as for the case where no unbalanced moment is transferred. He suggested that only a fraction K of the moment KM ($K = 0.33$) should be considered acting around the column perimeter.

A method for calculating the shear strength of slabs which are also subjected to unbalanced moment was given by Regan (1981) It was assumed that the unbalanced moment was transferred to the column by shear stresses acting along the line of contraflexure about the column. For a square column, the ultimate load capacity with an eccentricity e is given as a function of the ultimate concentric load capacity P_u;

$$P_{ue} = \frac{P_u}{1 + \frac{1.5e}{b+2d}} \qquad (2.19)$$

2.3.2 Edge and Corner Columns

Theoretical Approach

For punching at edge and corner columns, the approach is to apply the formulas for interior columns with a reduced control perimeter subjected to eccentric loading, and this method is adopted by some codes of practice. The importance of flexural effects, particularly for corner columns, implies that experimental failure loads will be largely dependent upon the design and detailing of the flexural reinforcement, making meaningful comparison with test results difficult.

The first theoretical approach to edge columns seems to be by Andersson (1963) who made three tests from which he observed that the criterion of failure appeared to be similar to that adopted in the Stockholm work on interior columns. He determined a nominal shear stress at a distance *d/2* from the inner face of the column. A part of the moment transmitted to the column is assumed to be provided by torsions at the side faces, and these torsions are assumed to create downward forces near the inner corners of the column. The corresponding upward forces at the slab edge are taken to be resisted by vertical reinforcement.

On the basis of plastic theory the sum of the two downward forces due to torsion as shown in Figure 2.27 is:

$$\Delta p = 2(\tau \frac{d^2}{4}) = \frac{T}{2(b_1 - \frac{d}{3})} \qquad (2.20)$$

Where the torque T is the sum of the torsions at the two faces. The torque T is assumed to be $0.4M = 0.4Pe$ where e is the eccentricity of the load from the centre of the column. The total downward shear is then $P + \Delta P$ and is assumed to be distributed around the part of the column which is in compression. The final nominal shear stress is then:

$$v = \frac{\frac{p}{d^2}\left[1 + \frac{0.4e}{2(b_1 - \frac{d}{3})}\right]}{\left[\frac{b_2}{d} + \frac{b_1}{d}\left(1 + \frac{b_1}{6e}\right) + \frac{\pi}{2}\right]} \qquad (2.21)$$

The application of the Kinnunen / Nylander theory to edge columns has been studied by Kinnunen (1971). The treatment of punching is in outline similar to Andersson's but the force increment ΔP is taken as $T/2b_1$, with the total torque T calculated from a yield line analysis of the slab. With this method of determining the torsion the calculated punching load becomes a function of the arrangement of reinforcement in the slab - the greater the proportion of the transferred moment accommodated by reinforcement crossing the inner face of the column the higher the punching resistance.

Both Anderson and Kinnunen determine the moment capacities of edge column connections on the basis of yield line theory. The local yield lines corresponding to the formation of a hinge between the slab and the column, with its axis at the inner face of the column are as shown in Figure 2.28.

Regan (1981) discussed the local strengths of connections with edge and corner columns in rather different terms. The starting point was the behaviour of a slab connected to an edge column at only the inner face as in Figure 2.29a. The pure bending resistance is clearly the ultimate moment at AA (M_f). When a shear force is added, provided the failure is still flexural, the ultimate moment about the column centre becomes:

$$M_u = M_f + Pb_1/2 \qquad (2.22)$$

As for beams without shear reinforcement, the shear resistance is taken to be independent of the moment and is expressed in terms of a limiting nominal vertical stress on the inclined area of the failure surface shown shaded in Figure 2.29a. The complete moment-shear interaction diagram, for inward eccentricity, is then shown as in Figure 2.29b.

The yield line solutions used by Andersson and Kinnunen imply the existence of torsion at the slab edge. Regan assumed that the resistance to these effects is lost when torsion cracking occurs at the slab edge and that thereafter the pure bending resistance is limited to the ultimate moment provided by the reinforcement perpendicular to the edge and crossing the "yield lines" in Figure 2.28_b.

The beam analogy approach described briefly in the context of interior connections with unbalanced moments is also applicable to edge column connections and is considerably simpler in this context. Its application is described by Hawkins and Corley (1971). The control section adopted as shown in Figure 2.30 is as in the ACI code. Two modes of failure termed moment-torsion and shear-torsion are possible.

In a moment-torsion failure the full flexural capacity is developed at BC.

In shear-torsion failure the critical actions are shear on BC and torsion on AB and CD.

The basic distinction between the two modes of failure lies in the conditions at the inner face (BC), where the situation is critical either for bending or for shear. The side faces are always predicted to reach a critical condition under combined actions with V and T alone or V, T and M influencing the failure.

A difference between this theory and others is the influence predicted for the applied moment parallel to the edge. This does not enter into any other theory in the same way although adequacy of top steel parallel to the slab edge is implicit in other methods and relatively explicit in Kinnunen's work (Kinnunen's work is however specifically related to situations in which redistributions from negative to positive moments parallel to the edge are impossible).

A recent theoretical approach to the resistances of edge and corner connections is of Pöllet (1983) who distinguishes two modes of failure - shear and moment/torsion.

For a moment/torsion failure, the failure surface is assumed to be as indicated in Figure 2.31.

It was assumed that the concrete carries stresses only in the compression zones. Shear stresses are calculated as average values while normal stresses are determined from a rectangular stress block.

The general nature of the results obtained from Pöllet's method is shown in Figure 2.32. It has some commonality with Regan's approach in the division of failure modes and the prediction of moment failures at resistances below yield line values.

Information from Tests

The work by Stamenkovic and Chapman (1972) included series of tests of models with edge and corner columns attached to slabs simply supported as in Figure 2.33. Edge column specimens were tested with moments parallel and perpendicular to the free edges. Corner column specimens were tested with moments parallel to one free edge. The results are shown in Figure 2.33 as ultimate moment-shear interaction diagrams. The moments are related to the centroid of the ACI control perimeters indicated.

For edge columns, moments parallel to the free edge can be seen to produce a linear interaction similar to that for an interior column. For the other two cases the interactions are different. Test arrangements of this type do not permit realistic redistribution of moments.

In a real structure, the attainment of a limiting flexural condition at an exterior column is not in itself a cause of failure as moments can be redistributed into the adjacent span. The moment at the exterior column then rises slowly due only to eccentric shear and failure occurs either overall as a bending failure or locally as a shear failure at the column.

Zaghlool, dePaiva and Glockner (1970) studied the behaviour and the strength of the column-slab connections in the presence of uniaxial and biaxial bending. The authors showed that the method proposed by Moe was conservative for corner columns. A value of K which would result in reasonable predictions of strength was found to be 0.4 instead of the value 0.33 determined by Moe for interior columns. They proposed a simplified method to determine the punching strength of corner columns. They assumed that the inclination angle α of the diagonal cracks to the horizontal equal to 45 degrees. Dowel action and aggregate interlock are negligible, and the compression zone carried no shear. Based on the assumption that failure will take place when the principal tensile stresses produced by the shearing forces exceed the tensile strength of the concrete, they proposed the following equation:

$$v_u=[5.6+(4\frac{d}{b})]\sqrt{f_{cc}} \qquad (2.23)$$

Equation (2.23) showed a good correlation with their tests.

The analysis of data from failures at exterior columns is considerably more difficult than that for interior columns, principally because of the greater influence of flexural effects and of the design and detailing of the flexural reinforcement. Even for corner columns, where there is general agreement on the critical yield line patterns, it can be difficult to calculate the moments at the negative yield lines because of uncertainty about the anchorages of reinforcement crossing them. It can also be difficult to define ratios of reinforcement to be used in equations for punching strengths.

Table 2.1 Relationship Between Punching Shear Strength and Strength of Reinforcement (Moe 1961)

Slab ref	Results with f_y = 399 N/mm^2			Results with f_y = 482 N/mm^2		
	f_{cc} N/mm^2	$\frac{P_u}{P_{flex}}$	$\frac{P_u(kN)}{\times\sqrt{25/f_{cc}}}$	f_{cc} N/mm^2	$\frac{P_u}{P_{flex}}$	$\frac{P_u(kN)}{\times\sqrt{25/f_{cc}}}$
S1	23.3	0.99	403	24.5	0.84	396
S3	22.6	0.92	383	25.4	0.81	375
S4	23.8	0.94	342	35.2	0.82	315
				20.5	0.87	345

Table 2.2 Distributions of Flexure, Torsion and Shear (Mast 1970)

Definition of perimeter		Percentages of moment resisted by		
x/ℓ	y/ℓ	Flexure	Torsion	Vertical Shear
0.05	0.10	58	12	30 (26, 4)
0.10	0.05	17	12	61 (26, 45)
0.04	0.04	34	16	50 (32, 18)
0.07	0.07	34	16	50 (32, 18)
0.10	0.10	34	16	50 (32, 18)

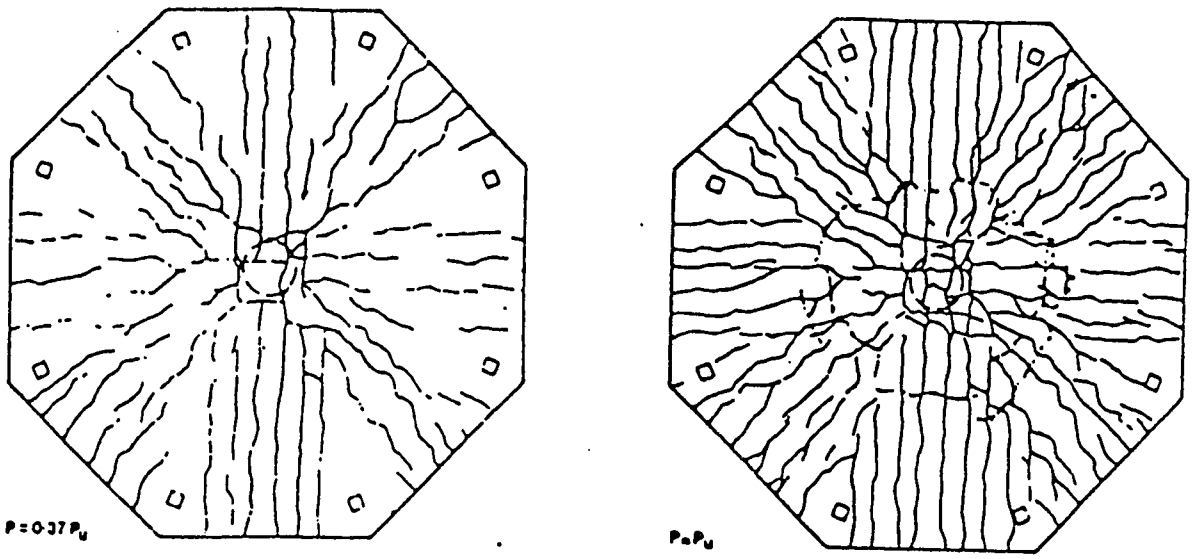

Figure 2.1 Cracking of A Symmetrical Two-way Slab
Slab p2 (Marti, Pralong and Thürlimann 1977)

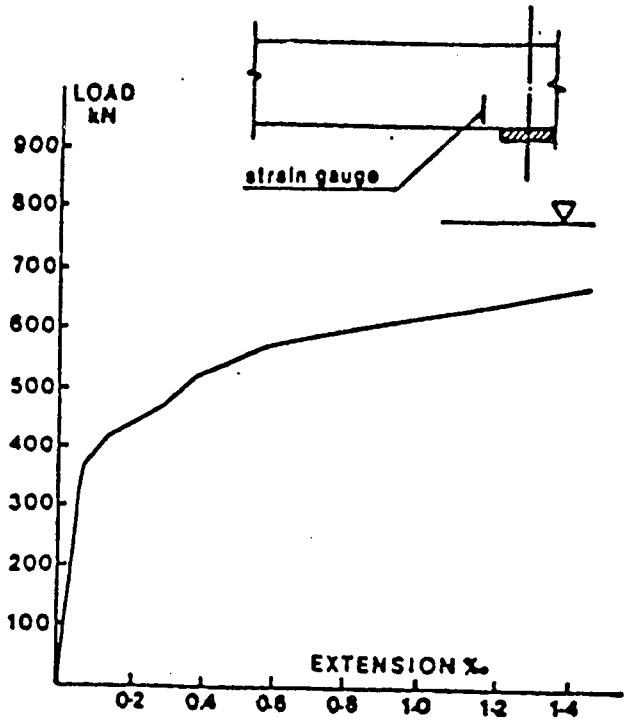

Figure 2.2 Interior Transverse Strain
-Regan Slab DT1 (Regan 1983)

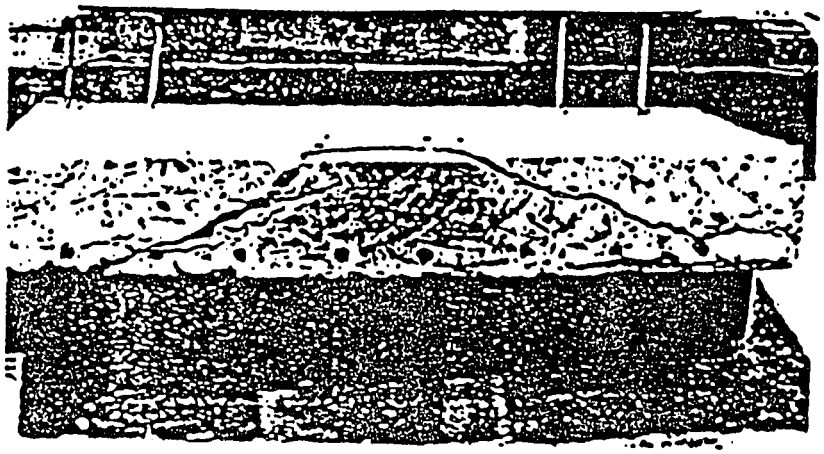

Figure 2.3 Cross-section View of Slab C1 after Failure (Grira 1990)

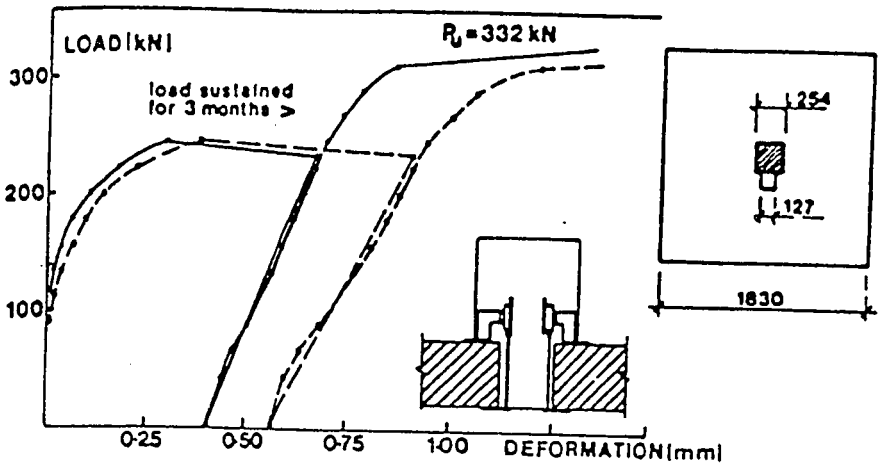

Figure 2.4 Vertical Deformation of A Slab-Moe's (1961) slab H15

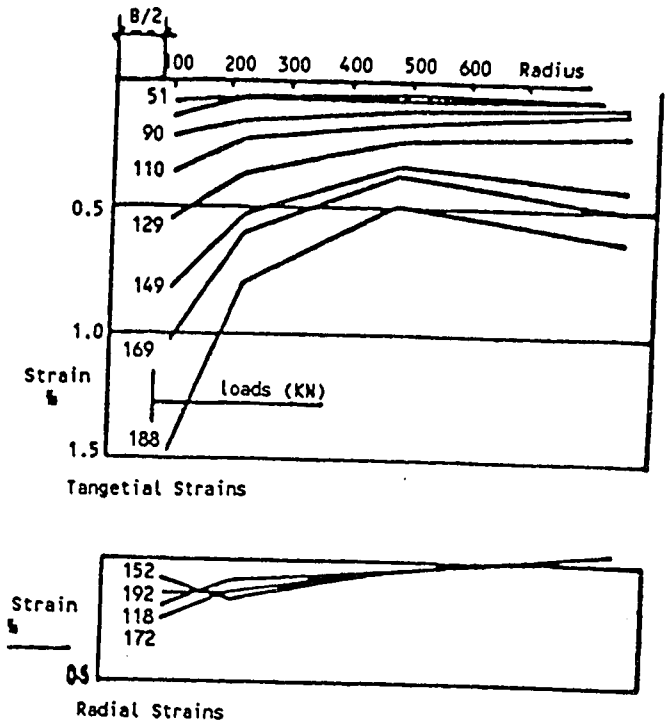

Figure 2.5a Radial Distributions of Strains in A Slab with Only Ring Reinforcement - Kinnunen and Nylander (1960) slab 15

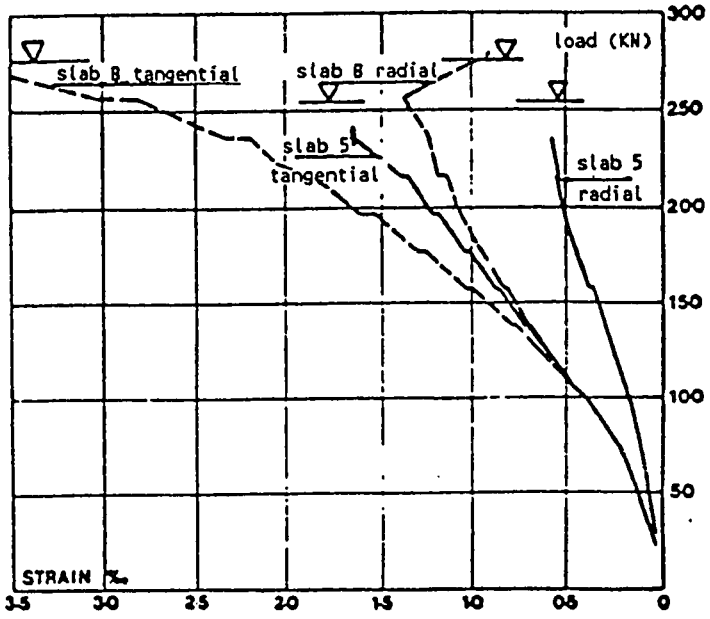

Figure 2.5b Radial and Tangential Strains on The Compressed Surfaces of Two-way Slabs -Kinnunen & Nylander slab 5&6

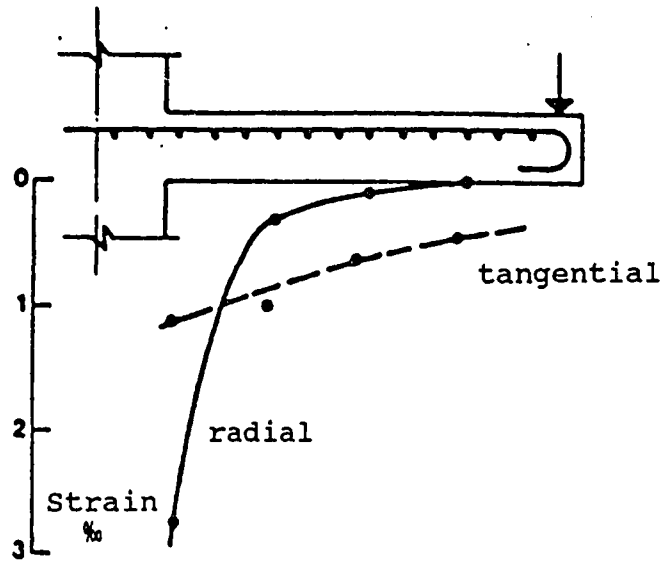

Figure 2.6 Distributions along A Radius of Radial and Tangential Strains of The Compressed Surface -Anis (1970) test B3

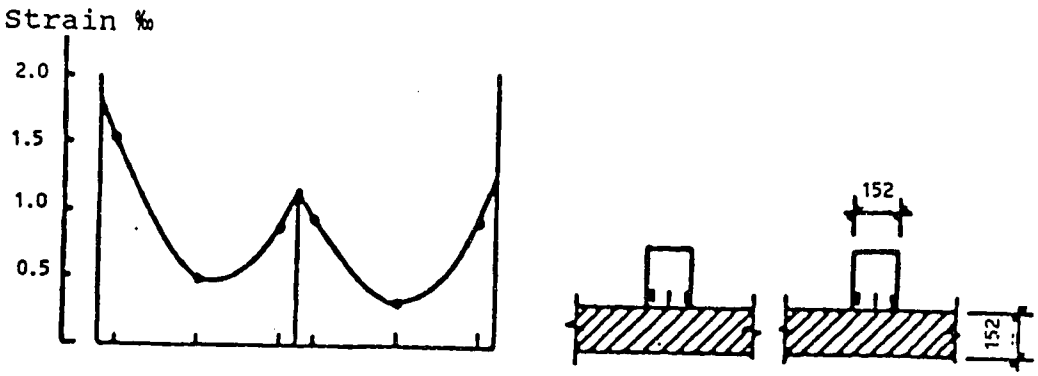

Figure 2.7 Vertical Strains at A Column Face - Moe's (1960) slab R2

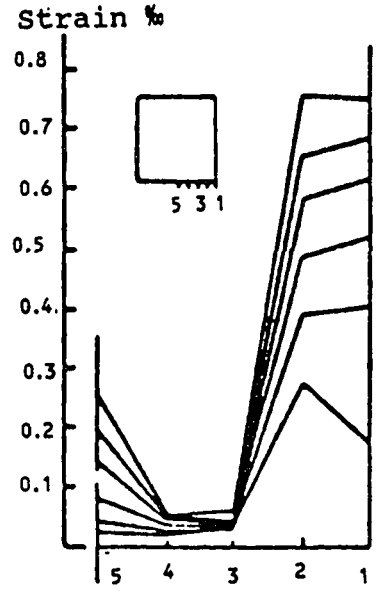

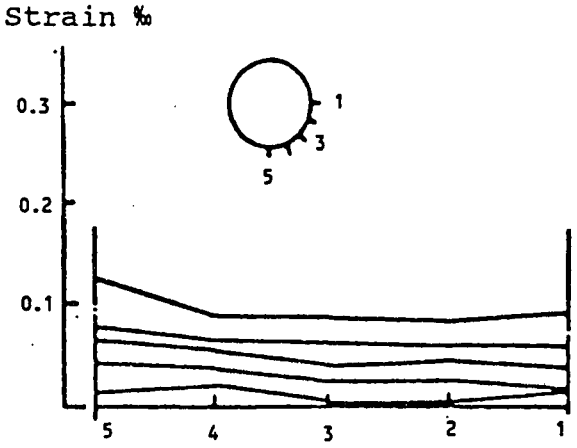

Figure 2.8 Vertical Strains at Column Faces
-Vanderbilt (1972)

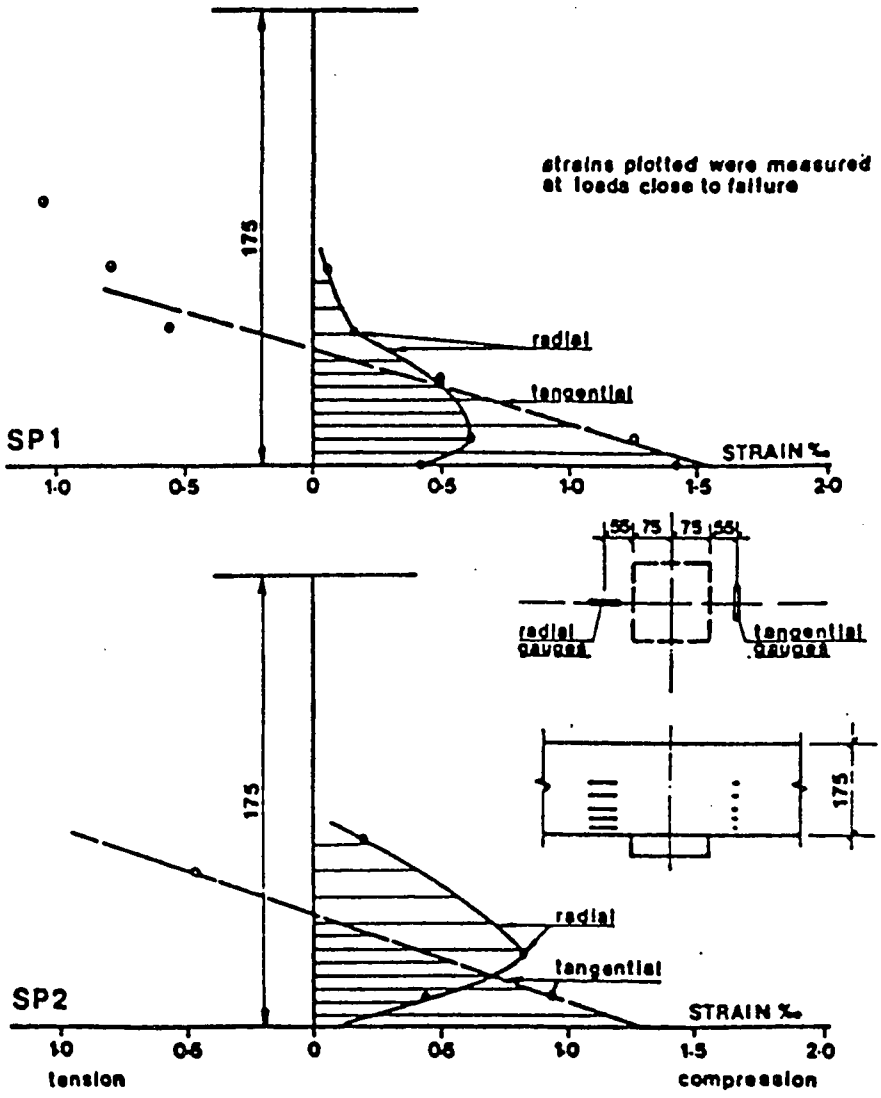

Figure 2.9 Interior Strains -Shenata (1982) slabs SP1&SP2

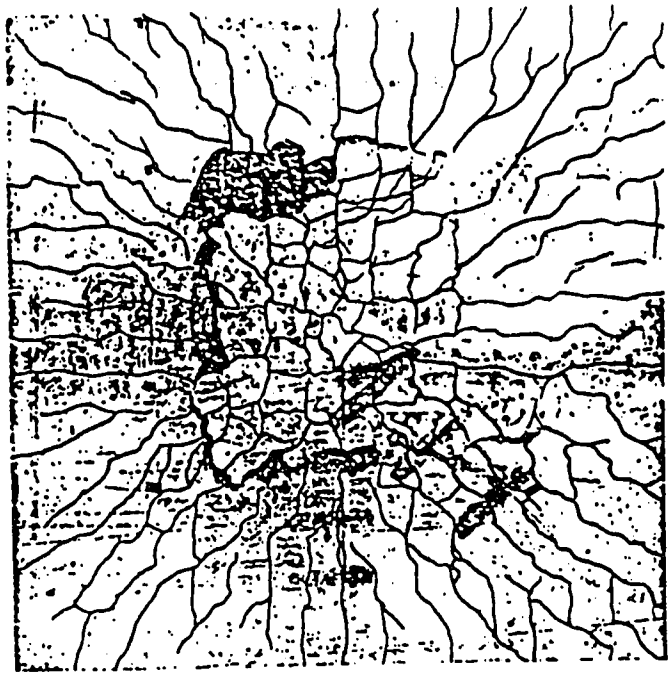

Figure 2.10 Crack Pattern at Failure for
A Typical Test Slab (Marzouk and Hussein 1991)

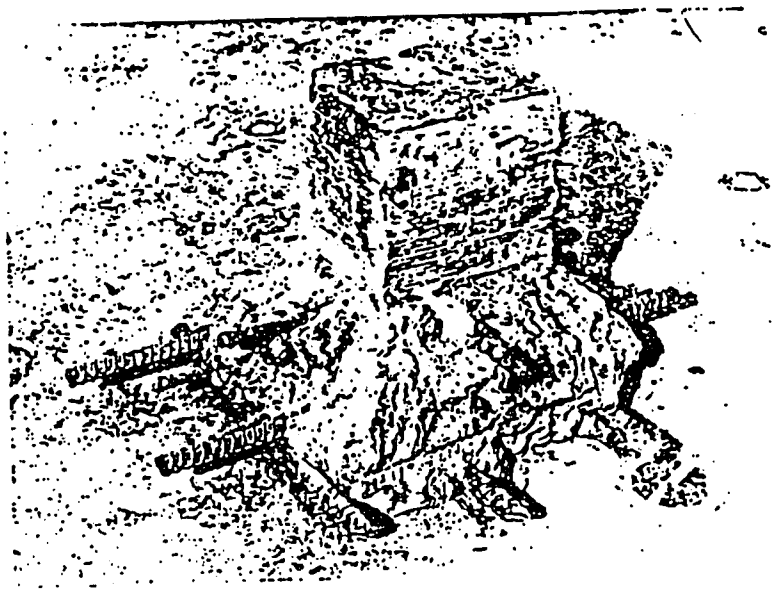

Figure 2.11 Failure Surface of A High-strength Concrete Slab
(Marzouk and Hussein 1991)

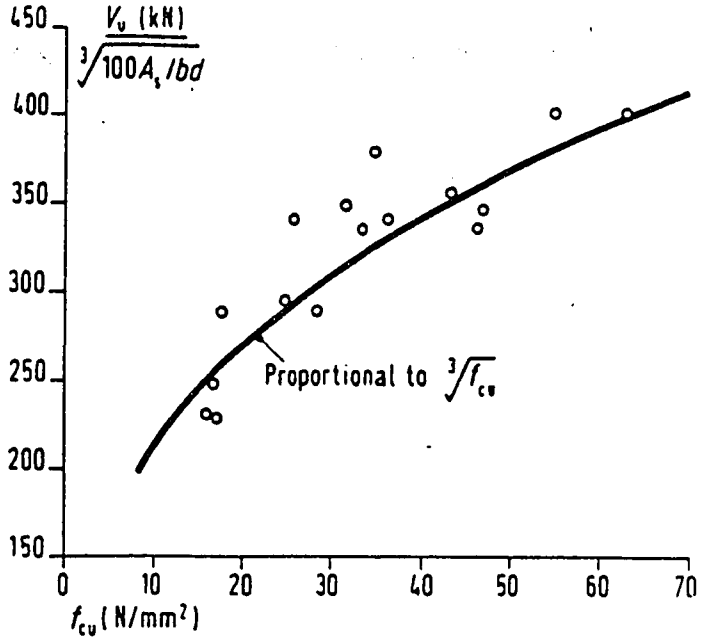

Figure 2.12a Influence of Concrete Strength on Punching Resistance (Regan 1981)

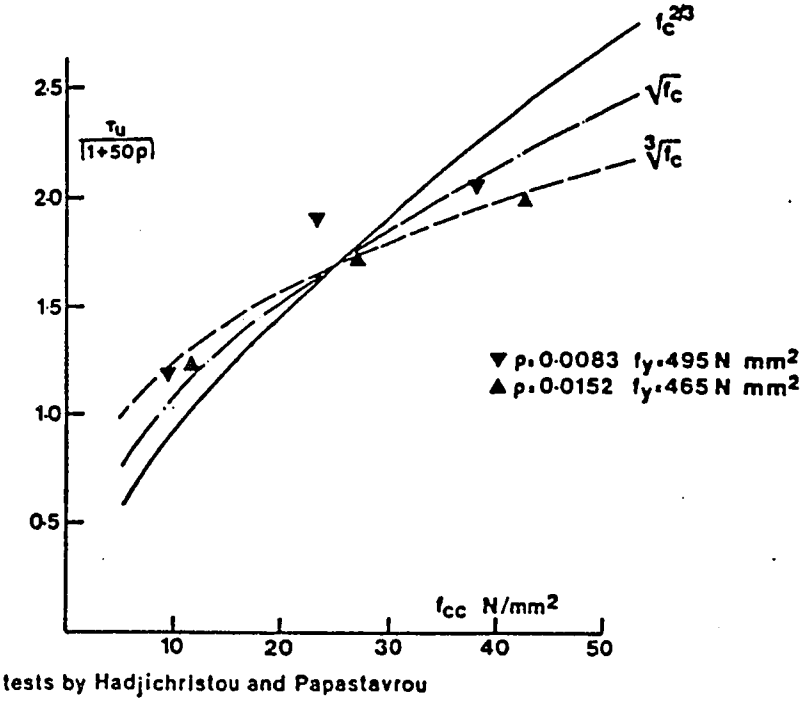

Figure 2.12b Variation of Punching Resistance with The Compressive Strength of Concrete (Regan 1985)

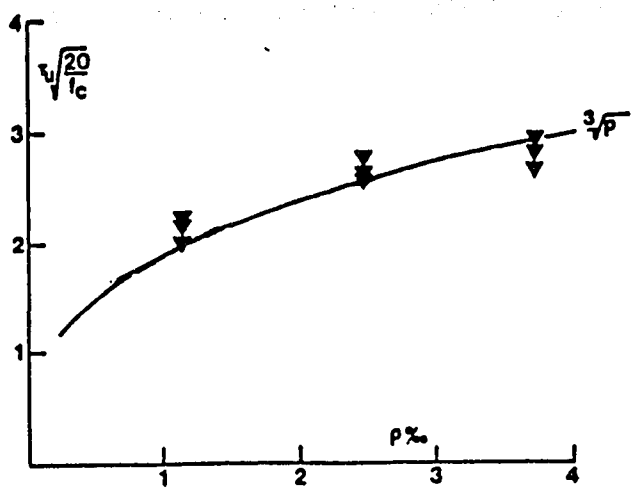

tests by Elstner and Hognestad

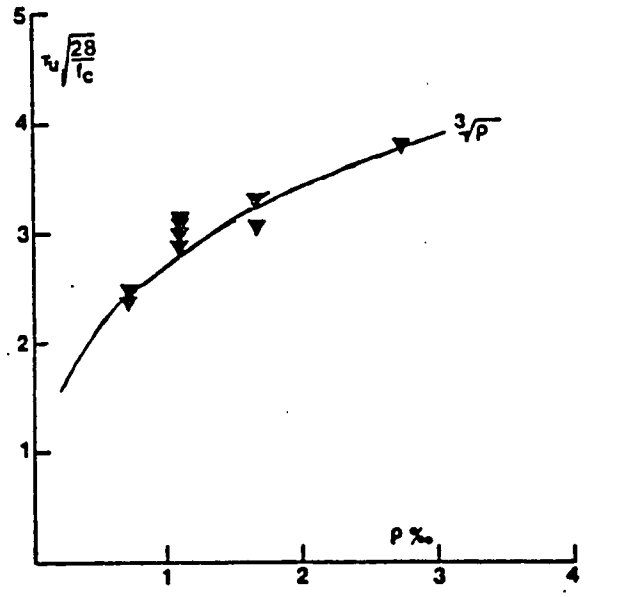

tests by Base

Figure 2.13 Influence of Reinforcement Ratio on Punching resistance (Regan and Braestrup 1985)

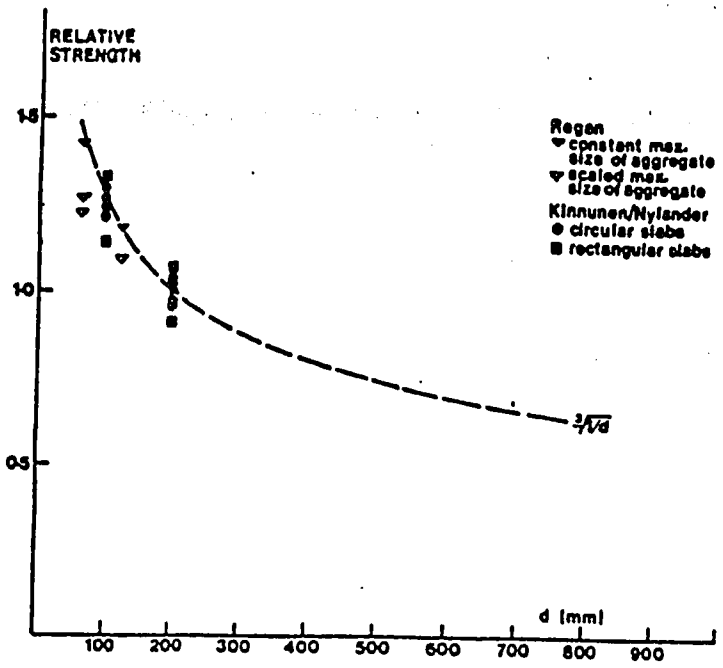

Figure 2.14 Influence of Slab Depth on Unit Punching Strength (Regan and Braestrup 1985)

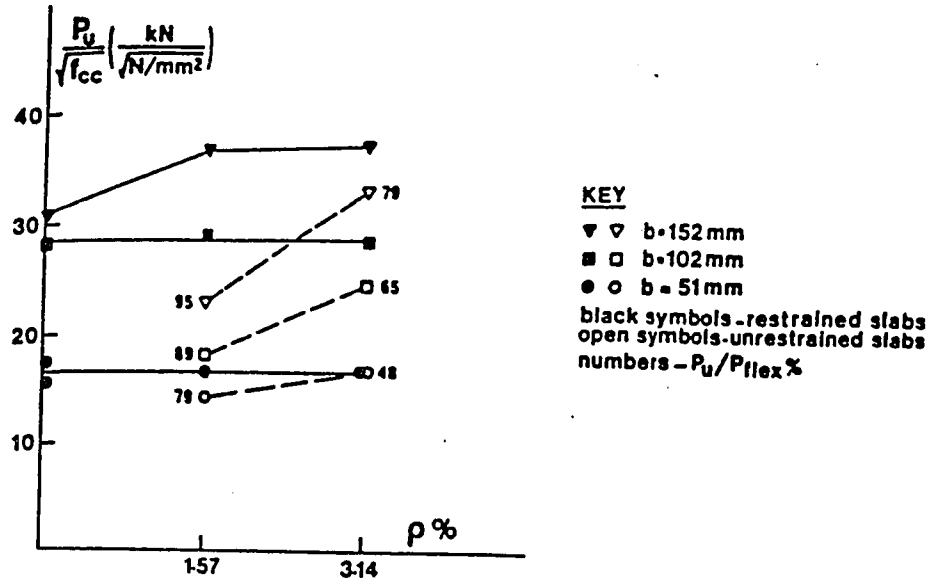

Figure 2.15 Influence of In Plane Restraint on Punching Resistance - tests by Taylor and Hayes (1965)

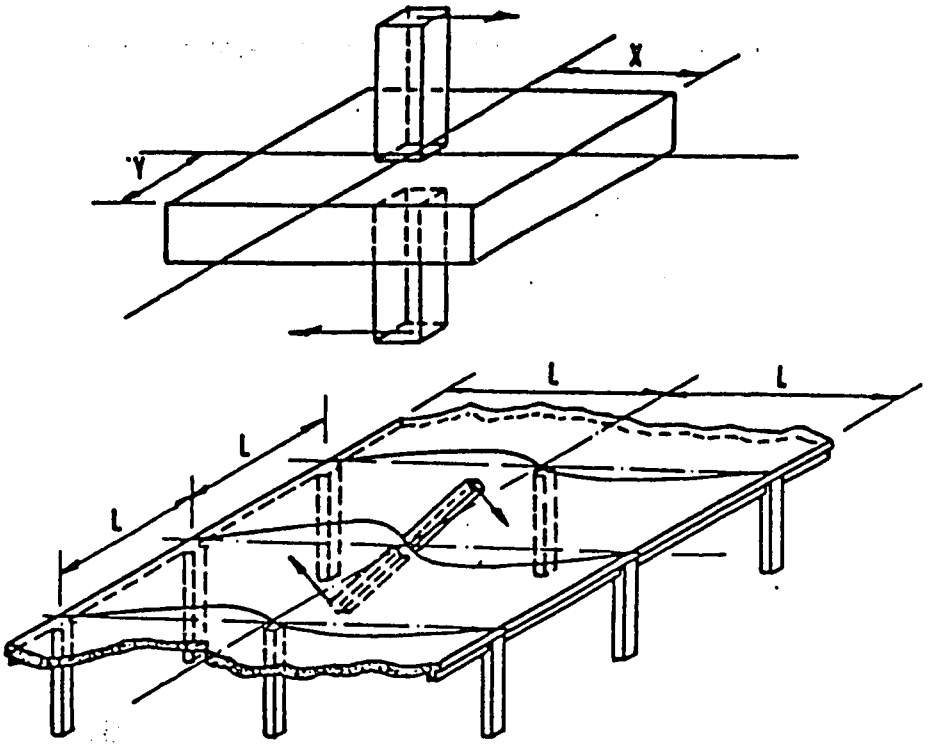

Figure 2.16 Structural Model Analyzed by Mast 1970

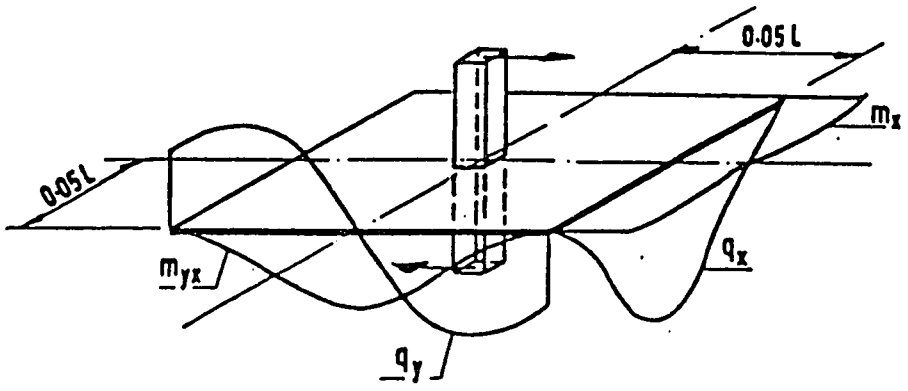

Figure 2.17 Example of Moment and Shear Distributions According to Mast 1970

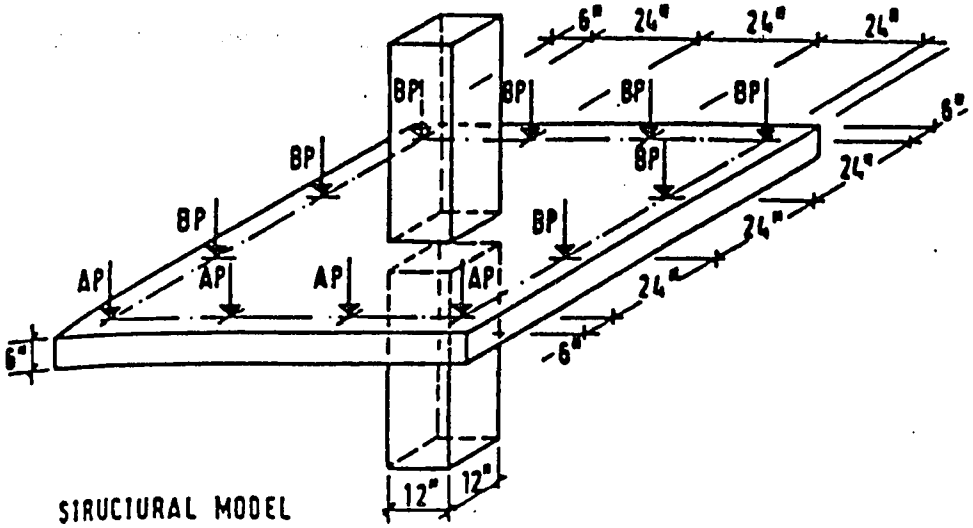

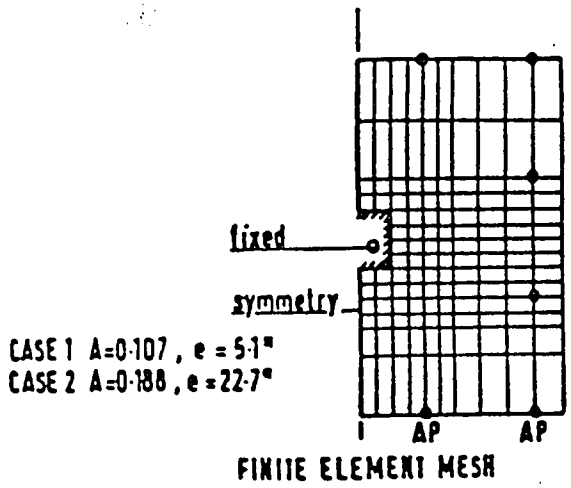

Figure 2.18 Yamazaki's (1975) Slab-column Specimens

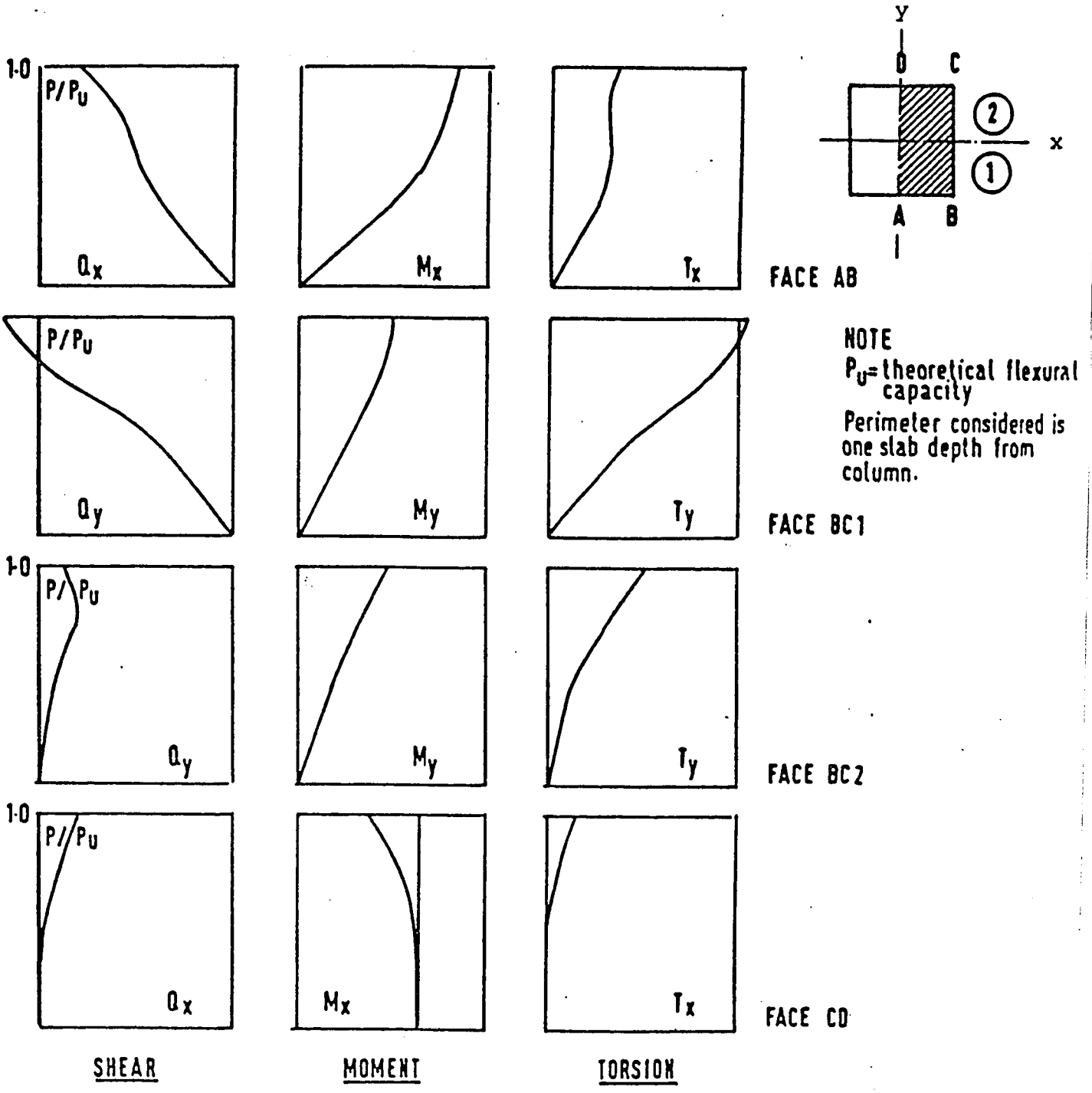

Figure 2.19 Yamazaki Shear Moments and Torsions Showing Inelastic Effects

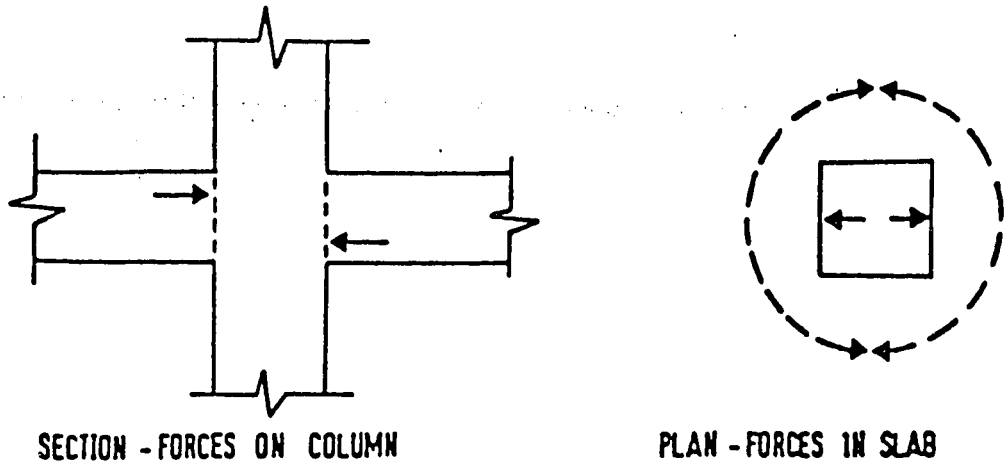

Figure 2.20 Transfer of Moment by Opposed Compressions

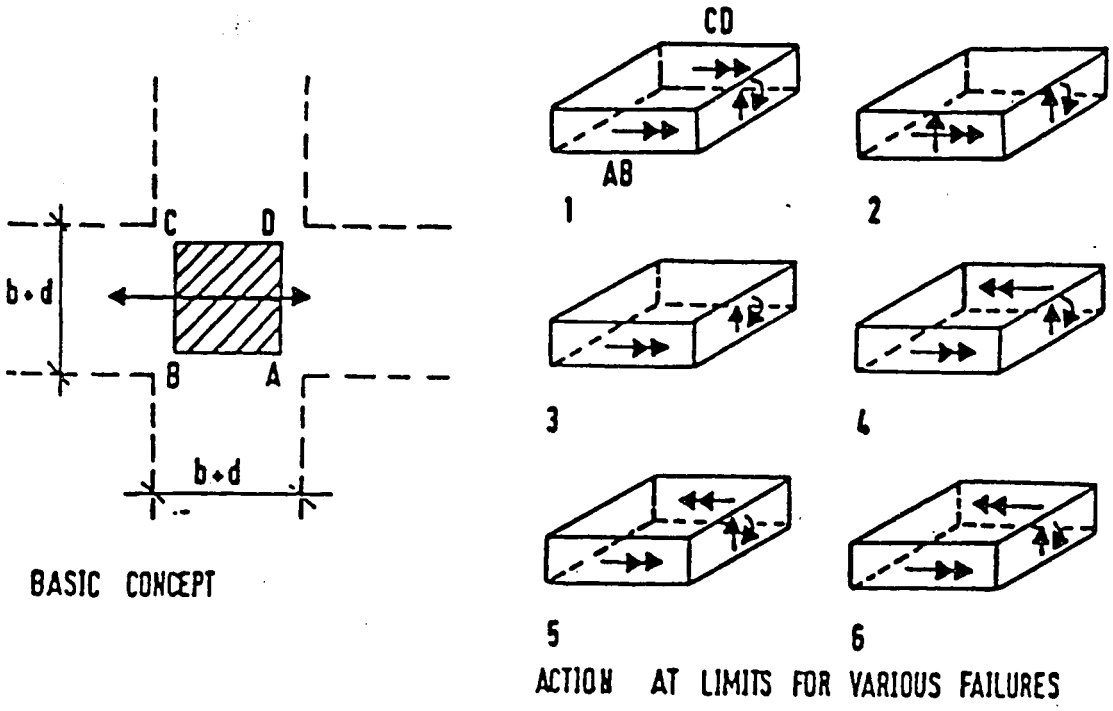

Figure 2.21 Beam Analogy for Interior Column-slab Connections

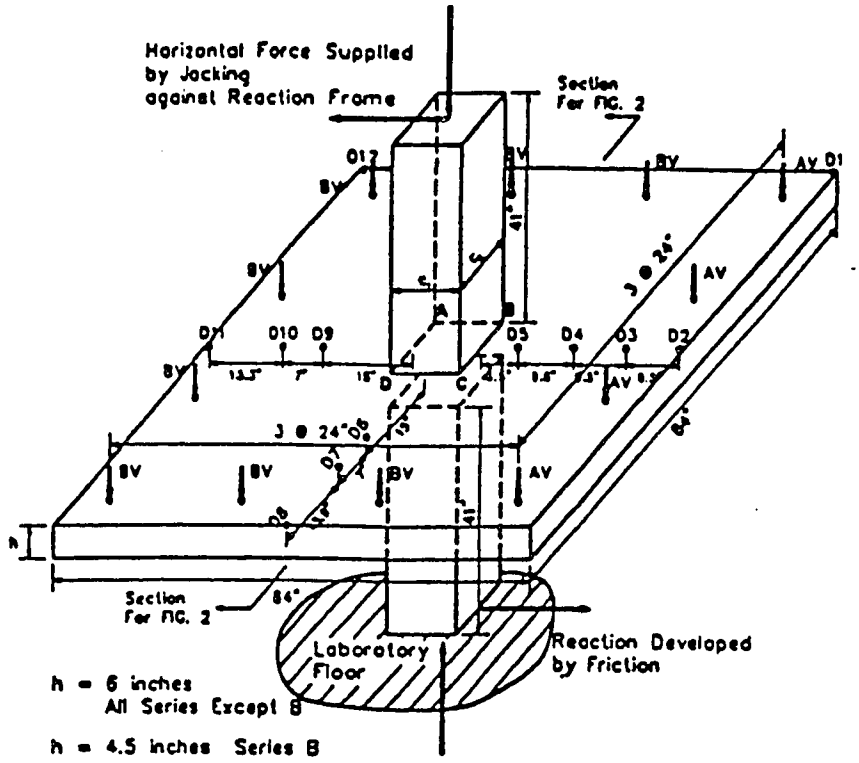

Figure 2.22 Dimensions and Loading Arrangement for Typical Specimen (Hawkins, Bao and Yamazaki 1990)

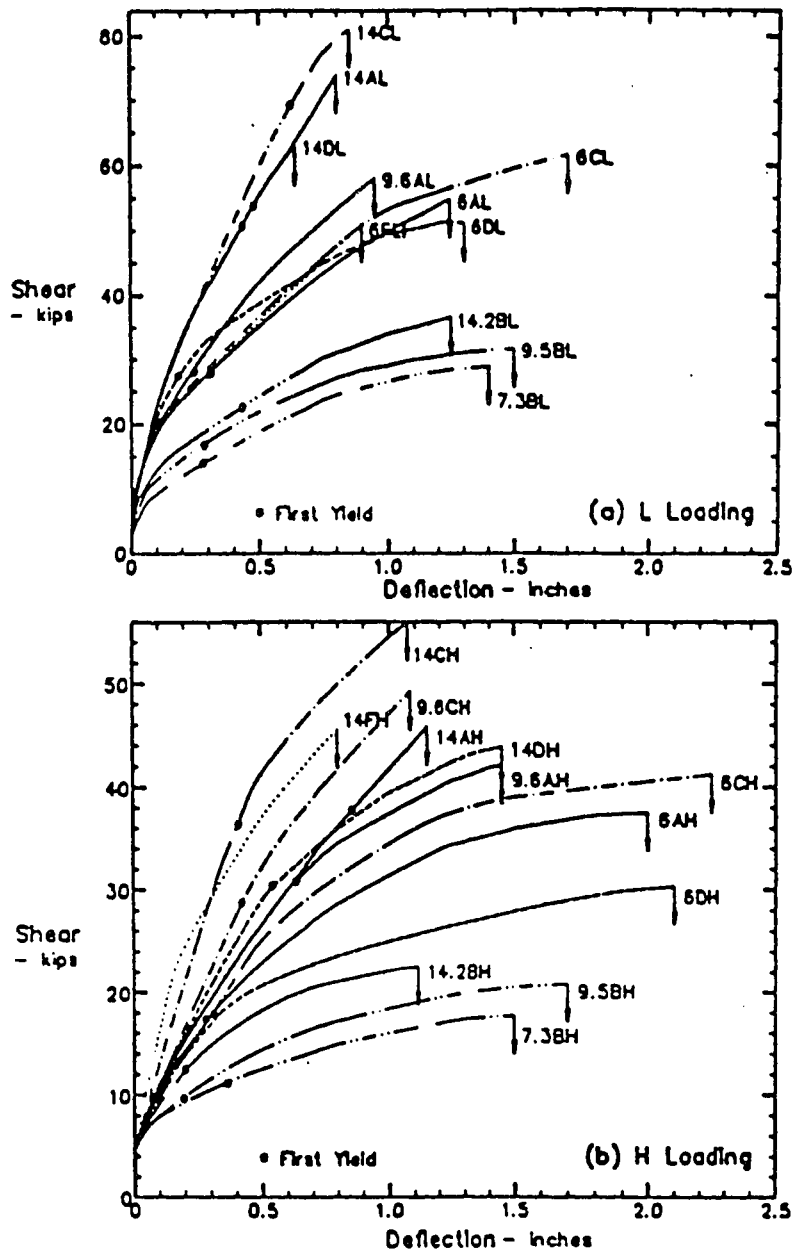

Figure 2.23 Shear-deflection, D2, Curves -series A,B,C and D (Hawkins, Bao and Yamazaki 1990)

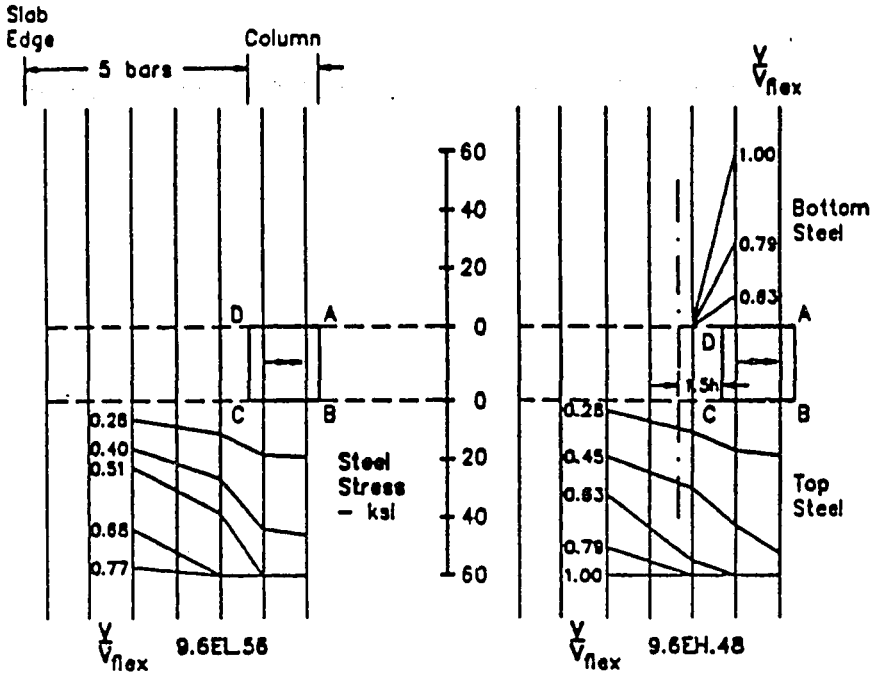

Figure 2.24 Distribution of Steel Strains
(Hawkins, Bao and Yamazaki 1990)

(a) Low moment transfer

(b) high moment transfer

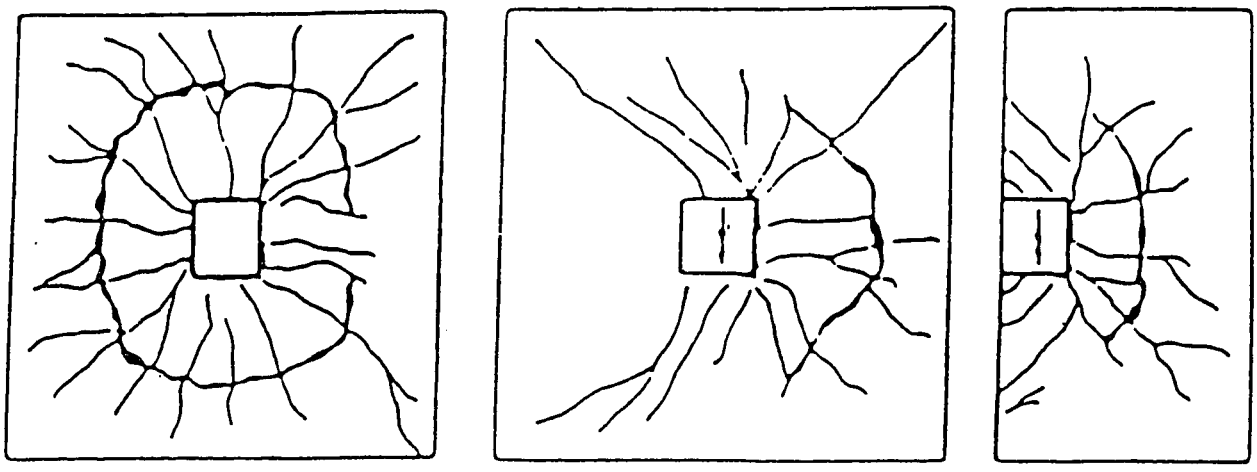

Figure 2.25 Typical Punching Failures:

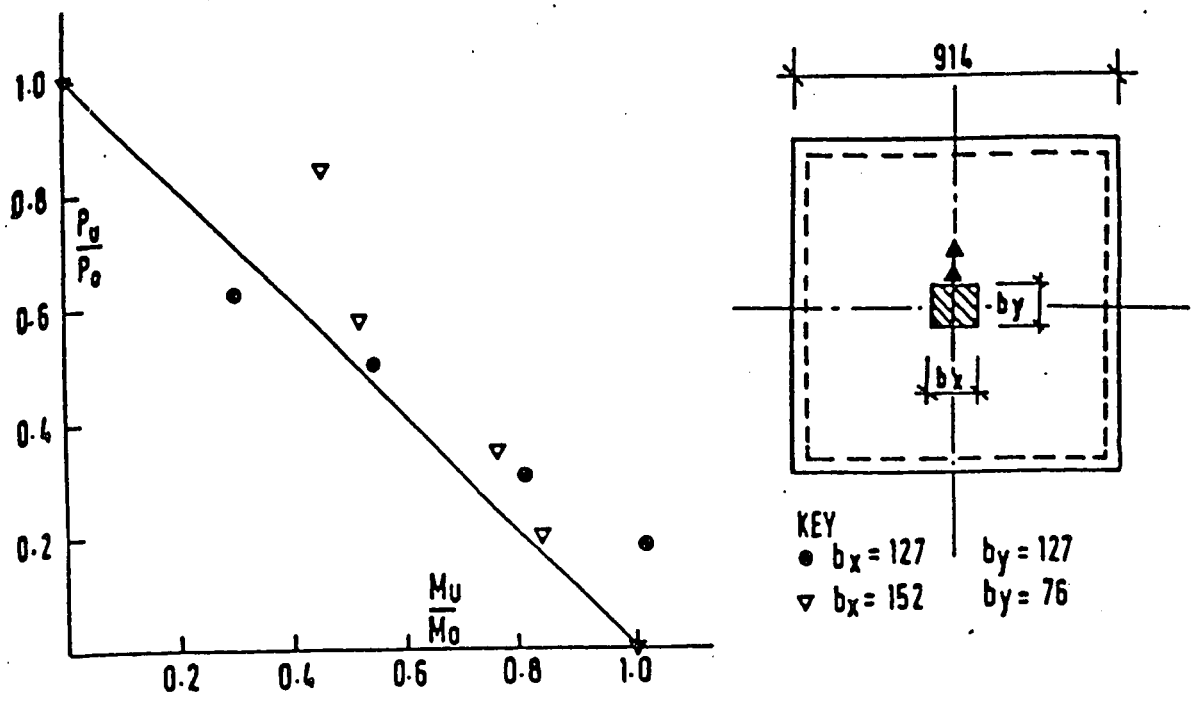

Figure 2.26 Moment-shear Interaction at Internal Columns
Results of Tests by stamenkovic & Chapman 1972

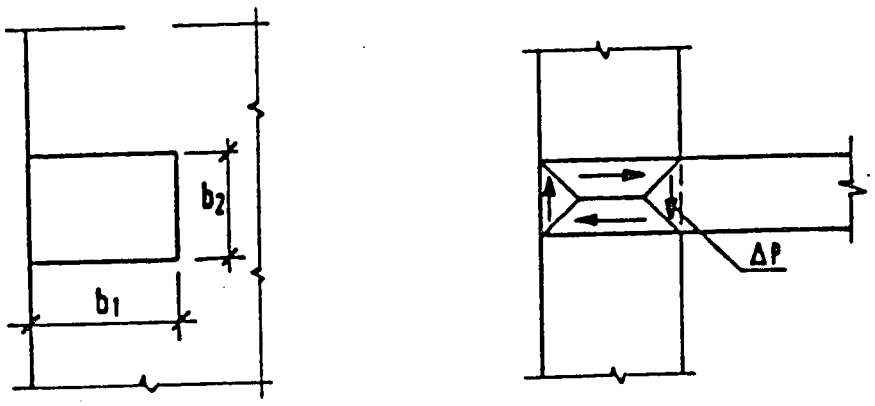

Figure 2.27 Torsion Producing Downward Shear at
Inner Part of Column Perimeter -by Andersson 1963

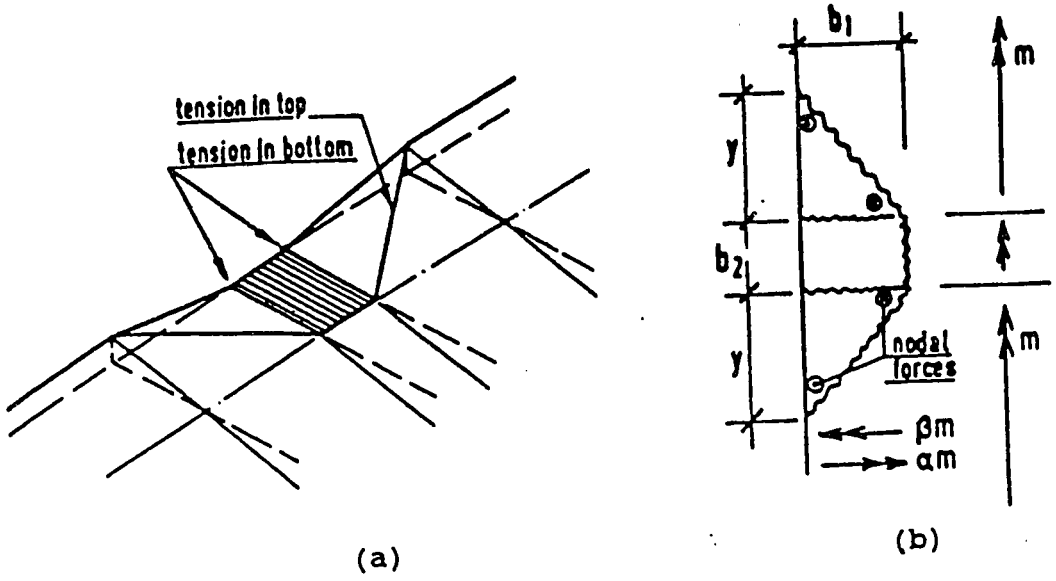

Figure 2.28 Local Yield Lines at An Edge Column

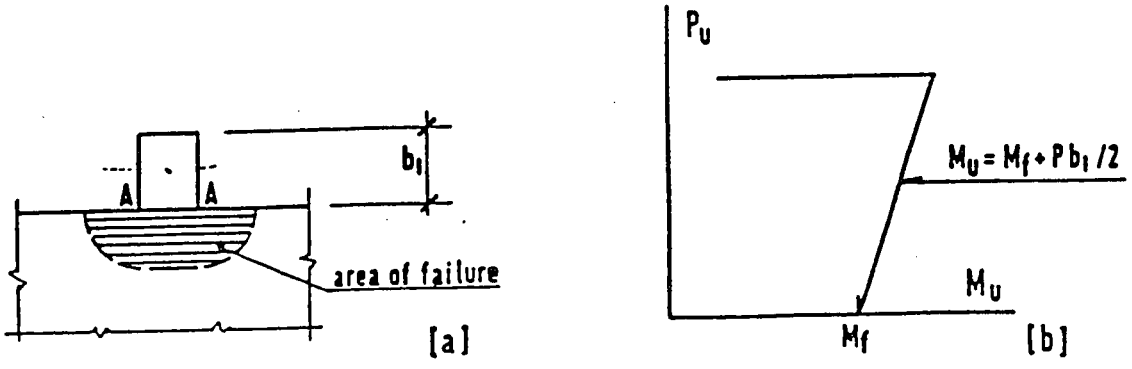

Figure 2.29 Column Connected to Slab at One Face Only
(Regan and Braestrup 1985)

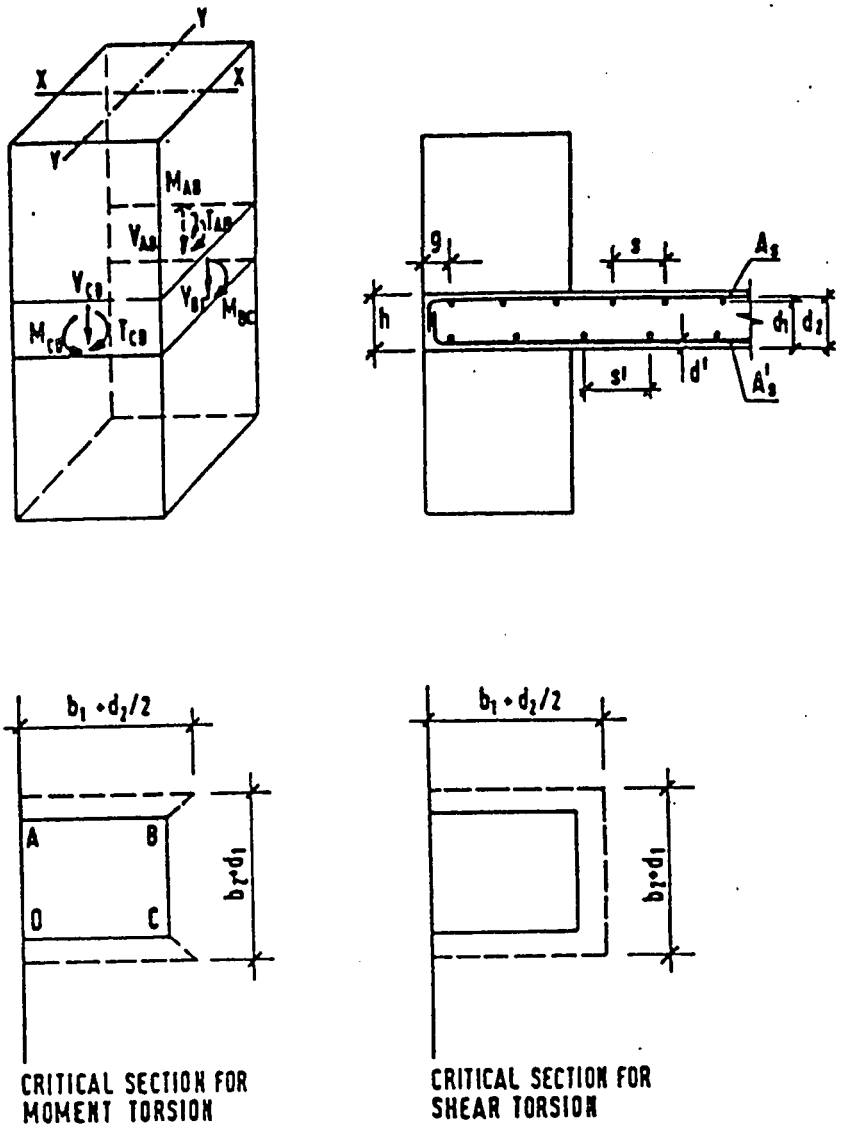

Figure 2.30 Beam Analogy for An Edge Column-slab Connection (Hawkins and Corley 1971)

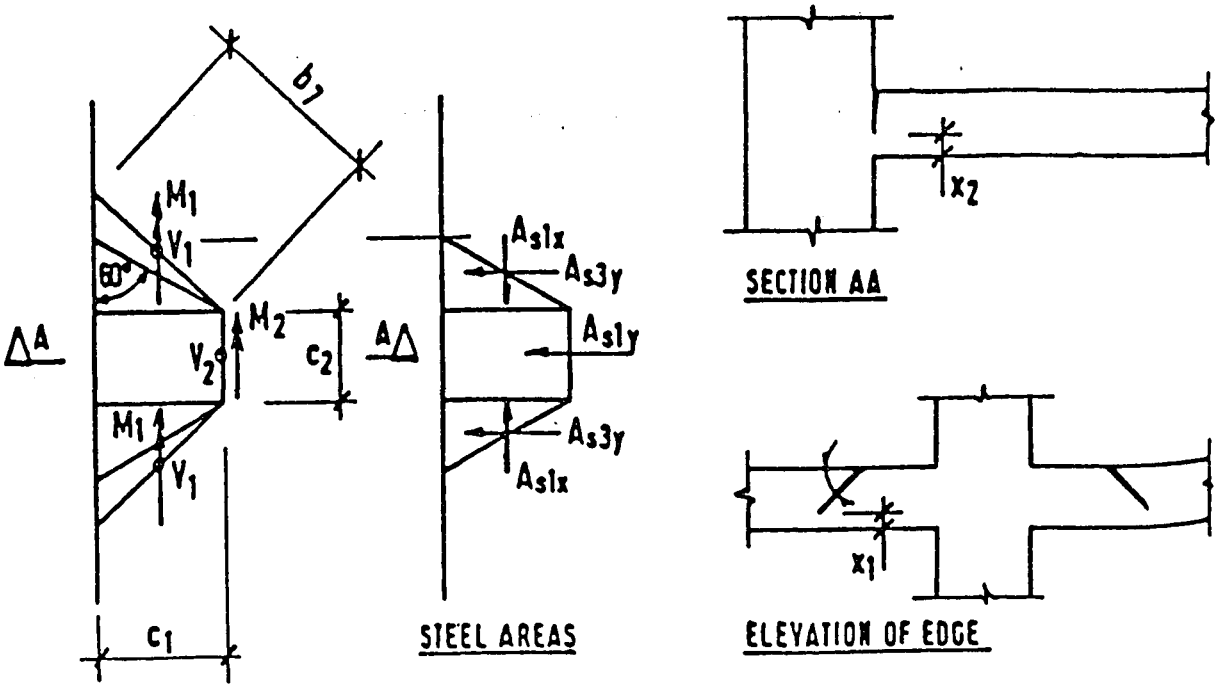

Figure 2.31 PÖllet's (1983) Theory
moment/Torsion Mode of Failure

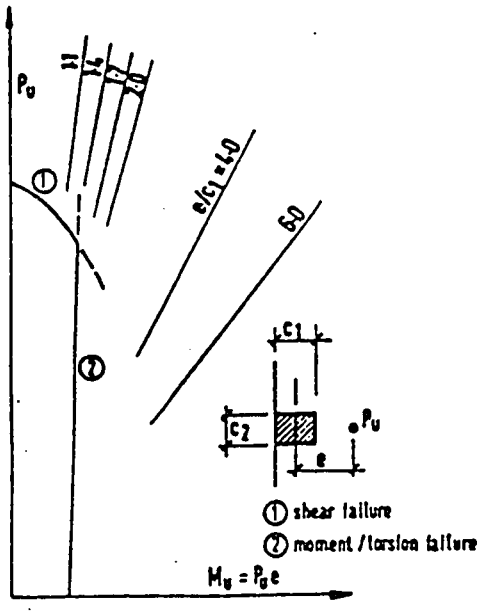

Figure 2.32 Typical Moment/Shear Interaction at An
Edge Column according to PÖllet 1983

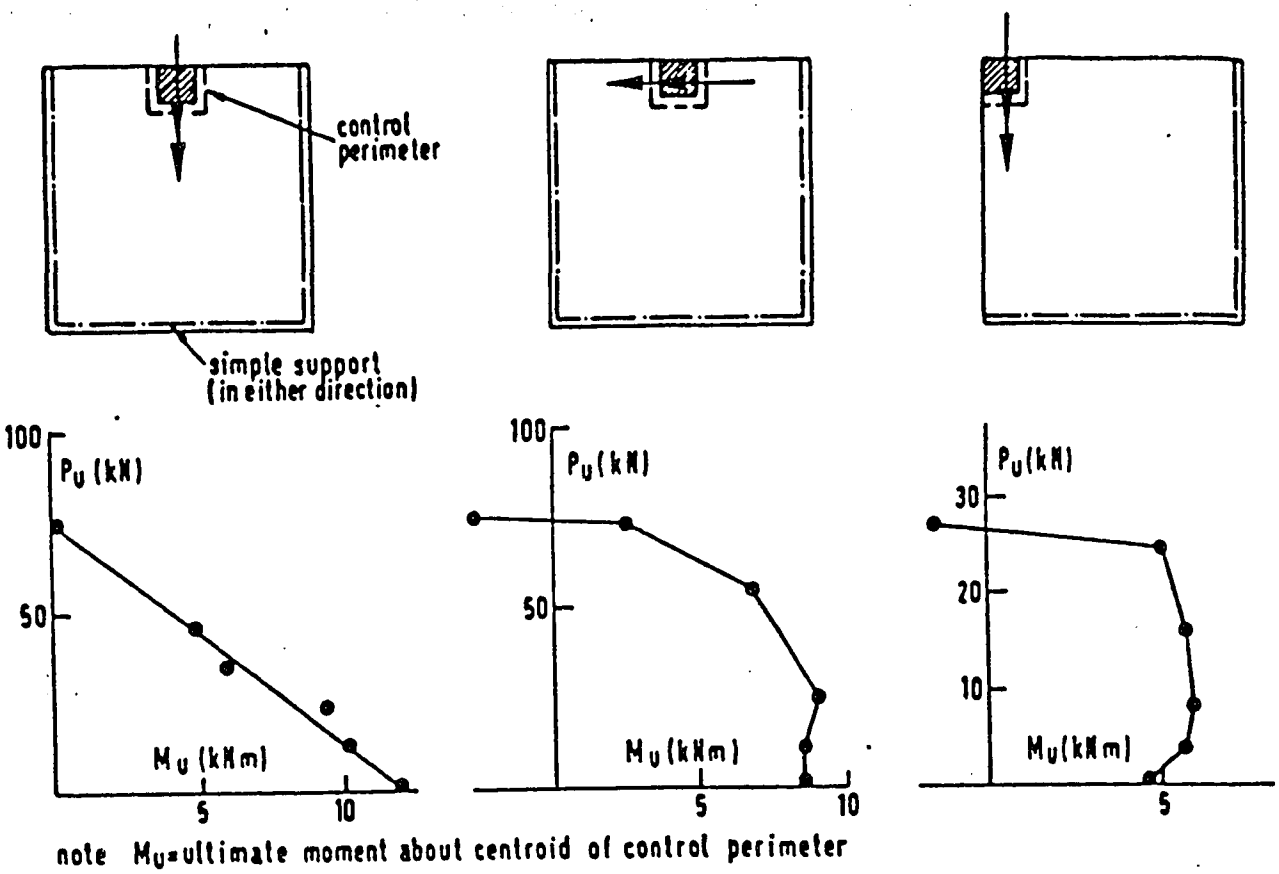

note M_U=ultimate moment about centroid of control perimeter

Figure 2.33 Results of Tests by Stamenkovic and Chapman 1972

CHAPTER 3

CODE RULES

3.1 Introduction

Punching is a subject on which there is no consensus at a theoretical level. However, many empirical procedures have been developed for the prediction of the ultimate punching resistant load of a slab-column connection. These procedures were based on assumptions which are reliable only over the limited range of data from which they were derived. However, most current codes use empirical equations for punching shear design because of their simplicity.

3.2 Control Surface Approach

The control surface approach should be regarded as a simple empirical method, which when intelligently applied gives strength predictions which are reasonably realistic and consistent. Consequently, it has been adopted by a large number of building codes.

In reality the punching load of a slab is influenced by, among other factors, the dimension b of the loaded area and the depth h of the slab, a dependence which is reflected by the various definitions of the critical perimeter. The nominal shear stress depends on the distance of the control surface from the column or loading area and is higher for perimeters closer to the loaded area. Suitable adjustments of the shear strength parameter mean that recommendations using very differently defined perimeters give

similar predictions of punching capacity for typical test specimen dimension (ie. $b/h \approx 2$). However, for more extreme geometric ratios, methods using perimeters far from the loaded area tend to be unsafe for small values of b/h, whereas perimeters close to the load become unsafe when b/h is large, provided that the shear strength parameter is not varied.

Regan (1981) tried to use a "true failure surface" approach to determine the nominal stress. The inclined surface area is as follows:

$$A_c = d\sqrt{1+\cot^2\theta}(\Sigma c + \pi d \cot\theta) \tag{3.1}$$

The nominal vertical stress at punching failure is defined as:

$$\sigma_{vu} = \frac{V_u}{A_c} \tag{3.2}$$

where V_u is the ultimate shear force acting across A_c, which is shown in Figure 3.1. The results are not necessarily better than that of current codes definition of "critical perimeter" though the equation is more complicated. In reality, the average angle θ varies widely and is difficult to determine.

The ACI 318 (American Concrete Institute 1989) and CSA(CAN3-A23.3-M90) (Canadian Standards Association 1990) codes are based mainly on Moe's (1961) work, while the BS 8110 (British Standard Institution 1985) code is based on Regan's work

(1974). The CEB-FIP Model Code for concrete structures was published by the Comité Euro-International du Béton (CEB) and the Federation International de la precontrainte (FIP) 1990. These current building code specifications for the strength of reinforced concrete slabs are based on the test results of slabs made with relatively low compressive strengths, varying mostly from 14 to 40 MPa.

The main differences involve the definition of the control surface and the corresponding choice of concrete strength parameter. The empirical interdependence of the two makes their individual definitions more or less arbitrary.

Code Rules for Critical Perimeter:

1. ACI 318-89

ACI Building Code Requirements define the nominal shear stress as $\tau = P/ud$, where the control perimeter u is defined as the shortest curve with a minimum distance $0.5d$ from the loaded area. Thus the control perimeter should have rounded corners, but for square or rectangular load or reaction areas, the Code states, the critical section may have four straight sides as indicated in Figure 3.2. The effective depth d of the slab may normally be taken as that to the mean plane of an orthogonal arrangement of tension reinforcement.

2. BS 8110-85

The British code of Practice defines the nominal shear stress as $\tau = P/ud$, where u is the perimeter of the smallest rectangle with a minimum distance $1.5d$ from the loaded

area. Thus the control perimeter is larger than for ACI-codes. The area of the control surface is the same whether the loaded area is a square or the inscribed circle. The effective depth d is the arithmetic mean corresponding to the layers of reinforcement as shown in Figure 3.2.

3. CEB-FIP 1990

CEB-FIP 1990 defines the nominal shear stress as $\tau = P/ud$, the control perimeter u is taken to be at a distance $2d$ from the column periphery and should be constructed so as to minimize its length, as shown in Figure 3.2. The effective depth d of the slab is assumed constant and may normally be taken as that to the mean plane of an orthogonal arrangement of tension reinforcement.

3.3 Code Equations for Nominal Shear Stress

Code of practice recommendations are written in terms of nominal shear stresses calculated with reference to slab depths and lengths of control perimeters and the results of theoretical analyses can often be expressed in similar terms. The definition of the control perimeter and that of any term allowing for a depth or size effect are then the empirical means of expressing the influences of all the overall geometric parameters.

The code rules differ considerably with respect to the definition of the control perimeter, the calculation of the nominal shear stress, and the choice of concrete strength parameter.

Safety factors have been removed from the following Code equations to give expressions for characteristic resistances, i.e., values which should be attained by 95% of test results. The uniform use of characteristic strengths does not in itself ensure a fair comparison between levels of safety actually achieved by different Codes as there can be differences between their partial safety factors for resistances (γ_m) and loads (γ_f) and between specified (characteristic) loads themselves.

For the following code equations, the notation used is as follows:

NOTATION

b	side dimension of square column or loaded area
Σb	length of periphery of column or loaded area
c	diameter of a circular column or loaded area (mm)
d	average effective depth of tension reinforcement
d_x , d_y	effective depths of tension reinforcement in the x and y directions
f_c'	cylinder crushing strength of concrete
f_{cu}'	cube crushing strength of concrete
f_y	yield or 0.2% proof stress of reinforcement
h	overall thickness of slab (mm)
P_u	shear strength (force) (N)
u	length of control perimeter (mm)
v_c	the nominal shear stress of the slab (MPa)

ρ	average ratio of reinforcement
ρ_x, ρ_y	ratios of reinforcement in the x and y directions

3.3.1 ACI 318-89

The nominal shear stress for nonprestressed slabs and footings *vc* shall be the smallest of:

$$v_c=0.083\times(2+4/\beta_c)\sqrt{f_c'} \tag{3.3}$$

$$v_c=0.083\times(\frac{\alpha_s d}{u}+2)\sqrt{f_c'} \tag{3.4}$$

$$v_c=0.083\times 4\sqrt{f_c'} \tag{3.5}$$

$$P_u=v_c u d \tag{3.6}$$

where $d = (d_x + d_y)/2$

$u = \Sigma b + \pi d$ (circular columns)

$u = \Sigma b + 4d$ (rectangular columns)

f_c' is the specified concrete cylinder strength, inserted in MPa.

β_c is the ratio of ,longer to shorter dimension of the loaded area. Thus the ratio $\beta_c > 2$ are penalized.

α_s is 40 for interior columns, 30 for edge columns, 20 for corner columns.

3.3.2 BS 8110-85

$$v_c=0.79(100\rho)^{1/3}(400/d)^{1/4} \tag{3.7}$$

$$P_u=v_u ud < 0.8\sqrt{f'_{cu}}u_0 d \tag{3.8}$$

where $u = 4\ (c + 3d)$ for circular loaded areas

$u = 4\ (b + 3d)$ for square loaded areas

$\rho = (\rho_x + \rho_y)/2$

ρ is calculated for a width equal to $(c + 3d)$ *or* $(b + 3d)$

$\rho \leq 0.03$

$400/d \geq 1$

For characteristic concrete strengths greater than 25 N/mm^2, v_c may be multiplied by $(f'_{cu}/25)^{1/3}$. The value of f'_{cu} should not be taken as greater than 40MPa.

3.3.3 CEB-FIP 1990

The concrete shear strength parameter is defined as

$$v_c=0.12\xi(100\rho f'_{ck})^{1/3} \tag{3.9}$$

$$P_u=v_c ud \tag{3.10}$$

where $u = \pi\ (c + 4d)$ for circular loaded areas

$u = 4b + 4\pi d$ for square loaded areas

$\xi = 1 + (200/d)^{1/2}$ with d in mm.

ρ = ratio of flexural tensile reinforcement extending for a distance equal to $3d$ beyond the section considered, except at end supports where the extension may be considered adequate.

3.3.4 Discussion

The main differences among the three Codes are described as follows:

• The **control perimeters** used by BS 8110-85 and CEB-FIP are larger than that of the ACI code. In BS 8110, the control perimeter has square corners whether the loaded area is square or circular, whereas CEB-FIP uses rounded corners in all cases. In the ACI code, the control perimeter is taken to have the same shape as the loaded area with rounded corners.

The use of a small distance for control perimeter, such as the half effective slab thickness adopted by the ACI code results in unconservative values for large loaded areas (Regan and Breastrup 1985). The 1990 version of CEB-FIP and the British code get consistent prediction by adopting a distance much larger than ACI code.

• ACI 318-89 code does not take account of **reinforcement ratio**, nor is there any reduction in effective control surface area for large punches. In BS 8110-85 the ratio of flexural reinforcement is calculated for a width of slab equal to that of the loaded area plus 1.5d each side. In the CEB-FIP Model Code, the reinforcement ratios are calculated over a width 3d distance from the loaded area, which is greater than that of BS 8110-85.

• The range of slab depth over which a **size effect** is considered on punching resistance in BS 8110 is 100 mm $\leq d \leq$ 400 mm, while the ACI Code ignores size effects.

• In BS 8110 the concrete strength is limited as $f'_{cu} \geq 25$ MPa, where f'_{cu} is characteristic concrete strength. The Code has no clear rules for concrete characteristic strength f'_{cu} less than 25 MPa.

3.3.5 Comparison with Test Results

a. Size Factor

Figure 3.3 shows the test results obtained by Regan (1986), as a graph of $[P_u/d^2 (40/f_{cu})^{1/3}]$ plotted against d, which shows the BS 8110 size factor $[\xi \propto (1/d)^{1/4}]$ and this agrees reasonably well with the test results and lies between the data for scaled and unscaled aggregate.

b. Concrete Strength

As it has been indicated in Chapter 2, the function $v_c \propto (f_{cc})^{1/3}$ or $v_c \propto (f_{cc})^{1/2}$ reasonably represents the trends of the test data (Figure 2.12b), which shows that ACI 318-89 using the function of $v_c \propto (f_{cc})^{1/2}$ and BS 8110-85 and CEB 1990 using the function of $v_c \propto (f_{cc})1/3$ to predict the punching shear strength of the reinforced slabs are equally reasonable.

Nevertheless, an experimental study designed to obtain data relating punching shear capacity to concrete cylinder strength with the aim of deriving an improved code equation for calculating early-age punching shear capacity was done by Gardner (1990).

Concrete strengths ranged from 14 to nearly 56 MPa and steel ratios ranged from 0.5 to 5 percent. The cube root relationship and shear perimeter approach of the British Standard for punching shear was adopted:

$$v_c = 0.99[(\rho f_c')^{1/3}](400/d)^{1/4} \qquad (3.11)$$

It was determined that Regan's method, and that of BS 8110-85, had significantly lower coefficients of variation than either ACI 318 or Bažant and Cao's method. The coefficient of variation was taken as the measure of goodness of the equations. The cube-root relationship between shear strength and concrete strength was stated to be preferable to the square-root relationship currently used by ACI 318-89.

The results of comparisons between computed and experimental strengths for sixty-eight slabs failing by punching from previous researches obtained by Regan and Breastrup (1985) are shown in Figures 3.4 and 3.5 where c is distance between sections of contraflexure on either side of the column and B is diameter of column. To allow a relatively uniform presentation of comparisons, the punching strengths calculated have been multiplied by factors λ to give average ratios of calculated and experimental strengths equal to unity, ie. $(P_{test}/\lambda P_{calc})_{mean} = 1.0$.

The values of λ are 1.46 and 1.00 for ACI and BS 8110, respectively.

The main interest here is in the scatter of the ratios $\lambda P_{calc}/P_{test}$ and in systematic trends to errors in treatments of individual variables.

With ACI 318-83 the range of $P_{test}/\lambda P_{calc}$ is again from about 0.7 up to 1.3. Figure 3.4a shows that the use of $v_c \propto (f_{cc})^{1/2}$ does not seem to cause any marked errors but the

lack of a size factor (Figure 3.4c) does mean that test/calculated ratios tend to be low for thicker and high for thinner slabs. The neglect of the influence of steel ratio ρ also introduces a systematic trend for the ratio of experimental to calculated strength to increase with increasing reinforcement. The treatment of column size in terms of a conforming perimeter *d/2* from the column face does not seem to cause any systematic error nor does the lack of any treatment of the span/depth ratio. Since there were no changes between the ACI 318-83 and ACI 318-89 recommendations for punching shear, the above comments are also apply to ACI 318-89.

For BS 8110 the range of $P_{test}/\lambda P_{calc}$ is reduced to 0.8 to 1.2. There appears to be no systematic error with respect to any of the parameters considered although unconservative errors may well be anticipated for $B/d < 1.0$, Where B is diameter of nominal diameter of column = $\sum b/\pi$ and d is the average depth of tension reinforcement.

CEB-FIP 1990 was revised from CEB-FIP 1978 based on Regan and Breastrup's (1985) work. The function of $v_c \propto (f_c')^{2/3}$ in CEB 1978 overestimated the influence of the compressive strengths of reinforced slabs and was revised to $v_c \propto (f\acute{c})^{1/3}$. The control perimeter was changed from distance of *d/2* to *2d* from loaded area. These changes make the CEB-FIP 1990 very similar to BS 8110.

c. Arrangement of Reinforcement

Figure 3.6 shows the results of 7 slabs tested by Regan (1986). Ultimate loads, corrected for variations of concrete strength and effective depth plotted against ratios of

flexural reinforcement determined for the widths specified in BS 8110. The strengths are also plotted against the reinforcement ratios averaged over the full widths of the slabs. It is apparent that concentration of reinforcement toward the loaded area has no significant beneficial effect in terms of punching resistance. The scatter of results is greater for BS 8110 where the steel ratio is calculated for more narrow width and less when the ratio is averaged over the full width, while ACI 318-89 should take the reinforcement ratio into account.

This conclusion is supported by the results of test by Elstner and Hognestad (1956), and Moe(1961). The available tests have all been of specimens representing the intersections of column strips in flat slabs. It is reasonable to assume that reinforcement very far from the column can have little influence on punching resistance and it would probably be appropriate to calculate steel ratio for column strips and not full column-to-column widths.

Lateral Restraint

The punching resistances of slabs can be enhanced when the boundary conditions are other than those of simple support. However, none of the three Codes discussed takes any account of lateral restraint or of boundary moments. All of them become increasingly conservative by certain amount.

Conclusion

For the calculation purpose, all codes assume shear stress is uniformly distributed over the slab depth and the critical perimeter. The function for the calculation of the ultimate nominal punching stress depends on parameters that differ from one code equation to another. Test results showed that certain parameters, such as the compression strength of concrete, the geometry of a slab column connection and sometimes the flexural reinforcement, have an effect on the punching shear resistance. Based on theoretical considerations that essentially support the equilibrium condition in the vertical direction (for example $\sum V = 0$) and observations made during tests, empirical formulas have been derived. The results obtained were adjusted to those of tests by statistical methods. This way of proceeding has the advantage of being simple and gives the numerical values that corresponds very well to those measured during the tests. This procedure does not contribute to the understanding of the punching shear phenomenon and can lead to a wrong interpretation of the behaviour of a slab-column connection.

3.4 Transfer of Moment in Slab-column Connections

Most connections in flat slab structures must be designed to transfer moment as well as shear. When a flat slab structure resists lateral forces, every connection transfers moment. For gravity loadings only, there is always moment at edge and corner columns, and there can be moment transfer at interior columns due to unequal lengths for adjacent spans, pattern loadings,

3.4.1 ACI Code Rules:

When gravity load, wind, earthquake, or other lateral forces cause a transfer of moment M_u between a slab and column, a fraction of the unbalanced moment $\gamma_f M_u$ shall be transferred by flexure. The code requires that the fraction be transferred by flexure within an effective slab width between lines that are one and one-half slab thicknesses outside opposite faces of the column or loaded area. The fraction of unbalanced moment $\gamma_v M_u$ not transferred by flexure shall be transferred by eccentricity of shear, which is assumed to vary linearly about the centroid of the critical sections.

A fraction of the unbalanced moment is given by:

$$\gamma_{vx} = 1 - \frac{1}{1 + (2/3)\sqrt{b_1/b_2}} \tag{3.12}$$

where b_1 and b_2 are the sides of the control perimeter of a rectangular column, with the side b_1 being parallel to the moment vector.

The shear stress v_u can be calculated from:

$$v_u = \frac{V_u}{A_c} + \frac{\gamma_{vx} M_{ux}}{J_{cx}} y \tag{3.13}$$

V_u and M_{ux} are factored shear force and moment determined at a centroidal axis x of the critical section; A_c is the concrete area of assumed critical section; In this equation, it is assumed that moment exists only about centroidal axis x, and y is the coordinate of any point on the critical section. The symbol J_{cx} used in Equation 3.11 is

a property of the assumed critical section; analogous to the polar moment of inertia. The commentary implies that the same equation can be used for edge and corner columns.

The stress distribution is assumed as illustrated in Figure 3.7 for an interior or exterior column.

The factored shear force V_u and unbalanced moment M_u are determined at the centroidal axis c-c of the critical section (Figure 3.7). For J_{cx} at an interior column:

$$J_{cx}=\frac{d(c_1+d)^3}{6}+\frac{(c_1+d)d^3}{6}+\frac{d(c_2+d)(c_1+d)^2}{2} \qquad (3.14)$$

Similar equations may be developed for A_c and J_{cx} for columns located at the edge or corner of a slab.

For square or circular columns 60 percent of the moment should be considered transferred by flexure across the perimeter of the critical section, and 40 percent by eccentricity of the shear about the centroid of the critical section. For rectangular columns, it is assumed that the portion of the moment transferred by shear decreases as the width of the face of the critical section

resisting the moment increases.

If a supporting member does not have a rectangular cross section, it is to be treated as a square support having the same area as illustrated in Figure 3.8.

The Code requires that concentration of reinforcement over the column by closer spacing or additional reinforcement shall be used to resist moment on the effective slab width.

3.4.2 BS 8110-85 Code Rules

The equations for moment transfer in slab-column connection in BS 8110-85 are simpler than those in ACI 318-89. For slab interior column connections, the maximum design shear stress is expressed as follows:

$$v_{max}=\frac{P}{ud}[1+\frac{1.5e}{x}] \tag{3.15}$$

where x is the length of the perimeter considered parallel to the axis of bending; For interior column it is $(b_x + 3d)$.

$e = M_t / V_{avag}$

M_t is the design moment transmitted from the slab to the column at the connection.

V_{avag} is the design shear at the connection

At corner column and at edge columns where bending about an axis parallel to the free edge is being considered, the shear stress is calculated from:

$$v_{max}=1.25\frac{P}{ud} \tag{3.16}$$

For edge columns where bending about an axis perpendicular to the edge is being considered, the shear stress should be calculated as follows:

$$v_{max}=\frac{P}{ud}(1.25+\frac{1.5e}{x}) \qquad (3.17)$$

Alternatively, v_{max} may be taken as $1.4\ P/ud$ for approximately equal spans. According to the Code v_{max} should not exceed $0.8\sqrt{f'_{cu}}$.

3.4.3 CEB-FIP 1990 Code Rules

If the dispersion of the force is non-symmetrical due to the transfer of an unbalanced moment M_{sd} from the slab to a column the maximum shear at the control perimeter may be calculated as :

$$v_{sd}=\frac{P_{sd}}{ud}+\frac{0.6M_{sd}}{wd} \qquad (3.18)$$

where w is a property of the control perimeter $w = \int e\ dl$ shown in Figure 3.9. For a rectangular column:

$$w=[\frac{c_1^2}{2}+c_1c_2+4c_2d+16d^2+2\pi dc_1] \qquad (3.19)$$

where c_1 is the column dimension parallel to the eccentricity of the load.

c_2 is the column dimension perpendicular to the eccentricity of the load.

dl is an elementary length of the perimeter.

e is the distance dl from the axis about which the moment M_{sd} acts, and

the subscript l refers to perimeter u_l.

For edge column connections, the distribution of shear around the perimeter in Figure 3.10a should be determined to calculate v_{sd}. However, provided that the eccentricity of loading in the direction perpendicular to the slab edge is in the direction of the interior of the slab and there is no eccentricity parallel to the edge. v_{sd} may be calculated on the assumption of uniform shear on the perimeter u_l^* shown on Figure 3.10b.

Where a moment M_{sd} acting in the direction parallel to the slab-edge is transferred to the column, It should be taken to produce an additional shear stress equal to $0.6\, M_{sd}/W_d$ where W is calculated for the perimeter u from Figure 3.9.

For slab-corner column connections, the distribution of shear around the perimeter in Figure 3.11a should be used to calculate v_{sd}.

However, if the eccentricity of loading is towards the interior of the slab, v_{sd} may be calculated on the assumption of uniform shear on the perimeter u_l. shown on Figure 3.11b.

3.4.4 Discussion

According to Hawkins, Cao and Yamazaki(1990), the ACI 318-89 provisions for determining the strength of slab-interior column connections transferring moment are reasonable for design purposes. The provisions give conservative results when the slab flexural reinforcement ratio within lines that are 1.5 slab thicknesses either side of the column exceed 0.7 percent. The conservatism of the provisions increases as the reinforcement ratio increases. However, the warning of impending failure decreases. ACI

318-83 provisions are nonconservative for reinforcement values less than 0.7 percent. However, the flexural capacity of the reinforcement in the column region then controls and significant deformations occur before any punching failure.

Their research results show that the test-to-calculated ratios increase with increasing ρ value. For low ρ values especially, the ACI procedure is likely to severely underestimate the flexibility of the connection.

In the CEB-FIP and ACI the effects of eccentricities in two directions are taken to be additive but in the British draft it is stated that the equation "should be applied independently for the moments and shears about both axes of the column and the design checked for the worst case".

The British view may be reasonable if the moments arise solely from pattern loading of a slab with uniformly spaced columns. In more general cases it can not be justified rationally. On the other hand the direct addition of e_x and e_y would seem overconservative in terms of a linear distribution approach. In such a method the maximum shears from the two moments coincide only at the corners of rectangular control perimeters which are themselves artificial. With more realistic rounded corners, as in the CEB code, the locations of the two maximums are different. However it is difficult, if not impossible, to assess the effects of bi-axial eccentricity on a purely theoretical basis.

Tests of simply supported slabs with restraint against vertical movement in either direction and for a range of load eccentricities, including pure moment loading, have been reported by Stamenkovic and Chapman (1972) as mentioned before, The results are

shown in Figure 2.27 as a graph of P/P_0 plotted against M/M_0. Although there is some scatter in the data the results can be seen as reasonable support for the linear interaction predicted from the simplified methods of codes.

In the CEB/FIP Model Code (1990) edge and corner column connections are treated by the same expression as used for interior connections subjected to eccentric loads. The eccentricities e are measured from the centroid of the control perimeter. For columns near, but not at, slab edges the Model Code defines critical perimeters as shown in Figure 3.12a.

The ACI code does not distinguish between interior and exterior columns. Thus in principle the maximum shear stress is calculated as:

$$v_{max} = \frac{p}{ud} + \frac{\gamma_{v1} P e_1}{J_1} + \frac{\gamma_{v2} P e_2}{J_2} \qquad (3.20)$$

Where the eccentricities e_1 and e_2 are measured from axes through the centroid of the control perimeter.

γ_{v1} and γ_{v2} the proportions of the applied moments that are assumed to be resisted by shear are apparently calculated by the same expression as for internal columns although it might be more reasonable to replace $(b_1 + d)$ by $(b_1 + d/2)$ where the latter is the overall dimension of the control surface and J_1 and J_2 are calculated for the surfaces shown in Figure 3.13.

The research work conducted by Ghali and Elgabry (1990) shows that the co-efficient used by ACI 318-89 agrees with test results for interior and edge column connections, but needs to be modified for corner column connections and connections with holes.

In the British Code, corner column connections and edge connections subjected to moments perpendicular to the slab edge are treated by a single expression independent of the eccentricity of the load:

$v_{max} = 1.25\ v_{avg} = 1.25\ P/ud$

As Regan (1985) pointed out, in ordinary cases the effects of moments at edge columns need not be analyzed precisely provided the shear stress V/ud is increased by 40% before being compared with the permissible limit. This approach is similar to the British Code where the percentage increase is only 25%.

The work by Stamenkovic and Chapman (1970) included series of tests of models with edge and corner columns attached to slabs simply supported as in Figure 2.33. Edge column specimens were tested with moments parallel and perpendicular to the free edges. Corner column specimens were tested with moments parallel to one free edge. The results are shown in Figure 2.33 as ultimate moment-shear interaction diagrams. The moments are related to the centroid of the ACI control perimeters indicated.

For edge columns, moments parallel to the free edge can be seen to produce a linear interaction similar to that for an interior column. For the other two cases the interactions are clearly different. Test arrangements of this type do not permit realistic redistribution of moments.

In a real structure the attainment of a limiting flexural condition at an exterior column is not in itself a cause of failure as moments can be redistributed into the adjacent span. The moment at the exterior column then increases due only to eccentric shear and failure occurs either overall as a bending failure or locally as a shear failure at the column. Tests of models permitting redistributions of moments have been reported by Cleland, Franklin and Long (1982), Kinnunen (1971), Regan (1981), Zakaria (1978), Zaghlool, De Paiva and Glockner (1970), Ingvarsson (1977) , Regan (1981) and Walker (1980).

The analysis of data from failures at exterior columns is considerably more difficult than that for interior columns, principally because of the greater influence of flexural effects and of the design and detailing of the flexural reinforcement. Even for corner columns, where there is general agreement on the critical yield line patterns, it can be difficult to calculate the moments at the negative yield lines because of uncertainty about the anchorages of reinforcement crossing them. It can also be difficult to define ratios of reinforcement to be used in equations for punching strengths.

Figure 3.14 from Regan and Braestrup (1985) shows the test data [Zaghlool, de Paive and Glockner (1970), Ingvarsson (1977) and Walker (1980)] compared with the British Code with P_u/P_{calc} plotted against P_u/P_{yl}, where P_{yl} is the overall yield line capacity. It seems that the British Code almost ignoring eccentricity is reasonable. However, the British Code overestimates punching strengths in a number of instances. In fact, even for internal columns the Code expression for "characteristic resistance" in fact predicts mean strengths (Regan and Braestrup 1985). Thus the existence of

experimental strengths lower than predicted ones is not, of itself, too surprising, but what may cause some concern is the apparently systematic trend for the ratios of experimental to calculated resistances to decrease with increasing eccentricity.

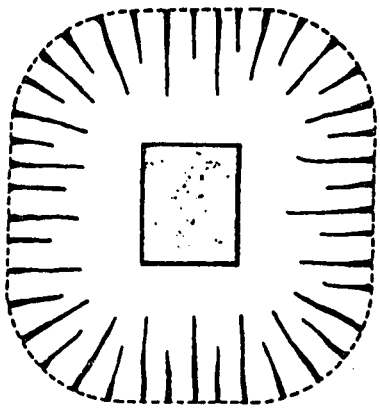

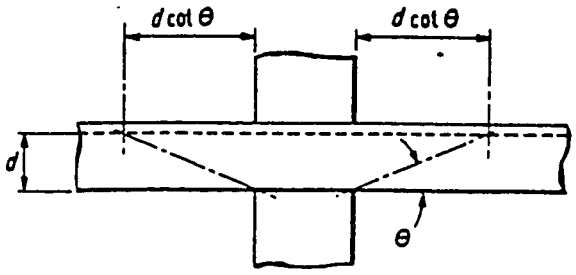

$$A_c = d\sqrt{1+\cot^2\theta}\left[\Sigma c + \pi d \cot\theta\right]$$

$$A_c = 2{\cdot}69d\left[\Sigma c + 7{\cdot}85d\right] \text{ for } \cot\theta = 2{\cdot}5$$

Figure 3.1 Fracture Surface Used in Calculation of Punching Resistance (Regan 1981)

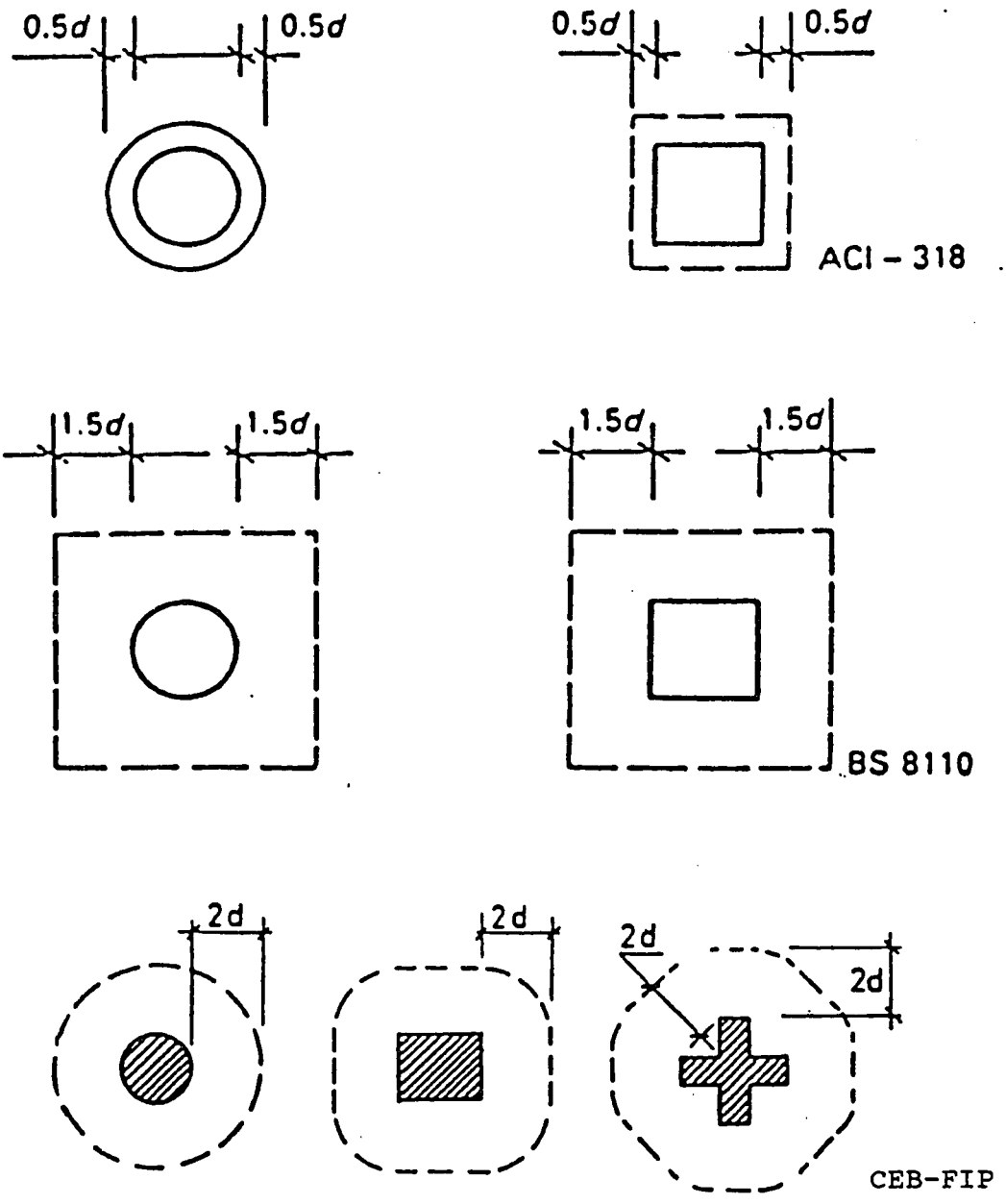

Figure 3.2 Control Perimeters at Interior Columns

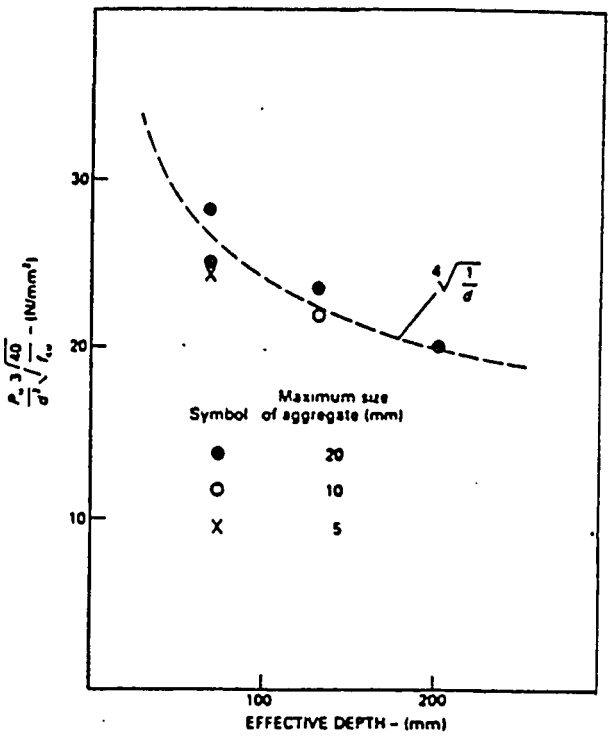

Figure 3.3 Influence of Effective Depth on Unit Resistance (Regan 1986)

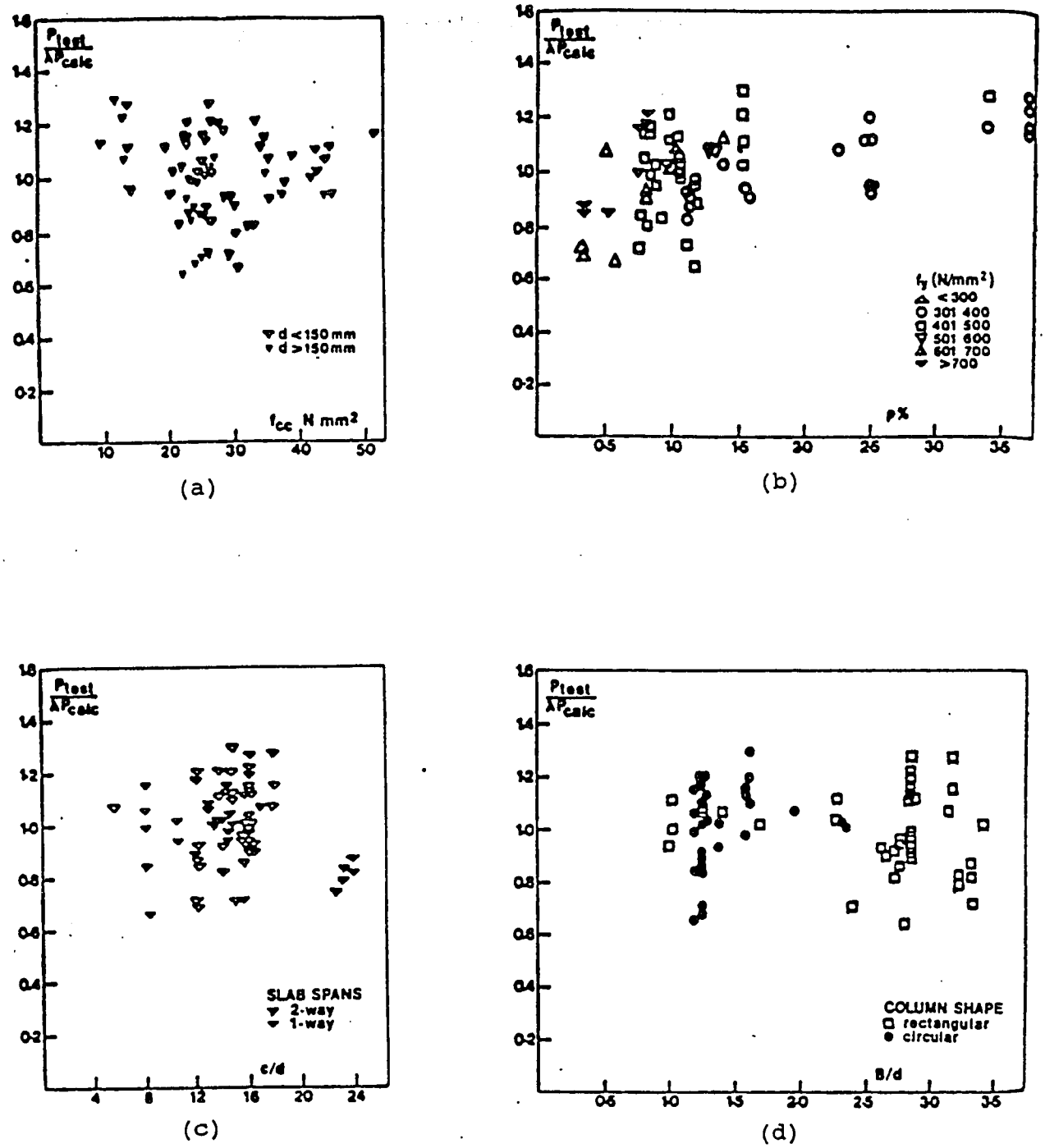

Figure 3.4 Comparison of Test Results with ACI 318-83 (Regan and Braestrup 1985)

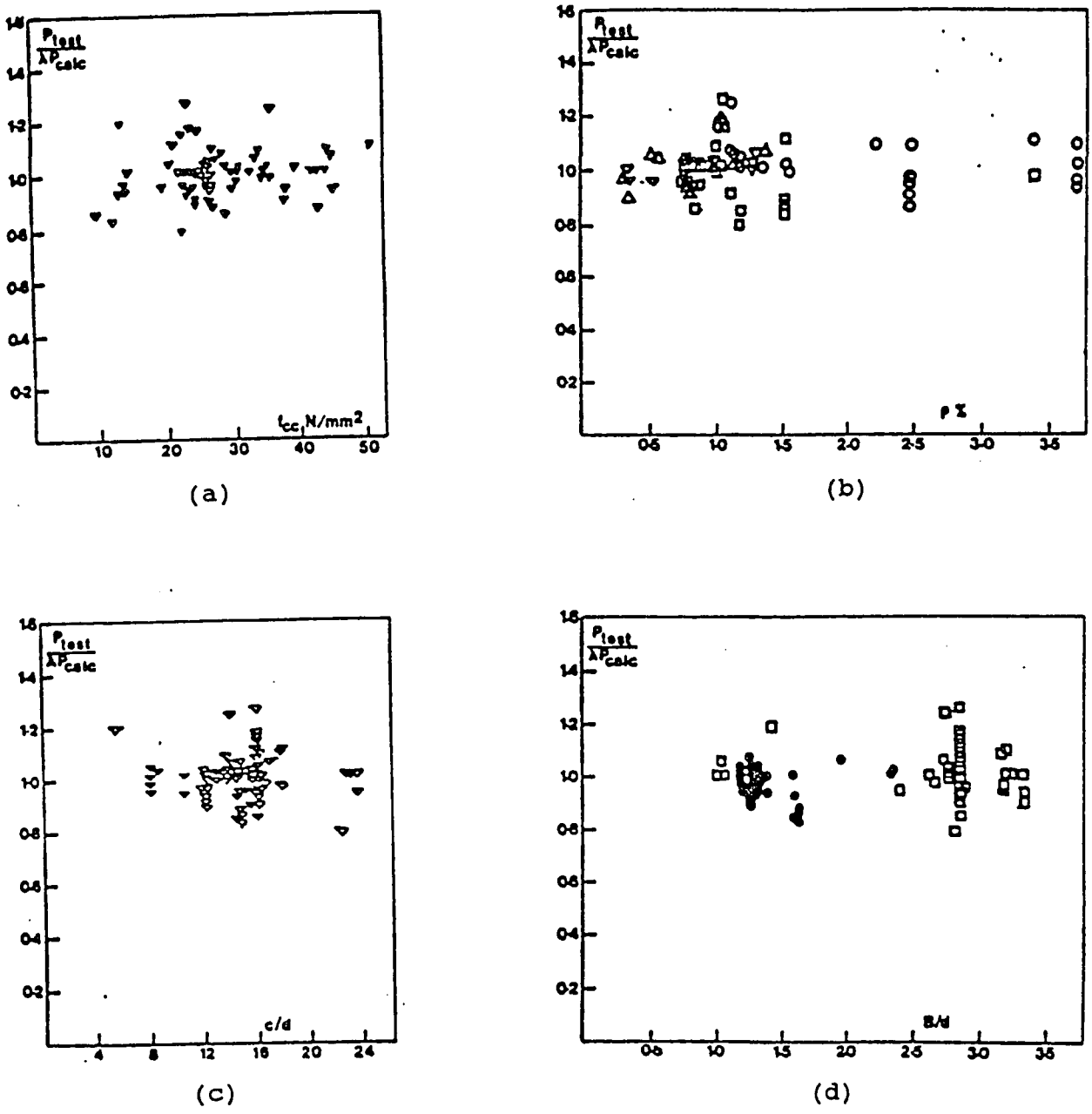

Figure 3.5 Comparison of Test Results with BS 8110-85 (Regan and Braestrup 1985)

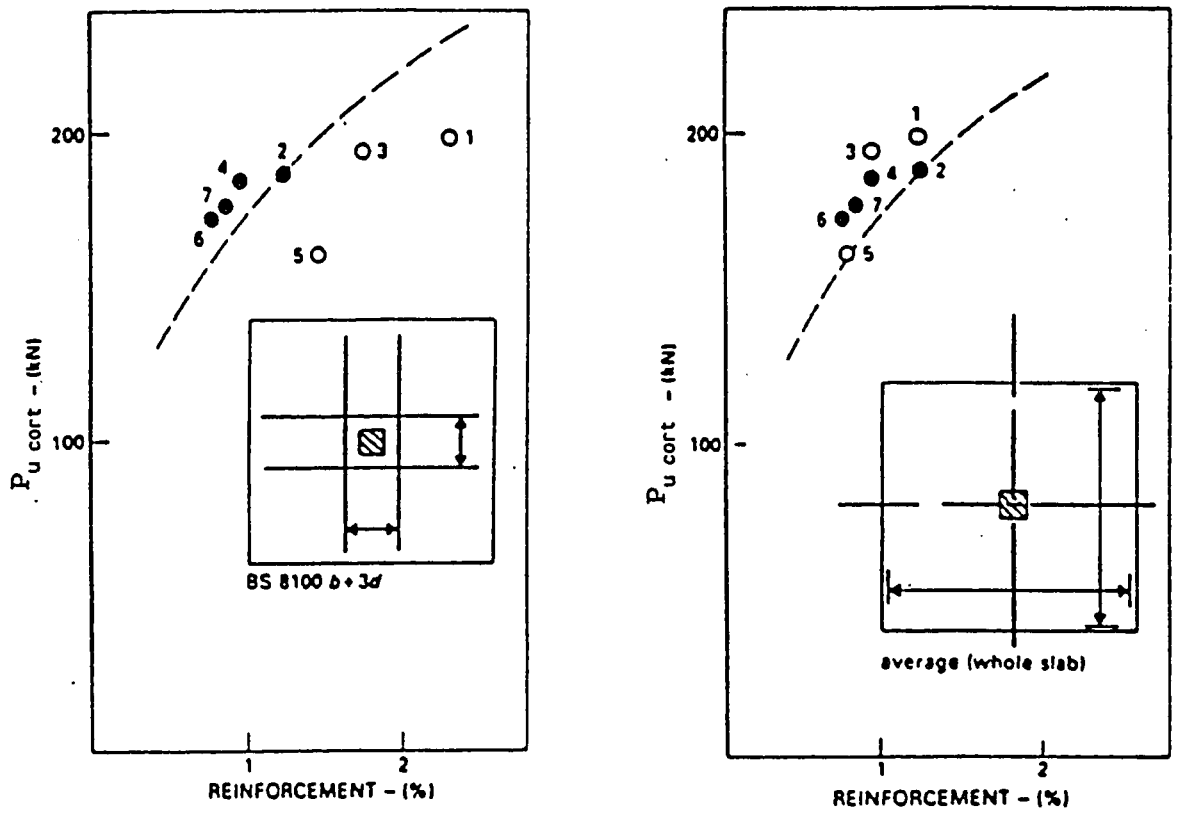

$$P_{u\ corr} = 3\sqrt{\frac{35}{f_{cu}}}\sqrt[4]{\frac{77}{d}}$$

Figure 3.6 Relationship of Punching Strength to Ratios of Reinforcement (Regan 1986)

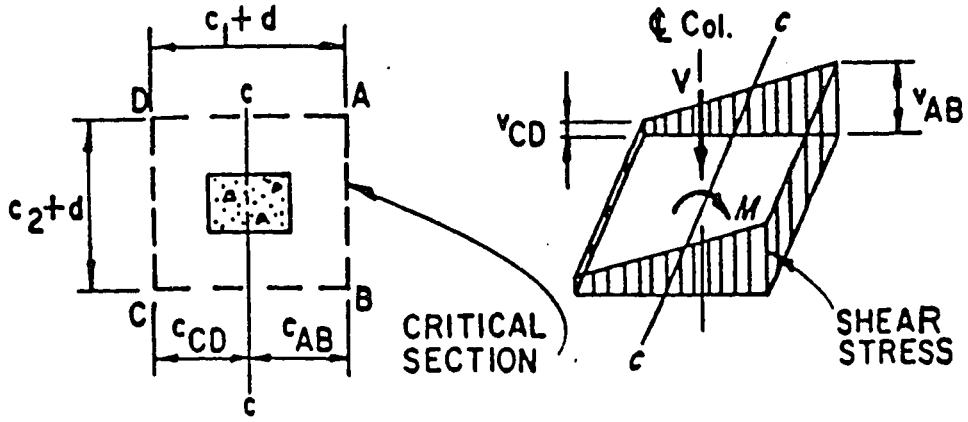

(a) INTERIOR COLUMN

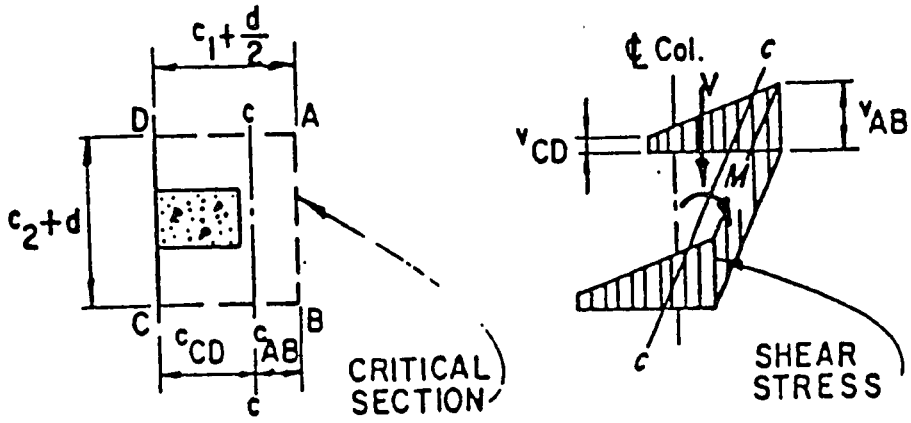

(b) EDGE COLUMN

Figure 3.7 Assumed Distribution of Shear Stress (ACI 318-89)

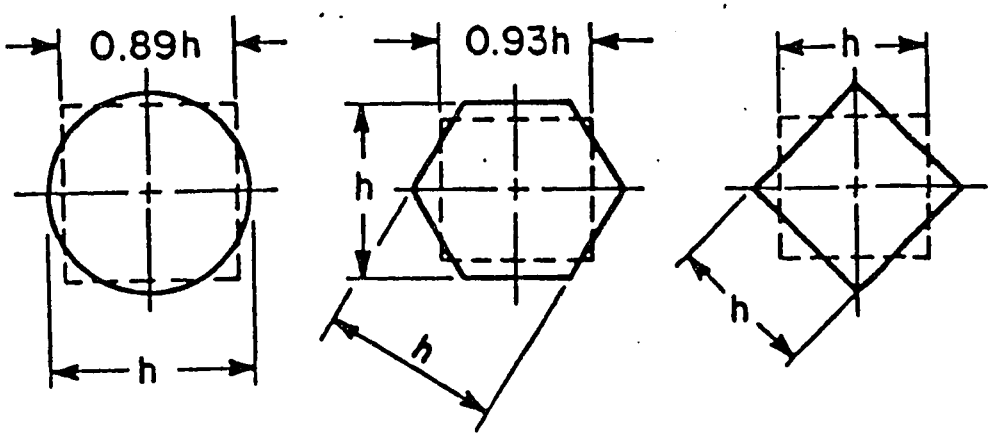

Figure 3.8 Example of Equivalent Square Section for Nonrectangular Supporting Members (ACI 318-89)

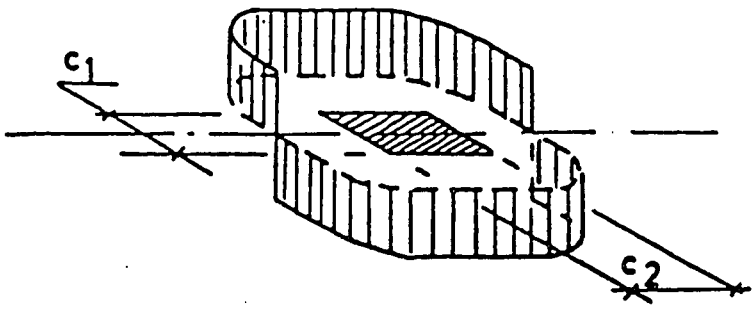

Figure 3.9 Shear Distribution (CEB-FIP 1990)

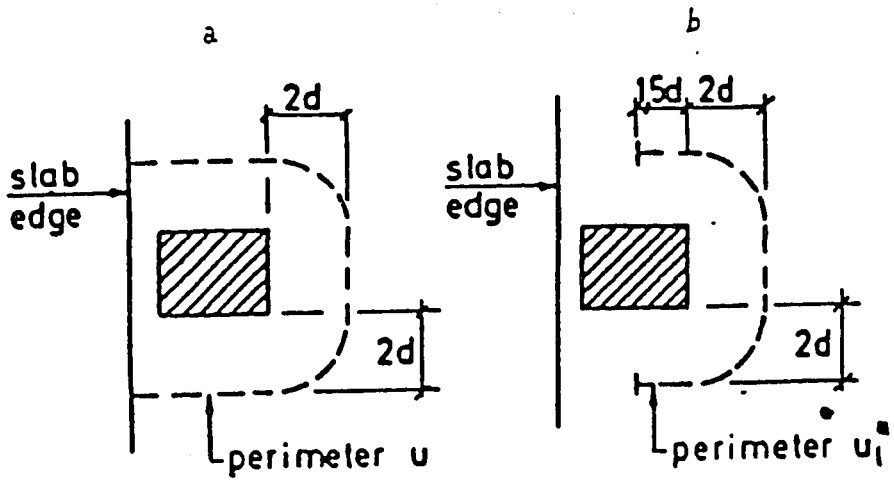

Figure 3.10 Control Perimeter at Edge Columns
(CEB-FIP 1990)

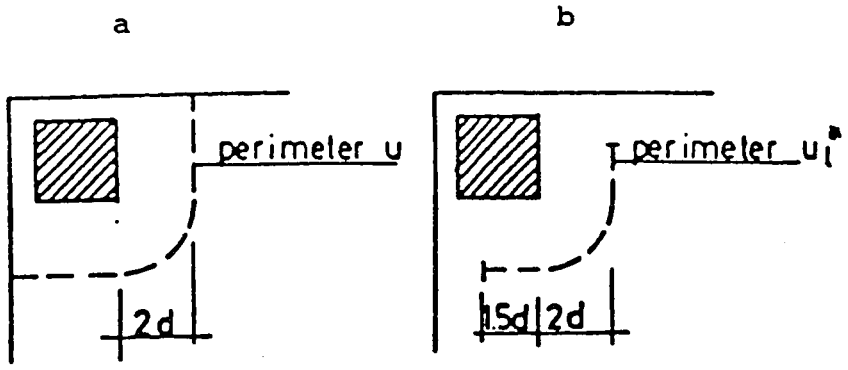

Figure 3.11 Control Perimeters at Corner Columns
(CEB-FIP 1990)

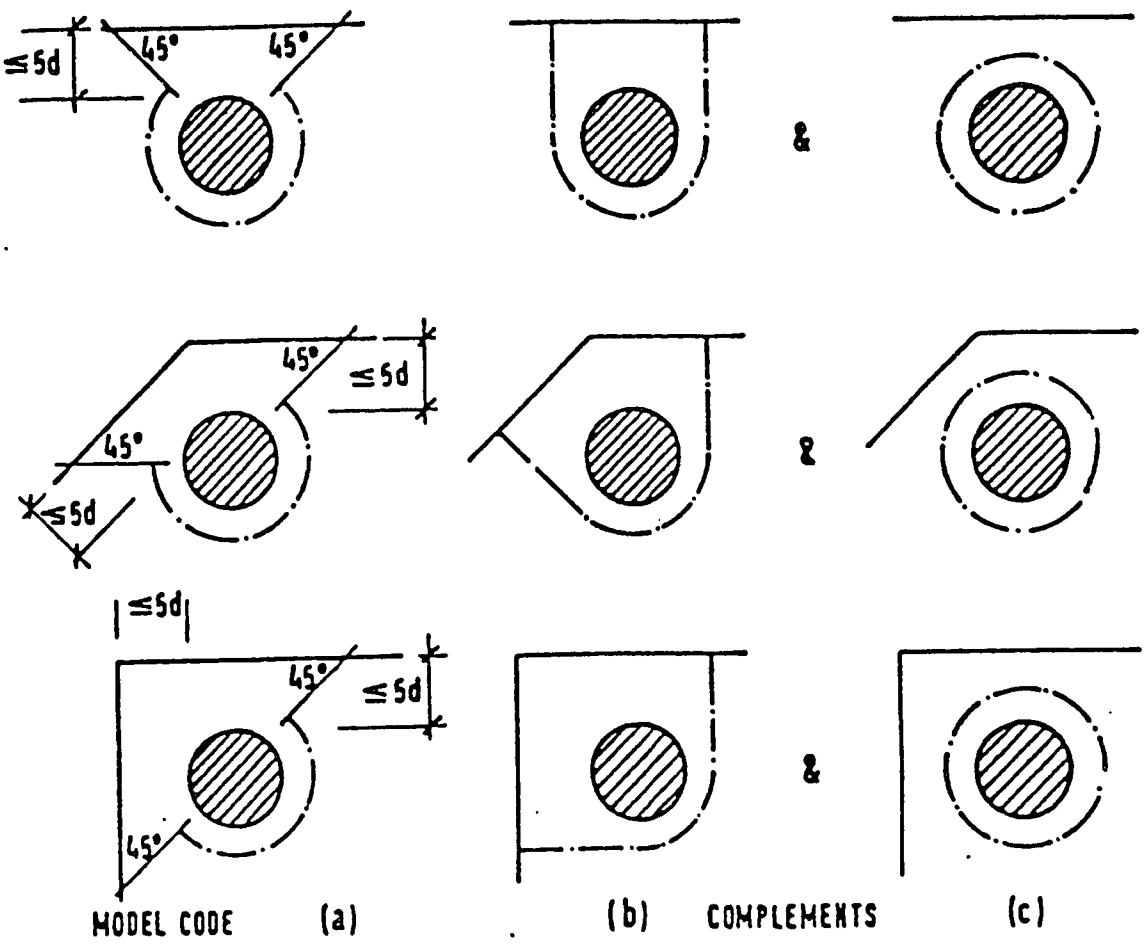

Figure 3.12 CEB Perimeters at Columns Near Slab Edges

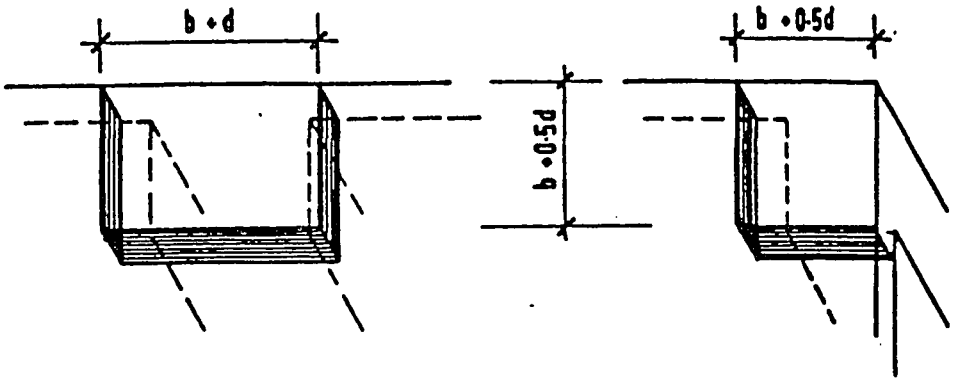

Figure 3.13 ACI Code Surfaces for Determining 'J' at Edge and Corner Columns

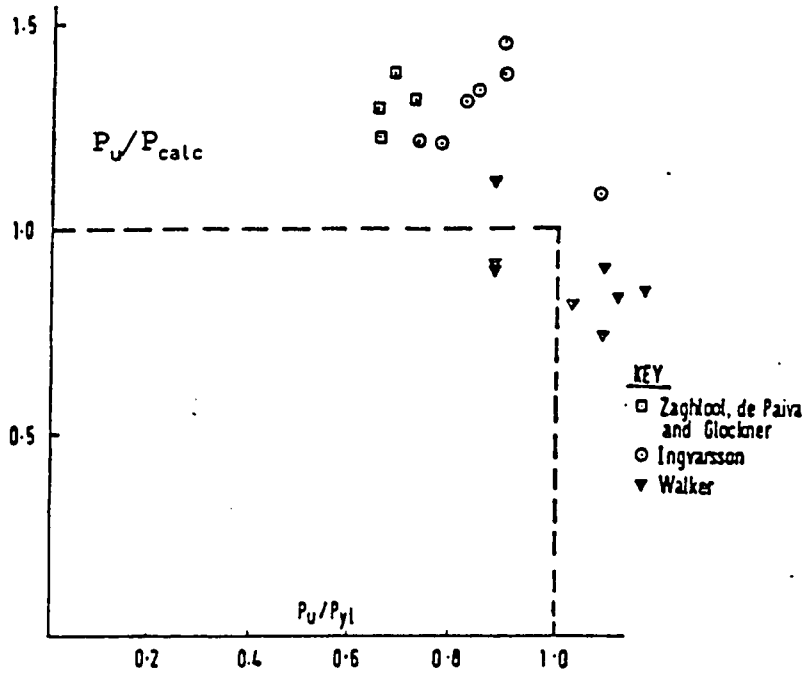

Figure 3.14 Comparison of Strength of Slabs on Four Corner Columns with Predictions by The British Code (Regan and Braestrup 1985)

CHAPTER 4

EXPERIMENT DESCRIPTION AND OBSERVATION

4.1 Introduction

The problem with flat slabs is that unless special precautions are taken, the residual shear resistance at a column following a punching failure is low. Punching even at a single column can cause a major redistribution of load effects. If punching failure occurs at an interior column, the shear load at the neighbouring columns is increased by about 12.5%, and large eccentricities are developed. A failure initiated at one column can thus rather easily spread horizontally, and once this happens the slab falls onto the next lower floor, where the extra loading is magnified by dynamic effects, causing progressive failure.

To avoid failures during construction, it is important to investigate the early-age punching shear strength. It is usual to calculate the available early-age shear capacity from the early-age characteristic strength of the concrete and assume the relationship between the characteristic strength and the shear strength.

Many experiments on punching shear conducted by previous researchers were small scale or on isolated slab-column connections. To collect more precise and practical data of punching shear stress on continuous flat slabs, a 2×2 bay (9 column) slab with span lengths of 2.743 m was loaded to failure. The main objective of this experiment was

to examine the continuous flat slab in real structures. Since the slab consisted of one interior column, four edge columns and four corner columns and the slab was subjected to the uniformly distributed load, the research can be extended to the punching strength with moment transfer at slab-column connection or the punching strength without moment transfer.

4.2 Description of The Experimental Model

Test Specimen

The slab was designed according to ACI 318-89 Code and the size of the slab was about half of the slab size in real structure. The dimensions of the test specimen are shown in Figure 4.1. The interior column (#1), the edge columns (#3 ~ #5) and the corner columns (#7 ~ #9) were all 254 mm × 254 mm square columns. Two 254 mm diameter circular columns were located at the middle of the south edge (column #2) and the south-east corner (column #6). The thickness of the slab was 140 mm.

The arrangement of the reinforcement is summarized in Figure 4.2. The clear concrete cover from the bottom of the slab to the bottom of reinforcing mats was 19 mm. The amount of reinforcement was calculated and distributed in such a way that the slab would have enough flexural strength to ensure a shear failure. At the slab-column connections, the reinforcement was extended to ensure enough anchorage length. At every edge and corner column connection, two bars were bent into the column and the other bars were bent into the slab. Twenty-two 95 mm × 95 mm wooden supplementary supports were placed underneath the slab at a distance of 127 mm from each column face

as shown in Figure 4.1 by the dash lines.

The deflections (which are response measurement) at locations D1 to D21 shown in Figure 4.1 were measured by dial gages. Dial gages were zeroed before each loading sequence.

Materials

CSA type 10 portland cement, river sand, and a coarse aggregate of 19 mm maximum size were used for the concrete mix. Five concrete cylinders were tested and the average concrete strength was 19.5 MPa. The average elastic modulus from testing two specimens was 20.9 GPa. Deformed reinforcing bars, #10M, with yield strength of 400 MPa were used in the slab.

Loading System

A uniformly distributed load was applied by means of 40 concentrated loads L_1 ~ L_{40} as indicated in Figure 4.1.

Because the tributary areas of slab associated with various tie bars were not identical, to apply a uniformly distributed load to the slab, different amounts of force were applied to the different loading points in the experiment. The loading points on the slab were divided into three groups according to jack pressure. All of the loading points in one group are connected to a common pump which had a pressure gage. Group 1 consists of the interior loading points (L17 to L40 in Figure 4.1) connected by the hose to a common pump. The edge loading points (L_1 to L_8 in Figure 4.1) are in Group 2 and

Group 3 consists of edge loading points (L_9 to L_{16} in Figure 4.1).

The box section steel beams were located under the Lab floor and 20 hydraulic jacks were installed on the top of the beams. The test slab was connected to the box section beams by high-tension bars which went through the lab floor and were fixed by washers and nuts at the loading points.

The load was generated by hydraulic jacks and applied to the testing slab in the following way. When the pump was pumped, jack lifts up against the Lab floor and it creates a downward force on the box beam which in turn pulls down the slab through the high-tension bars. Lateral supports were provided by small box section steel bars to prevent jack and high-tensile bars from buckling. Figure 4.3 describes the detailed configurations.

Test Procedure

In order to determine whether supplementary supports can increase the shear strength of the slab or not, and to avoid premature failure of the slab, the slab was loaded to a predetermined load with supplementary shores in place; unloaded; then reloaded with the supplementary shores removed, measurements taken, and unloaded. The supplementary supports were re-installed and the slab reloaded to a larger predetermined load. In each test, the loads were increased monotonically in increments. After applying the load, 2 minutes were allowed to elapse time to allow the load to become stable, and then the readings were taken. The interior slab/column connection failed at the lowest load with the edge and corner column connections remaining relatively intact. To continue

testing and to obtain the maximum possible use of the model the interior column connection was excessively shored and the slab reloaded, without supplementary supports at the edge or corner columns, and two edge column connections, #2 and #5, in Figure 4.1 failed. Again to reuse the slab, all four edge column connections were excessively shored to force a failure of the corner connection but it was not successful. After reducing and re-arranging the supplementary supports at the edge connections, the slab was loaded again until one corner and one shored edge connection failed.

The tests are indicated as follows and the uniform distributed load w given below does not include the dead load of the slab.

Test 1

With the supplementary supports, the slab was loaded from 0 to the uniformly distributed load $w = 20.7$ KN/m^2 not including the self-weight of the slab. For each increment, the deflections at D_1 to D_{22} are given in Table A.1 in the Appendix. The cracks on the test slab are depicted in Figure 4.4. The slab was unloaded after the data were collected.

Test 2

The supplementary supports were removed and the slab was loaded in the same way as in Test 1. Slab failure didn't occur and the slab was unloaded. The results were given in Table A.2 of the Appendix.

Test 3

The supplementary supports were replaced. The slab was loaded again from 0 to $w = 25.9$ KN/m^2, which exceeds the failure load derived from BS 8110-85 Code. Slab failure did not occur and the slab was unloaded. The measured deflections are shown in Table A.3 in the Appendix.

Test 4

The supplementary supports were removed again and the slab was loaded in the same way as Test 3. The results of deflection at points D_1 to D_{22} are given in Table A.4 in the Appendix.

Test 5

The supplementary supports were replaced and the slab was loaded from 0 to $w = 31.1$ KN/m^2 which exceeds the failure load calculated by both CEB-FIP 1990 and BS 8110 Codes. However, the slab didn't fail. The measured deflections are given in Table A.5 in the Appendix.

Test 6

The supplementary supports were removed and the slab was loaded in the same way as in Test 5. The interior slab-column connection failed when the load reached $w = 31.1$ KN/m^2. The failure pattern shown in Figure 4.4 is similar to that obtained from isolated specimens. The measured deflections are given in Table A.6 in the Appendix.

Test 7

In order to test punching shear strength at the edge and corner connections, supplementary supports were used to support the failed interior column connection as shown in Figure 4.5 (a). There were no supplementary supports in vicinity of the edge and corner column connections. The slab was loaded from $w = 0$ to $w = 31.1$ KN/m^2, which is the same as the interior column connection failure load. Two edge column connections #2 and #6 failed when the load on the slab reached 31.1 KN/m^2.

Test 8

In this test, the supplementary supports were placed under all failed connections and the two unfailed edge slab-column connections (#3 and #4) as shown in Figure 4.5 (d)-(g). There was no support under the corner column connections. The purpose of this test was to load the corner column connections to failure. The slab was loaded from $w = 0$ up to $w = 41.5$ KN/m^2. However, no failure occurred.

Test 9

Two props were removed from the edge column connections #3 and #4 and the arrangement of the supports around the edge columns is shown in Figure 4.5 (b) and (c). The slab was loaded in the same way as in test 9. The edge connection #3, with reshores, and the corner connection #6, without supplementary shores failed, when the load reached 41.5 KN/m^2.

4.3 Test Observation

Deflections

In order to check the loading system and find out whether the load was applied uniformly on the slab and whether the concentrated load points L_1 to L_{40} can approximate a uniformly distributed loading condition, the deflections at the centre point of each panel (D7, D10, D17 and D18 in Figure 4.1) were compared Figure 4.6a to 4.6c show the deflections at these points versus the applied uniformly distributed load *w*. Figure 4.6a represents the deflections at these points during Test 1 and Test 2 in which the slab was loaded from $w = 0$ to $w = 20.7\ KN/m^2$ with the supplementary supports in Test 1 and without the supplementary supports in Test 2, respectively. Figure 4.6b represents the deflections during Test 3 and Test 4 in which the slab was loaded from $w = 0$ to $w = 25.9\ KN/m^2$ with the supplementary supports in Test 3 and without the supplementary supports in Test 4, respectively. Figure 4.6c represents the deflections during Test 5 and Test 6 in which the slab was loaded from $w = 0$ to $w = 31.1\ KN/m^2$ with the supplementary supports in test 5 and without the supplementary supports in test 6, respectively. As far as the centre of each panel is concerned, the slab can be considered as approximately symmetric since the size difference of the edges can be ignored. Deflections at locations D7, D10, D17 and D18 should be the same under a uniformly distributed load. As shown in Figure 4.6a to 4.6c, the difference of the deflections among the above points are less than 20% under most of the loading conditions, especially when the load is small. However, as the load increases, the deflection at D10 becomes greater than that of other points, while D17 seems to have the least deflection compared to the

other points. The biggest difference between these two extremes is 20%. It is believed that uniformly distributed load has been achieved in our slab experiment.

From Figure 4.6a to 4.6c, it is not hard to observe that the deflection curves are initially steeper when there were supplementary supports than without supplementary supports. This means that the stiffness of the slab system is greater when supplementary supports are provided under the slab. For the same support condition, the deflection curves are flatter in the latter loading tests which indicates that the stiffness of the slab decreased after each test. The reduction of the stiffness was caused by residual cracks.

The deflection difference between the slab with supplementary supports and one without such supports is small.

Figure 4.7a to 4.7c show the configurations of slab deflection during Test 2, Test 5 and Test 6. From Figure 4.7a, it can be observed that the deflection along the centre line of the edge and corner columns are similar. This means that the overhang of the edges, which extended from column face a distance equal to the effective thickness, is too small to affect the behaviour of the slab. Figure 4.7b and 4.7c indicate that prior to the failure of the interior connection, the deflection close to the column is very small. Contrarily, in the middle of each panel the deflection increases very quickly as the load increases. When failure occurs, there is a sudden drop in the vicinity of the column and the deflection there increases more than 7 mm. Figure 4.7 also shows that the deflection on the column strip is smaller than that on the middle strip.

Crack pattern

The crack pattern of the slab is depicted in Figure 4.4 in which the punching failure surface is shown by a thickened and irregular line.

During Test 1, the radial crack (#2 in Figure 4.4) first occurred at the corner of the interior column caused by the concentration of stress at the corner. As the load increased, the flexural crack (#1 in Figure 4.4) from the centre of the interior columns extends toward the centre of the edge columns, then tangential crack #5 along the edge of the interior column stub occurred. At the end of Test 1, cracks were fully developed at the interior column connections. At the edge column connections, the crack (#1 in Figure 4.4) developed first and then tangential cracks #3 developed at distance d from the column faces. At corner column the tangential cracks #3 developed in two directions simultaneously at a distance *d* from the column faces. After unloading at the end of Test 1, most cracks recovered but cracks 1 and 2 did not fully recover. In the vicinity of the edge columns, because of the unbalanced moment transfer at these connections, there were more cracks developed towards the inside of the slab although there were some small cracks developed towards the free edges as shown in Figure 4.4. At the edge columns and corner connections, torsional cracks #4 were found as shown in Figure 4.4.

For slabs with shores and those without shores, the crack patterns and crack development processes were similar. The only difference is that the cracks on the slab without supplementary supports tend to extend easily.

After each test, the length and width of the crack increased. The widest crack was always along the middle of the centre crack #1, which was about 6 mm at the end of the

experiment and were smaller at ends but larger at the centre due to the moment redistribution effects or due to the fact that in the centre strip there is less reinforcement than in the column strips, as shown in Figure 4.2. The second widest crack #5 was along the edge of column faces and its width was 4 mm. Crack #2 was also wide at the interior column connection.

Failure

The interior slab-column connection failed due to punching that initiated adjacent to the column corners. Punching spread completely around the column quickly. The slab as a whole fell off the column as shown in Figure 4.8. For the edge and corner connections, rigid body rotations dominated and punching spread towards the interior columns as shown in Figure 4.9. Torsional cracks were observed at edge and corner connections.

It was found that the circular columns #2 and #6, which were at the edge and corner, failed more abruptly and deflected more than the square edge columns #3 and #5 perhaps because the perimeter of the circular column is smaller than that of the square ones. For #3, another reason was the presence of the supplementary supports.

There was marked bond distress with reinforcement closely spaced through the column as shown in Figure 4.10. As loading increased, inclined cracks appeared on the vertical surface of the most heavily loaded slab edge. Those cracks extended down to the outermost bars of the concentrated reinforcement. Simultaneously with the final punching failure at the column, a horizontal crack connected these inclined cracks, and the top

reinforcement was pulled out of the slab. This phenomenon was more pronounced at corner connection #6 and edge connection #2. It seems that reinforcement through the column should have larger spacings between the bars.

The average angle of inclination for each failure surface θ (refer to Figure 3.1) are calculated as following:

Interior connection #1	$\theta_1 = 18°$
Edge connection #2	$\theta_2 = 15°$
Edge connection #3	$\theta_3 = 18°$
Edge connection #5	$\theta_5 = 17°$
Corner connection #6	$\theta_6 = 17°$

These are smaller angles than those reported by Regan (1981).

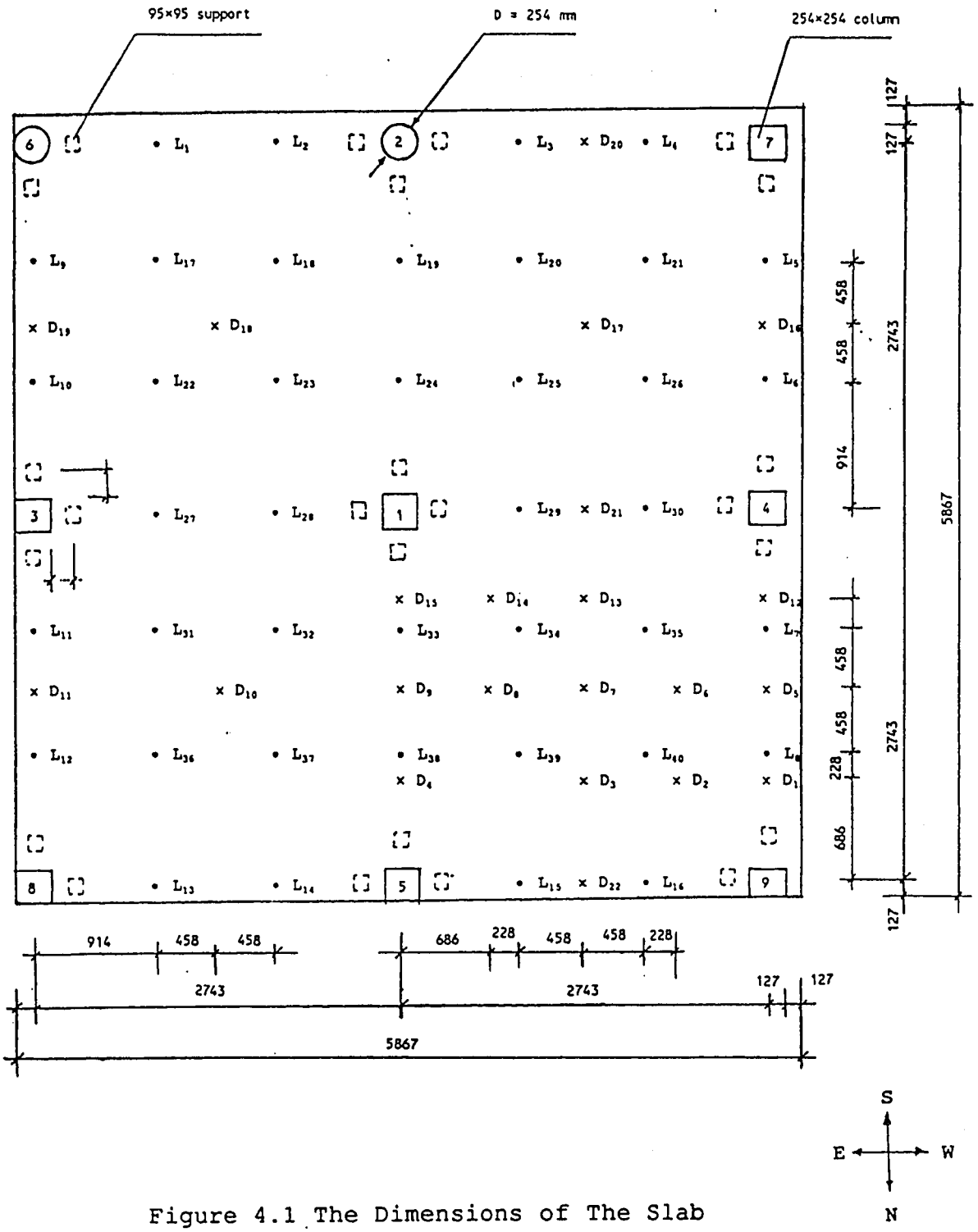

Figure 4.1 The Dimensions of The Slab

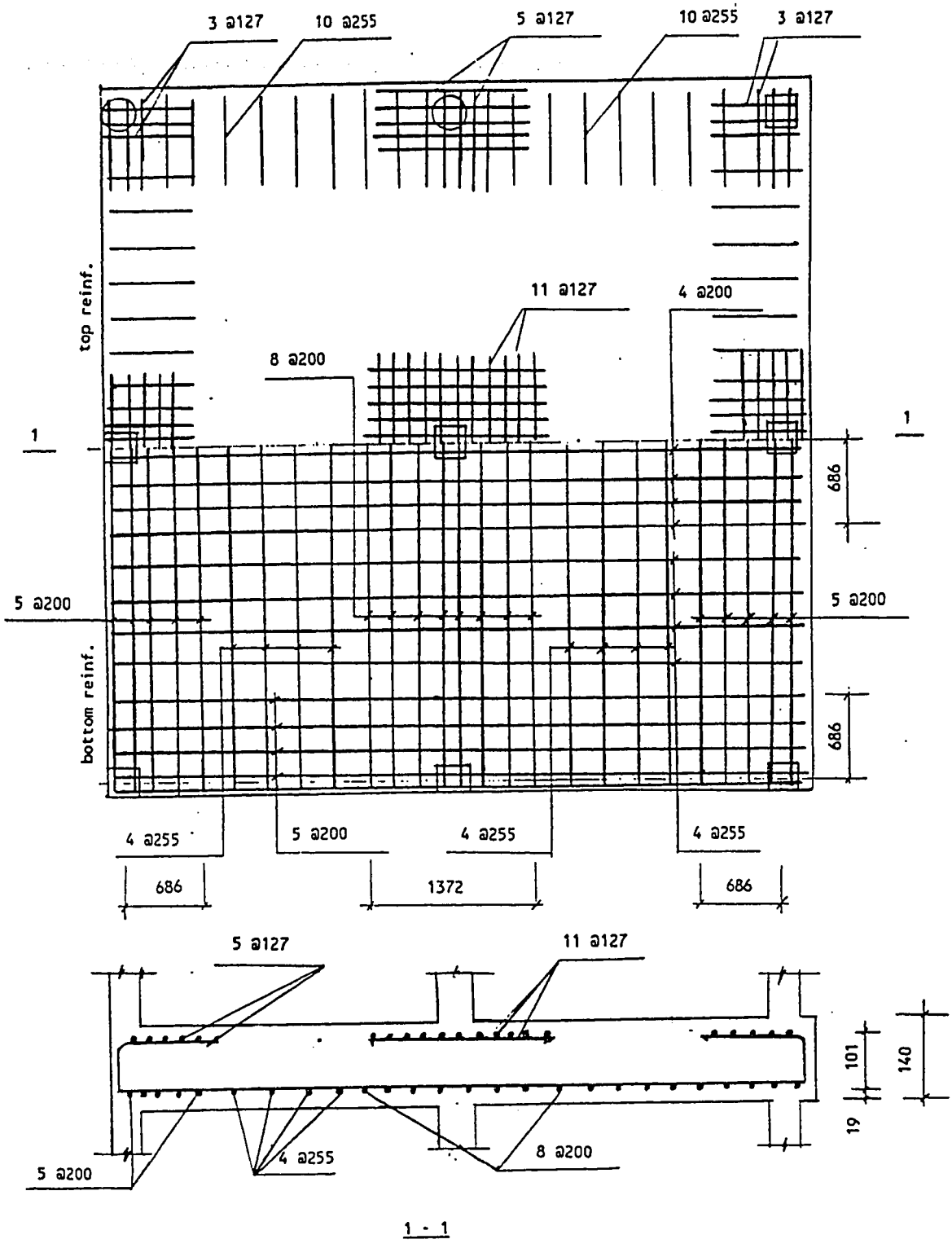

Figure 4.2 The Arrangement of Reinforcement of The Slab

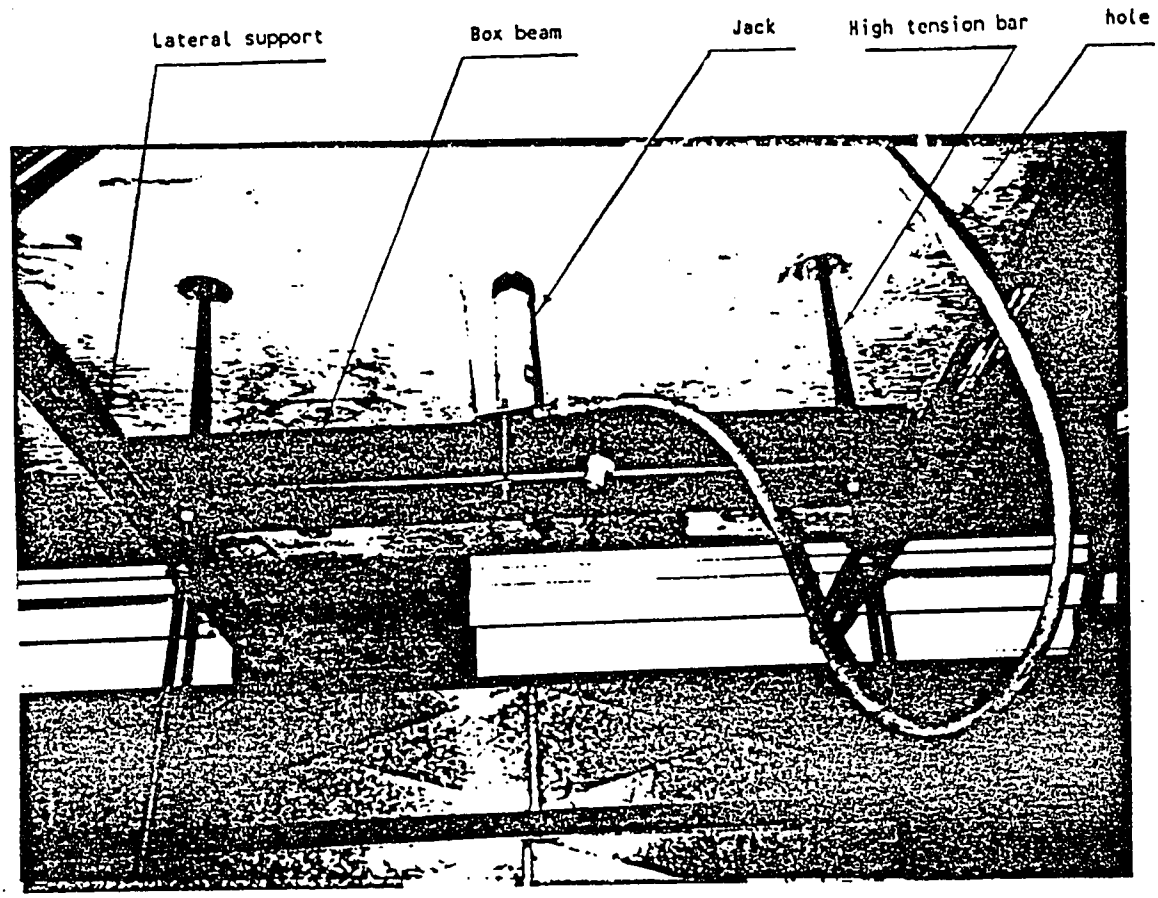

Figure 4.3 The Loading System

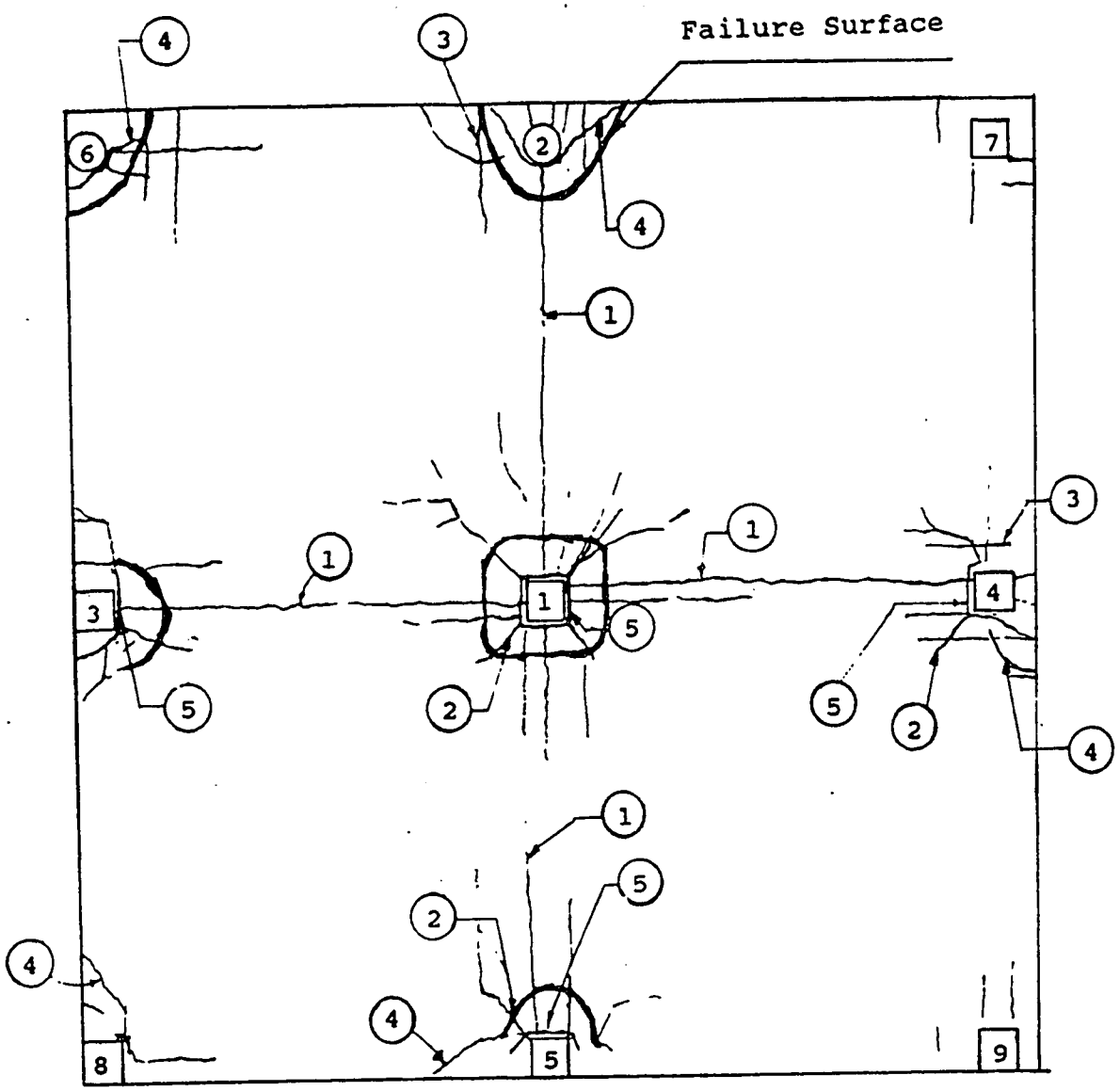

Figure 4.4 Top Surface Crack Pattern

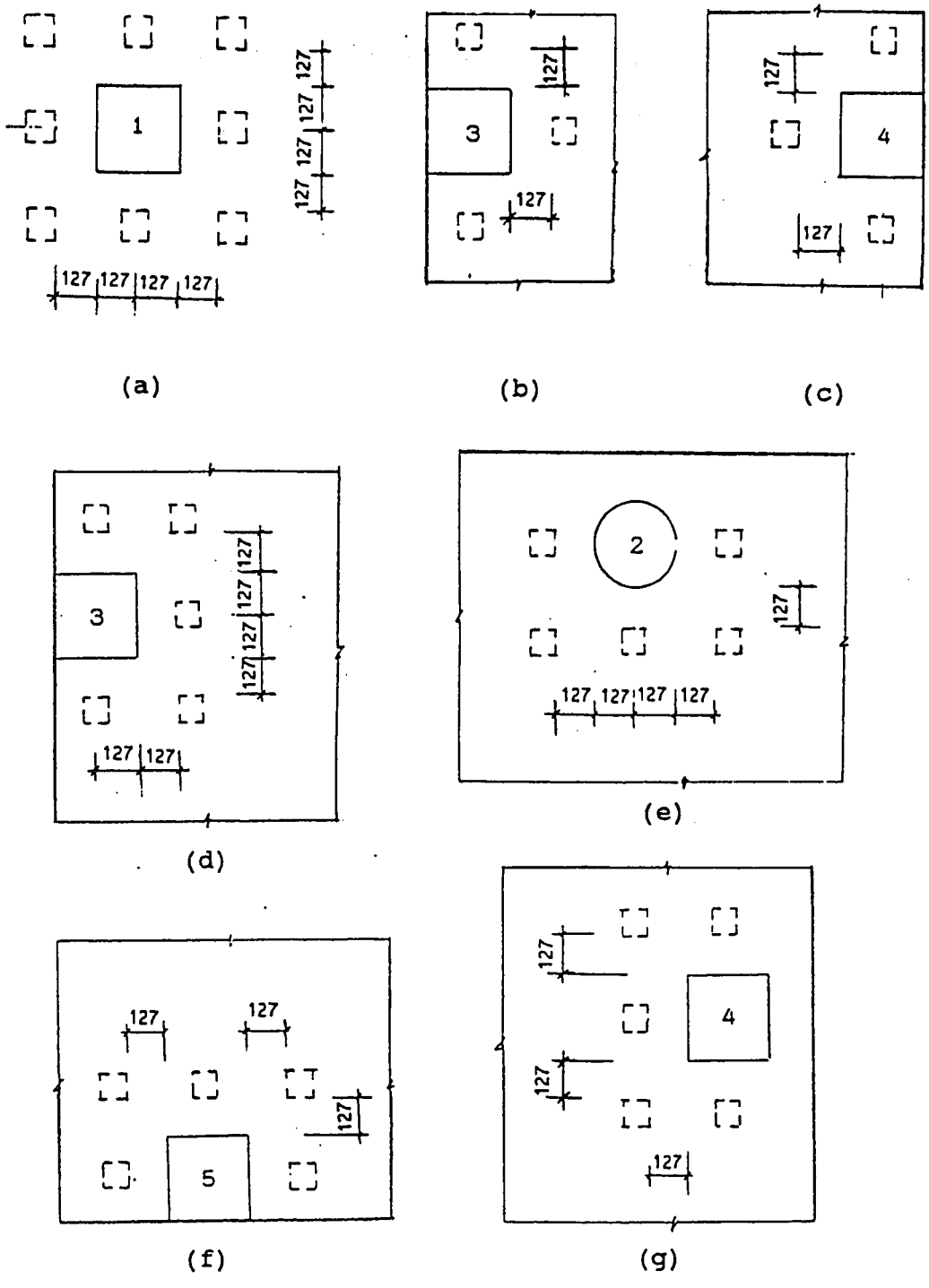

Figure 4.5 The Arrangement of Supplementary Supports

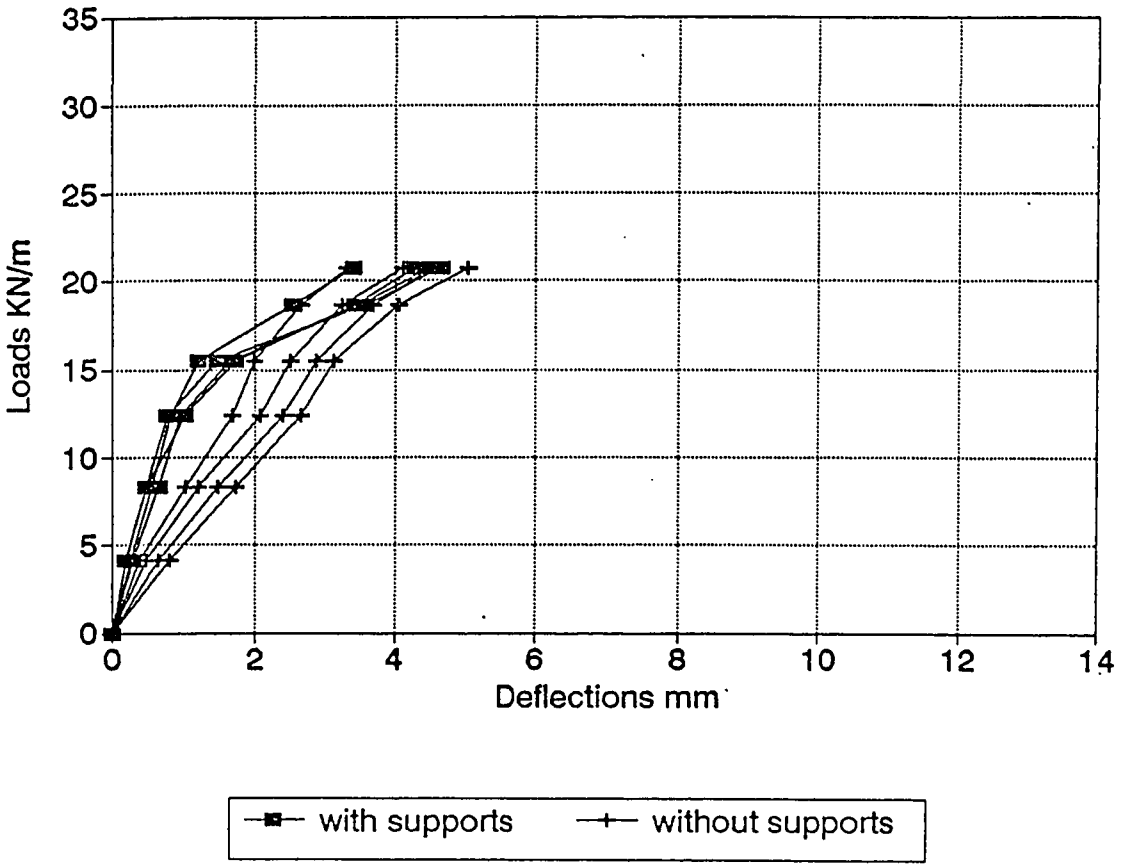

Figure 4.6a Deflection at Points D_7, D_{10}, D_{17} and D18 During Test 1 and 2

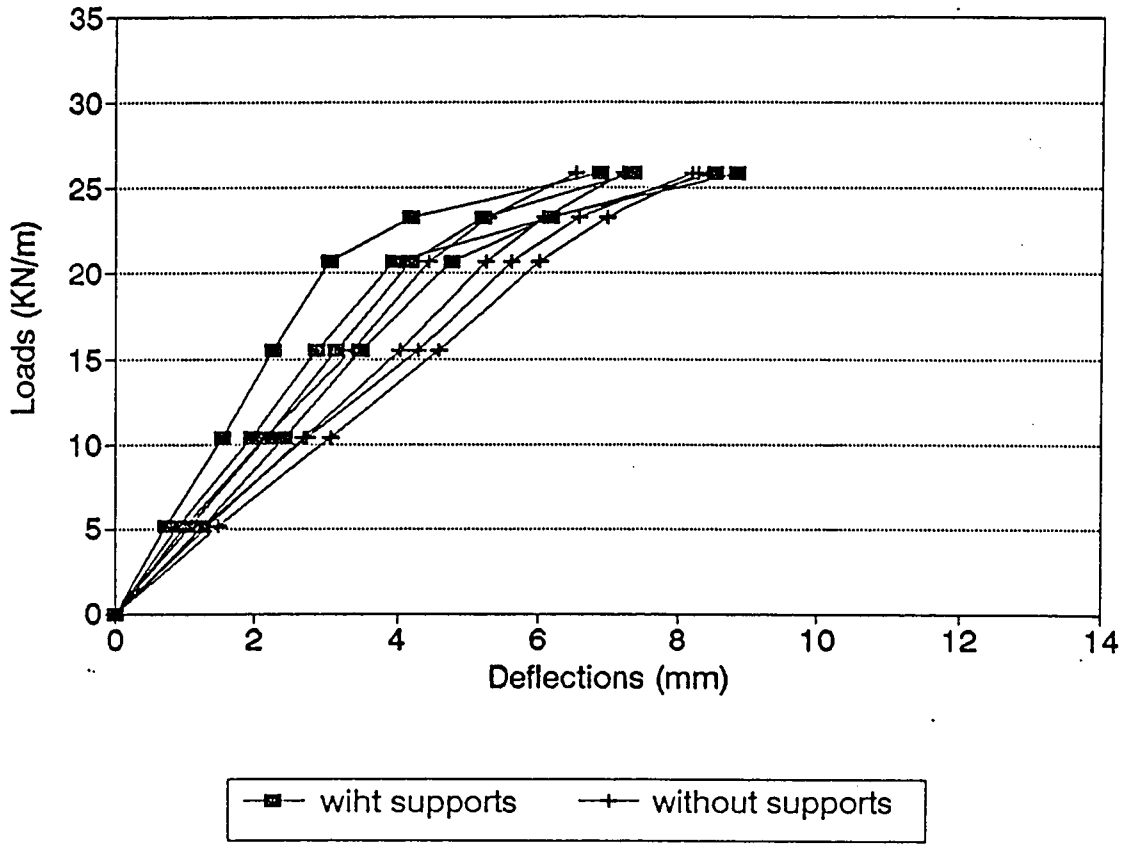

Figure 4.6b Deflection at Points D_7, D_{10}, D_{17} and D18 During Test 3 and 4

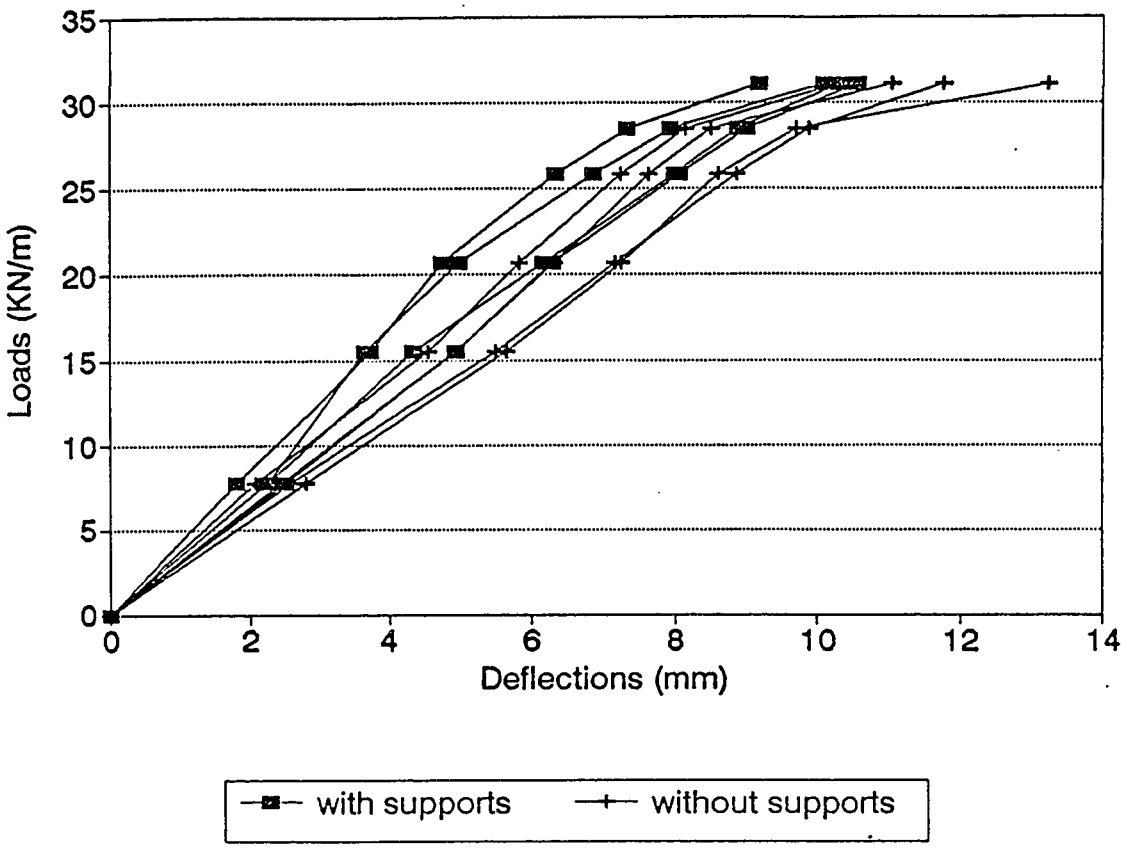

Figure 4.6c Deflection at Points D_7, D_{10}, D_{17} and D18 During Test 5 and 6

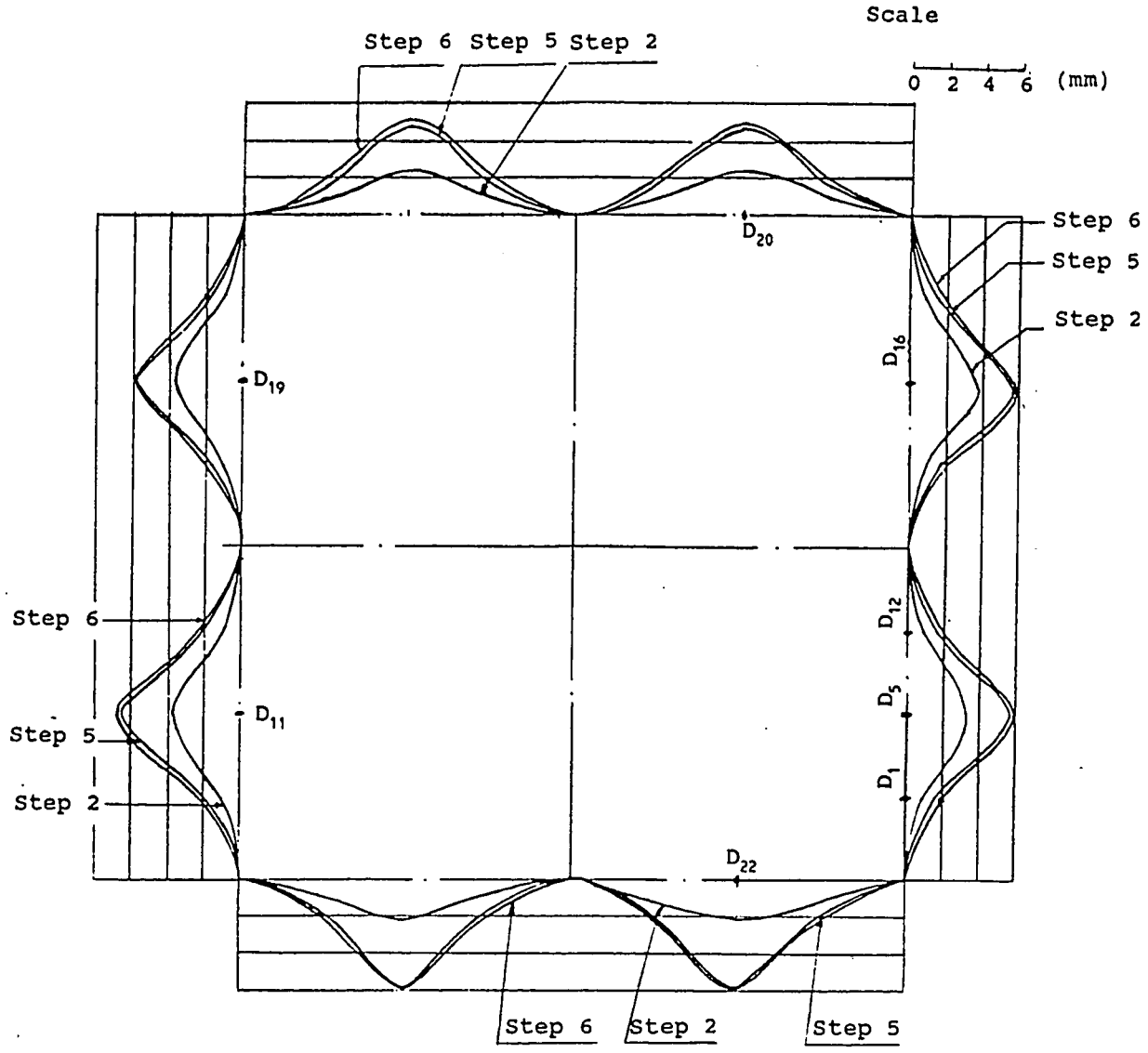

Figure 4.7a The Configuration of Deformation along Edges of The Slab

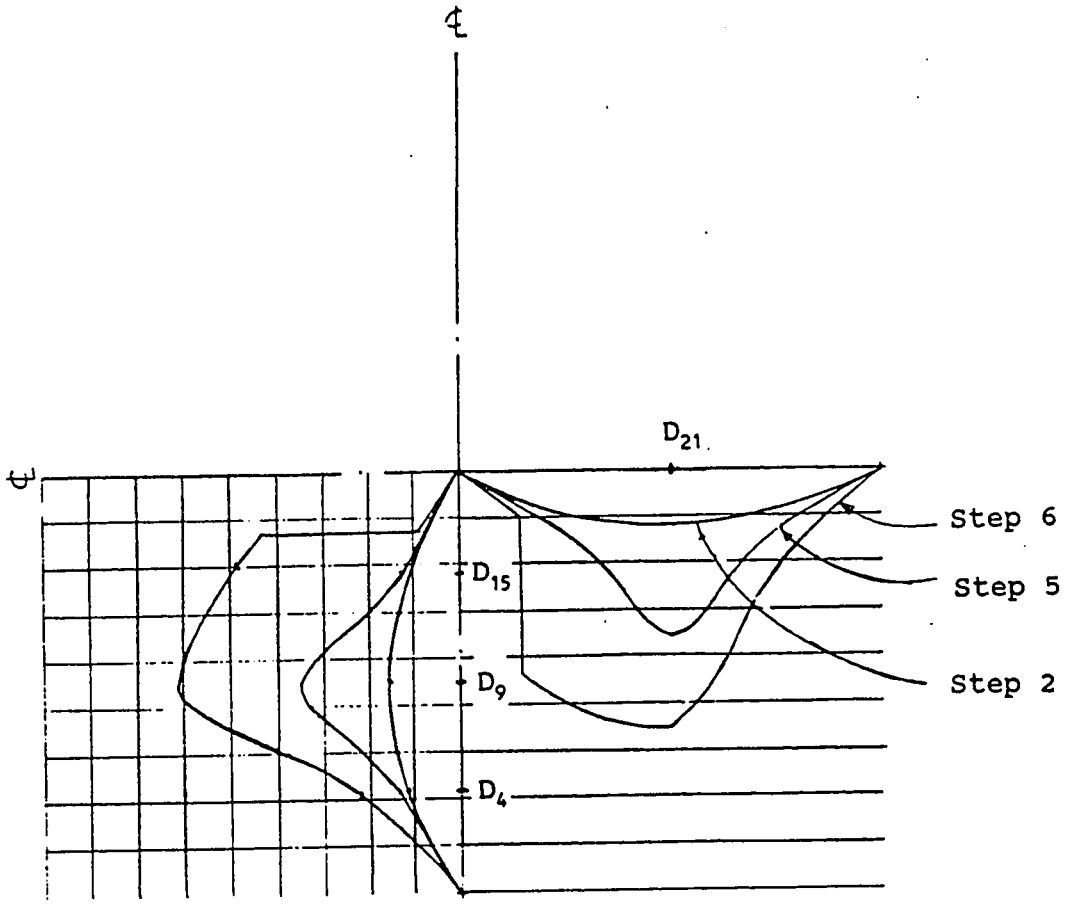

Figure 4.7b The Configuration of Deformation along The Centre of The Slab

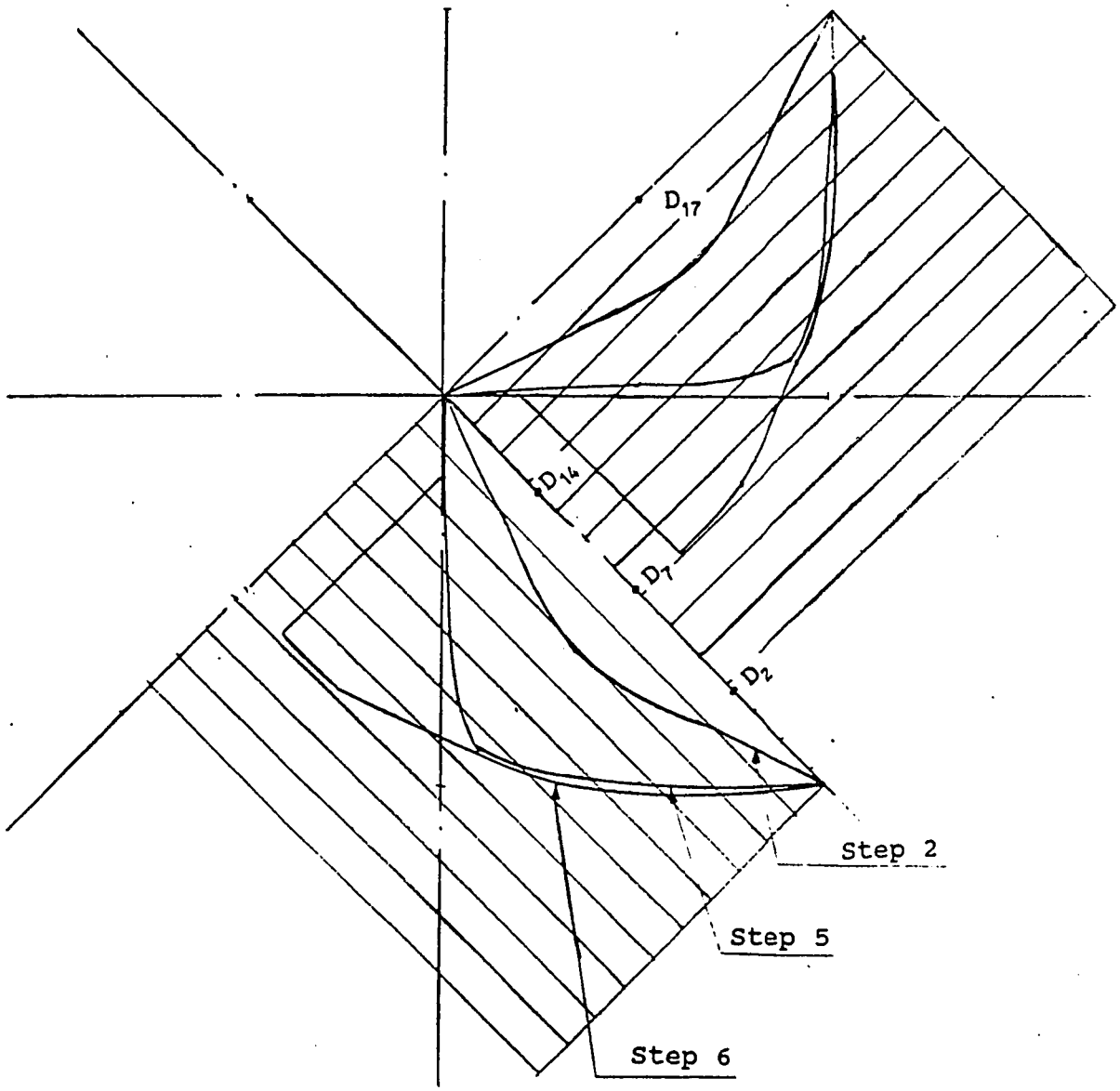

Figure 4.7c The Configuration of Deformation along The Diagonal of The Slab

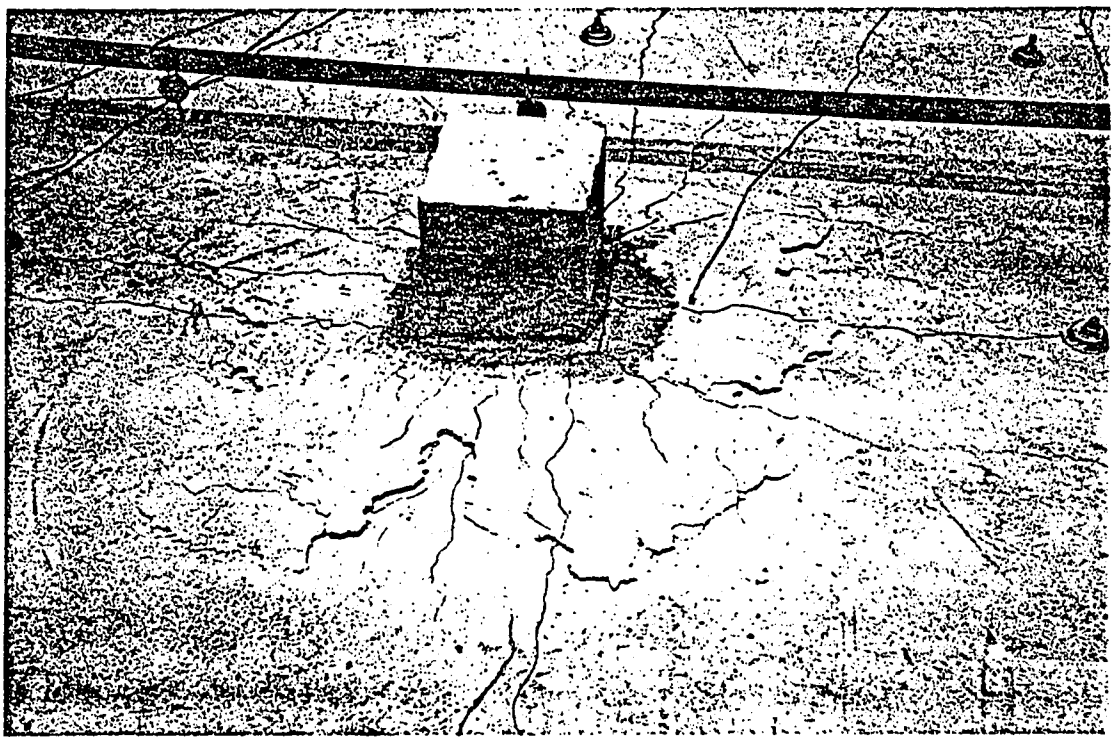

Figure 4.8 Failure Pattern of the Interior

Slab/Column Connection

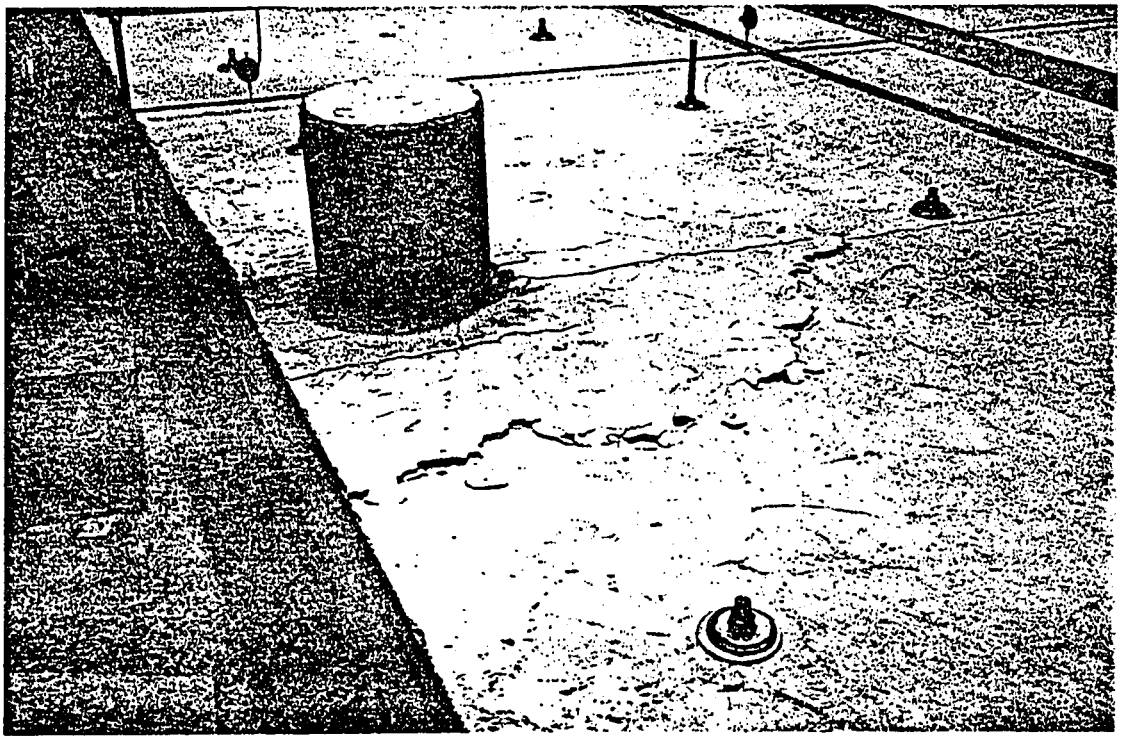

Figure 4.9 Failure Pattern of the edge

Slab/Column Connection

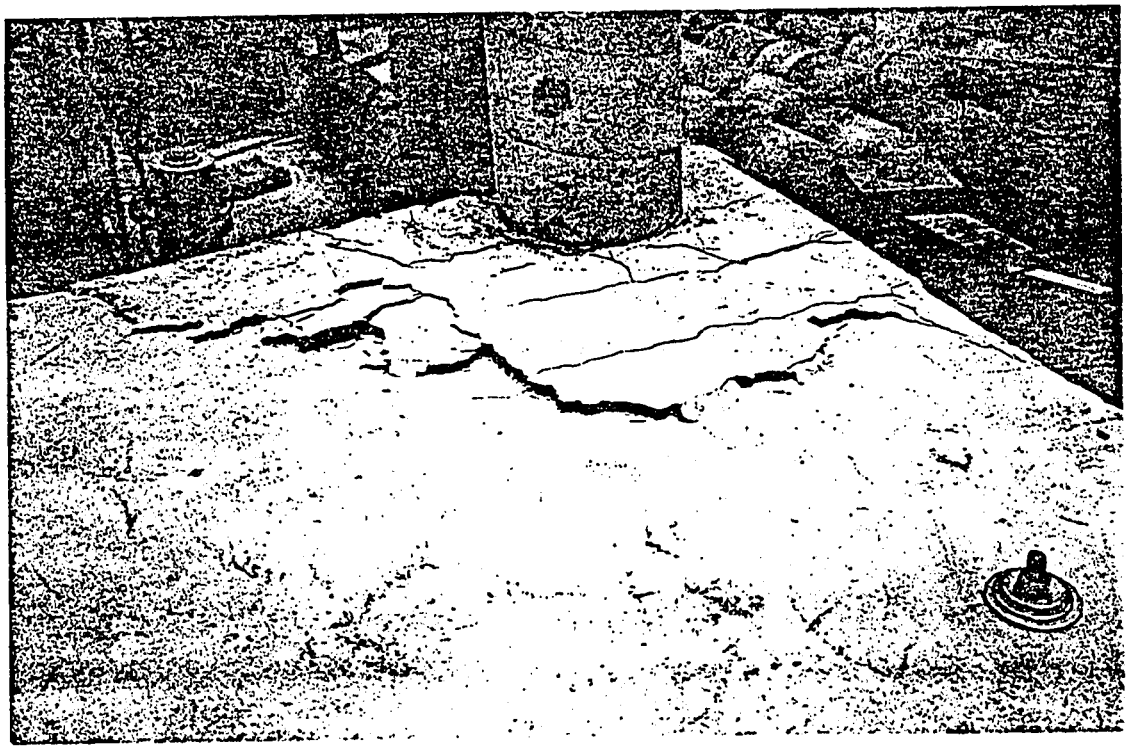

Figure 4.10 Failure Pattern of the Corner

Slab/Column Connection

CHAPTER 5

ANALYSIS OF THE EXPERIMENTAL RESULTS

5.1 Calculation of Ultimate Load

The experimental results, the ultimate punching shear loads calculated by ACI 318-89, BS 8110-85, CEB-FIP 1990 style equations using mean value coefficient and the service punching shear loads calculated by the three codes for the test slab are described in the following sub-sections.

5.1.1 Test Results

The experiment loads were not measured directly but were calculated from the hydraulic pressure. The pressure of the exterior hydraulic jacks was adjusted so that a uniform slab load was applied regardless of slab tributary area.

Since the area covered by each interior loading point $L_{17} \sim L_{40}$ is:

$$A_i = 0.914 \times 0.914 \text{ m}^2$$

by edge points $L_1 \sim L_8$ is

$$A_{e1} = 0.914 \times 0.711 = 0.78A_i$$

by edge points $L_9 \sim L_{16}$ is

$$A_{e2} = 0.914 \times 0.584 = 0.64A_i$$

The hydraulic pressure of the four jacks connecting edge loading points L_1 to L_8 was adjusted to 78% of interior hydraulic pressure and four jacks connecting edge loading

points L_9 to L_{16} was adjusted to 64% of the interior hydraulic pressure.

a. Interior Slab-Column Connection

The failure occurred when the interior jack reading was 6000 psi. The area of the hydraulic jack was 2.27 $(in)^2$. Therefore, the concentrated force at each interior loading point should be:

$(6000 \times 2.27)/2$ Lbs

There were four jacks round the interior tributary area 2.743 m × 2.743 m, therefore, the failure load in terms of uniformly distributed load at interior column-slab connection is:

$$w_l=\frac{6000\times2.27\times4.448\times4}{2.743^2}=32.2KN/m^2 \quad (5.1)$$

The slab self-weight:

$$w_D=2.4\times0.14\times9.81=3.3KN/m^2 \quad (5.2)$$

Total failure load:

$$w_f=32.2+3.3=35.5KN/m^2 \quad (5.3)$$

b. Edge Column Connections

The two edge column connections failed when the hydraulic pressure of the

interior jacks was 6000 psi, therefore, the failure load at connection #2 in terms of uniformly distributed load is:

$$w_f = \frac{6000 \times 2.27 \times 4.448 \times (\frac{3}{2} + 0.78)}{2.743 \times 1.625} + 3.3 = 34.3 KN/m^2 \quad (5.4)$$

and the failure load at connection #5:

$$w_f = \frac{6000 \times 2.27 \times 4.448 (\frac{3}{2} + 0.64)}{2.743 \times 1.50} + 3.3 = 34.8 KN/m^2 \quad (5.5)$$

c. Corner and Edge with Supports

Failure occurred at corner connection #6 and the edge connection #3 with supplementary shores when the hydraulic pressure reading was 8000 psi.

The failure load at connection #6 is:

$$w_f = \frac{8000 \times 2.27 \times 4.448}{1.625 \times 1.50} (0.78/2 + 1/2 + 0.64/2) + 3.3 = 43.4 KN/m^2 \quad (5.6)$$

at Connection #3 is:

$$w_f = \frac{8000 \times 2.27 \times 4.448 (\frac{3}{2} + 0.64)}{2.743 \times 1.50} + 3.3 = 45.3 KN/m^2 \quad (5.7)$$

5.1.2. Comparison with Code Expressions

Comparison with Code expressions is not straight forward because the code expressions use specified concrete strength, not mean strength, and the expressions were designed to be conservative.

Using the technique used by Gardner (1990), the mean coefficients were calculated to predict the failure shear stress of isolated column specimens using the control perimeter appropriate to the code as described in Chapter 3. For the ACI 318-89, BS 8110-85 and CEB-FIP 1990 the mean shear stresses are as follows (calculation for the coefficients are given in the Appendix B):

ACI 318-89:

$$v_c = 0.47\sqrt{f_{cm}} \tag{5.8}$$

BS 8110:

$$v_c = 1.33\sqrt[3]{\rho f_{cm}}\left(\frac{400}{d}\right)^{1/4} \tag{5.9}$$

CEB-FIP 1990:

$$v_c = 0.77\sqrt[3]{\rho f_{cm}}\left[1+\left(\frac{200}{d}\right)^2\right] \tag{5.10}$$

Understrength factors and load factors are set to unity in all calculations.

For the two circular columns (edge column #2 and corner column #6) the ACI Commentary is used for both ACI 318-89 and CEB-FIP 1990. According to ACI Commentary, if a supporting member does not have a rectangular cross section, it is to be treated as a square support having the same area as shown in Figure 3.8. Hence columns #2 and #6 can be considered equivalent to 226 mm × 226 mm square column.

The BS 8110-85 code as published uses very approximate expressions to calculate the shear strengths at edge and corner columns. For these columns a second set of calculations were done using ACI type shear/moment interaction and the equivalent 226 mm × 226 mm square column for the two circular columns.

Knowing:

f'_{cm} = 19.5 MPa

d_v = 120 mm

h = 140 mm

It is assumed that the interior column connection takes 28%, edge connection takes 12.5% and corner connection takes 5.5% of the uniformly distributed panel load in the calculation.

The calculations for ACI 318-89, BS 8110-85 and CEB-FIP 1990 are listed in Table 5.1, 5.2 and 5.3 respectively.

Table 5.1 Punching Shear Strength of The Slab

-by ACI Equation

	Interior Column	Edge #5 Column	Edge #2 Column	Corner Column
d (m)	0.12	0.12	0.12	0.12
b_0 (m)	1.496	1.002	1.172	0.699
v_c (MPa)	2.075	2.075	2.075	2.075
e_1 (mm)		98.3	146	122
$J_1 \times 10^{-3}$ m^4		1.40	2.78	1.63
γ_1		0.38	0.42	0.44
M_1 (KN m)		0.578 w_u	0.603 w_u	0.327 w_u
e_2 (mm)				58.5
$J_2 \times 10^{-3}$ m^4				0.69
γ_2				0.36
M_2 (KN m)				0.302 w_u
w_u (KN/m^2)	44.2	44.4	51.8	52.2

Table 5.2 Punching Shear Strength of The Slab

-by BS 8110-85 Equation

	Interior Column	Edge #5 Column	Edge #2 Column	Corner Column
b_0 (m)	2.456	1.482	1.736 * 1.652	0.995 * 0.939
ρ (%)	0.66	0.58	0.58	0.60
v_c (MPa)	0.907	0.870	0.870	0.880
e_1 (mm)		127	172	151
$J_1 \times 10^{-3}(m^4)$		3.79	6.40	3.55
γ_1		0.36	0.39	0.43
M_1 (KN m)		0.578 w_u	0.603 w_u	0.327 w_u
e_2 (mm)				88
$J_2 \times 10^{-3}(m^4)$				1.87
γ_2				0.37
M_2 (kn m)				0.302 w_u
w_u (KN/m^2)	29.7	32.9	38.6	50.8
*w_u (KN/m^2)		*30.9	*34.4	*34.0

*---Refer to the values obtained by using ACI linear shear/moment interaction.

d = 0.12 m

Table 5.3 Punching Shear Strength of The Slab

-by CEB-FIP 1990

	Interior	Edge #5	Edge #2	Corner
d (m)	0.12	0.12	0.12	0.12
b_0 (m)	2.524	1.368	1.340	0.737
ρ (%)	0.66	0.57	0.57	0.60
ξ	2.29	2.29	2.29	2.29
v_c (MPa)	0.89	0.85	0.85	0.86
w_u (KN/m^2)	32.0	37.1	36.3	45.9

The control perimeters of edge and corner column connections are defined according to CEB-FIP 1990 rules as shown in Figure 3.10 and 3.11 respectively, which means that the overhang is not taken consideration.

Table 5.4 Summary of Calculated Loads (KN/m^2)

	Interior	Edge #5	Edge #2	Corner	Edge shored
Exp.	35.5	34.8	34.3	43.4	45.3
ACI	44.2	44.4	51.8	52.2	
BS 8110	29.7	32.9	38.6	50.8	
Linear		30.9	34.4	34.0	
CEB	32.0	37.1	36.3	45.9	
ACI Service	13.9				
CSA Service	16.2				
BS 8110 Service	17.0				
CEB Service	11.4				

Comparison of Code Equation

Table 5.4 is a summary comparison of the calculated and measured results. The most reliable experimental result is for the interior column; the experimental results for the edge and corner columns will be conservative.

From Table 5.4 it can be concluded that the ACI 318-89 mean coefficient equation over-estimates the measured failure load but both BS 8110-85 and CEB-FIP MC 1990 are slightly conservative; perhaps because they were derived from results on isolated columns.

By comparing the results calculated using ACI linear interaction for ACI and BS 8110, The effect of combined shear and moment transfer appear to be adequately represented by the ACI 318-89 linear interaction equation.

The BS 8110 prediction is reasonable for the interior column connection, but for the edge and corner column connections the results are not consistent, due to using very simple expressions for corner and edge column connections.

CEB-FIP 1990 predictions are consistent and close to the experimental values.

It should be noticed from Tables 5.1 (ACI 318) that the calculated punching shear strength of edge #2 is much greater than that of edge #5, which means that taking consideration of the overhang in the control perimeter in this case is very unconservative.

From Tables 5.1 and 5.2, it is observed that represent a circular column by the same area of rectangular column to calculate shear strength does not cause significant error and simplifies the calculations.

It is recommended that ACI type linear shear /moment interaction type equation is preferred to the simplistic approximations of BS 8110-85.

Comparison of service load:

In order to compare service load defined by different Codes to the experimental results, the service loads are calculated taking account of load factor γ_G and material understrength factor γ_m. The values of γ_G *and* γ_m for the Codes are:

ACI 318-89 $\gamma_G = 1.4$

$\gamma_m = 1/0.7$

The overall safety factor $\gamma = 1.4/0.7 = 2.0$

CSA A 23-3M 1990 $\gamma_G = 1.25$

$\gamma_m = 1/0.6$

The overall safety factor $\gamma = 1.25/0.6 = 2.08$

BS 8110-85 $\gamma_G = 1.4$

$\gamma_m = 1.25$

The overall safety factor $\gamma = 1.4 \times 1.25 = 1.75$

CEB-FIP MC 1990 $\gamma_G = 1.35$

$\gamma_m = 1.50$

The overall safety factor $\gamma = 1.35 \times 1.50 = 2.025$

To accommodate the difference between mean strength and specified concrete strength a pseudo specified concrete strength was calculated from five measured concrete strength results.

Measured mean value = 19.5 MPa

Calculated standard deviation = 0.84 MPa

pseudo specified strength = Mean - 2.12×0.84 = 17.7 MPa

Where 2.12 is the 4 degree of freedom "t" distribution factor for 95% confidence.

Using the code defined load factors, the code expressions and control perimeters service loads were calculated and are also given in Table 5.4.

It is evident from Table 5.4 that the four codes predict different service loads for the interior column of the test slab. From the calculated results it seems that the safety factors are quite different among the codes. For CEB the safety factor is about 3 which is too conservative. The safety factor of ACI is about 2.4 which is reasonable although the calculated mean value of punching shear strength by ACI is unconservative. The safety factors of BS 8110 and CSA are less than 2 which are lower because the BS 8110 uses lower overall safety factor and the coefficient in the CSA code expression for punching shear is higher than in the ACI code.

Therefore, it is concluded that the CEB Code uses the highest safety factor for punching shear design and its prediction of punching shear is very conservative. The reason that the CEB-FIP 1990 equation under-estimates the shear strength may be the small coefficients used.

It appears that ACI gives a reasonable service load , CSA overestimates the service load. It is suggested that CSA should use the same coefficient in the equation for punching shear stress as the ACI code.

5.2 Recommendations

From Appendix B it can be seen that the variation of the coefficients in the shear stress equations are 18%, 12% and 12% for the ACI, BS and CEB codes respectively. Using a 95% coefficient limit for an infinite population gives reduction factors of 0.7, 0.8 and 0.8 respectively.

To obtained an ultimate/service load ratio of 1.4/0.7 with a 95% confidence level (assuming the experimental result to be 10% optimistic and $f_{cm} = 1.25\ f_{ck}$) the ACI perimeter equation should be changed to:

$$v_{cACI} = 0.47 \times \frac{35.5}{44.2} \times 0.7 \times 0.9 \sqrt{f_{cm}} = 0.27 \sqrt{f_{ck}} \qquad (5.12)$$

the original equation:

$$v_c = 0.33 \sqrt{f_{ck}}$$

Similarly the CSA A23.3M-84 expression should be changed to

$$v_{cCSA} = 0.27 \sqrt{f_{ck}} \qquad (5.13)$$

the original equation:

$$v_c = 0.4 \sqrt{f_{ck}}$$

Similarly to use a BS 8110-85 type equation with the BS 8110-85 control perimeter 1.5d from the column, load factor of 1.4 and material factor of 1.25:

$$v_{cBS}=1.33\times\frac{35.5}{29.7}\times0.9\times0.8(\rho f_{cm})^{\frac{1}{3}}(\frac{400}{d})^{\frac{1}{4}}=0.72(100\rho\frac{f_{cm}}{25})^{\frac{1}{3}}(\frac{400}{d})^{\frac{1}{4}} \quad (5.14)$$

the original equation:

$$v_c=0.79(100\rho\frac{f_{cu}}{25})^{1/3}(\frac{400}{d})^{1/4}$$

Using the CEB 1990 control perimeter 2d from column:

$$v_{cCEB}=0.77\times\frac{35.5}{32.0}\times0.9\times0.8\xi(\rho f_{cm})^{1/3}=0.148\xi(100\rho f_{ck})^{1/3} \quad (5.15)$$

the original equation:

$$v_c=0.12\xi(100\rho f_{ck})^{1/3}$$

Shear strength of circular section columns should be calculated as a square column of the same cross sectional area.

Steel ratio should be calculated over the width of the column strip, and should be concentrated for moment transfer at edge and corner columns and the minimum steel ratio should be 0.5%.

5.3 The Contraflexural Line

As mentioned in chapter 2, most punching shear tests were conducted on isolated square or circular slabs. The edges of the specimen have been at positions representative of lines of contraflexure in continuous slabs.

By using Timoshenko's (1970) Elastic Method introduced in Section 54 of "Theory of Plates and Shells", the line of contraflexure for an interior connection of a continuous slab can be shown to be close to a circle with a radius of 0.2L from the column centre where L is the span length, even though the shape of the column is square.

Figure 5.1a shows the total deflection of the experimental slab in Test 2, in which the slab did not have the supplementary supports and was loaded from 0 to $2/3w_f$, where w_f is the failure load of the interior column connection. By interpolation of the measured deflections of the slab, it was found that, for deflections δ = 1.0 mm and 2.00 mm, the contour is close to circular although some experimental scatter exists and the number of the measured points were not enough to derive a very smooth curve. The load condition immediately before failure at w = 28.5 KN/m^2 (not including the selfweight of the slab) is also studied, and the deflections δ = 4.0 mm and 5.0 mm are shown in Figure 5.1b. These curves also show that the line of contraflexure has a circular shape instead of square which was used by many researchers in their experiments.

5.4 The Effects of Supplementary Supports

One of the objects of this experiment is that the slab was also tested with supplementary supports. From Figure 4.6a to 4.6c it can be observed that the supports can

increase the stiffness of the slab, as the deflection curves of same location are steeper with supplementary supports than the slab without the supports. The effect on the deflection of the slab near ultimate load is not pronounced. Nevertheless, the effect on shear strength is great.

It can be observed from the experimental results that the failure load of an edge column is 34.4 KN/m^2 (including the selfweight of the slab) when the slab does not have the supplementary supports and the failure load is 44.8 KN/m^2 when it has the supplementary supports. This means that the shear strength at failure can be increased by 30% by using supplementary support in this case.

From Figure 4.4, it can be seen that the failure surfaces of edge column connections #3 and #5 are similar which means that the supplementary supports increase shear strength by taking part of the applied load, not by increasing the critical perimeter of the connection. However, with supplementary supports an increased control perimeter, as shown in Figure 5.2, can increase the calculated shear strength by about 20 percent by using the ACI Code, and about 25 percent by using BS 8110 and CEB-FIP.

It is suggested that supplementary supports in the vicinity of the column-slab connection should be arranged as shown in Figure 5.3. This pattern of arranging the supports at an interior column connection will reduce shear concentration at column corner and more effectively increase the shear strength.

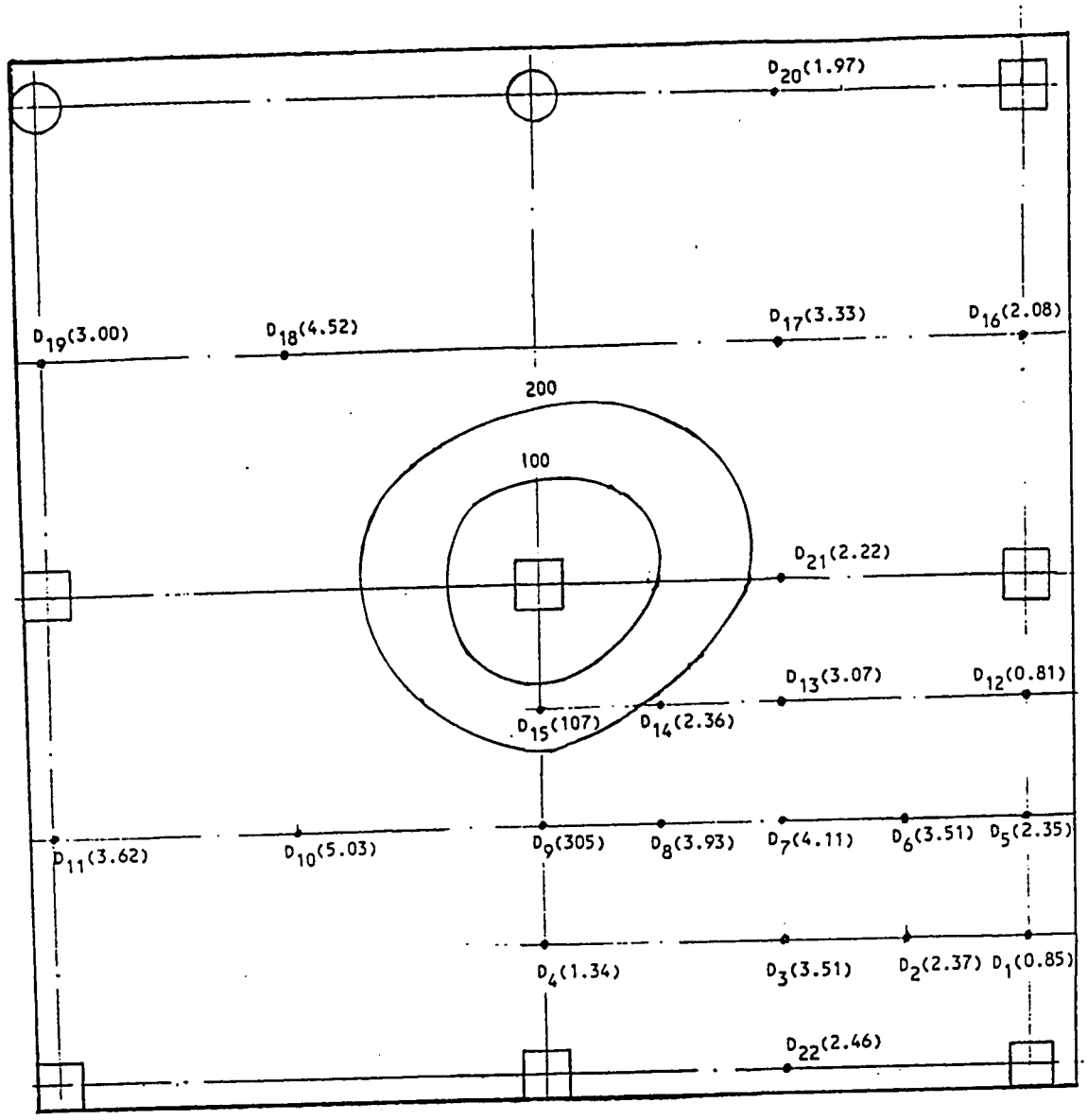

Figure 5.1a Contours of Uniform Deflection when w = 20.7 KN/m^2 (without shores)

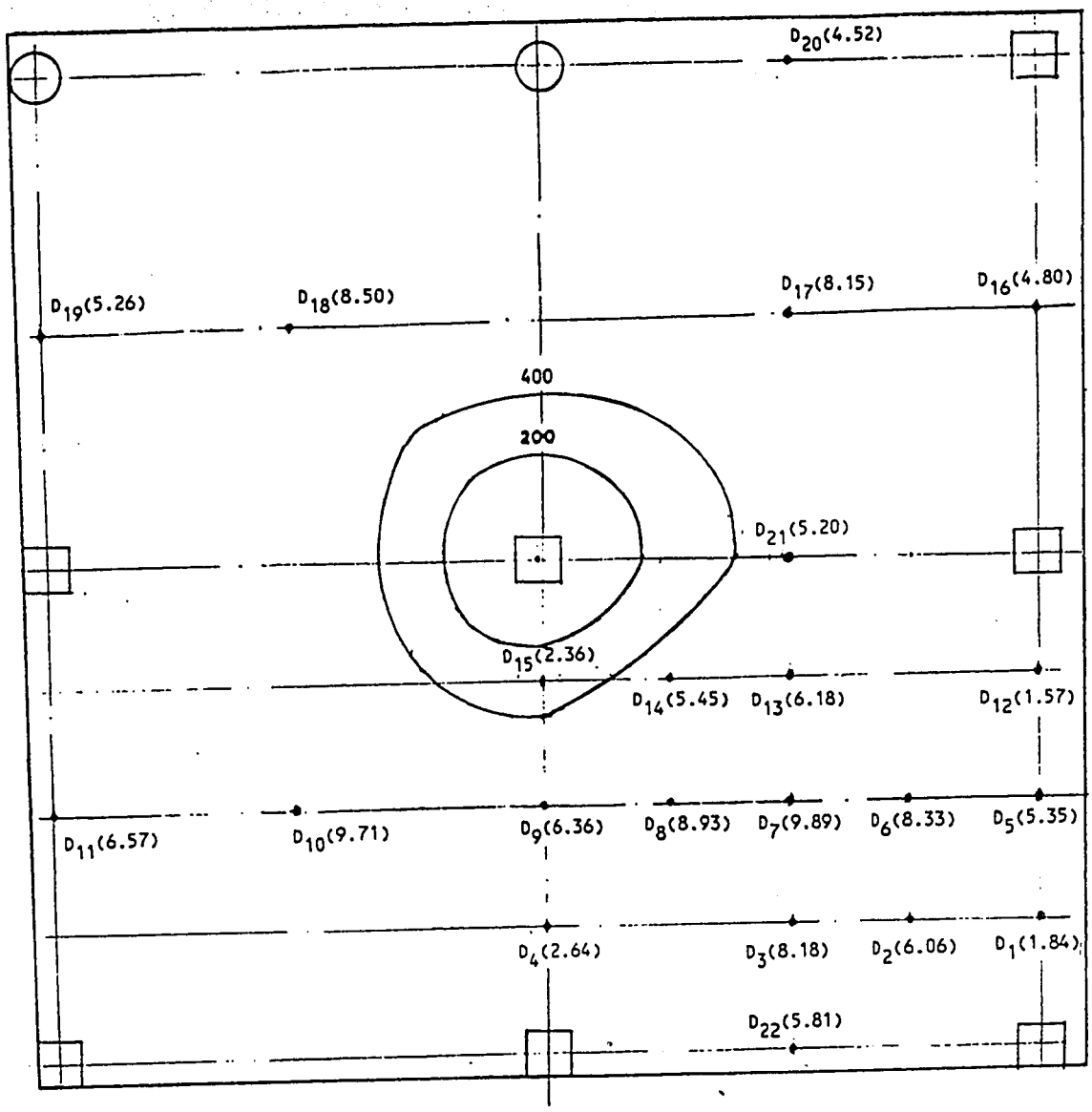

Figure 5.1b Contours of Uniform Deflection
when w = 28.5 KN/m^2 (without shores)

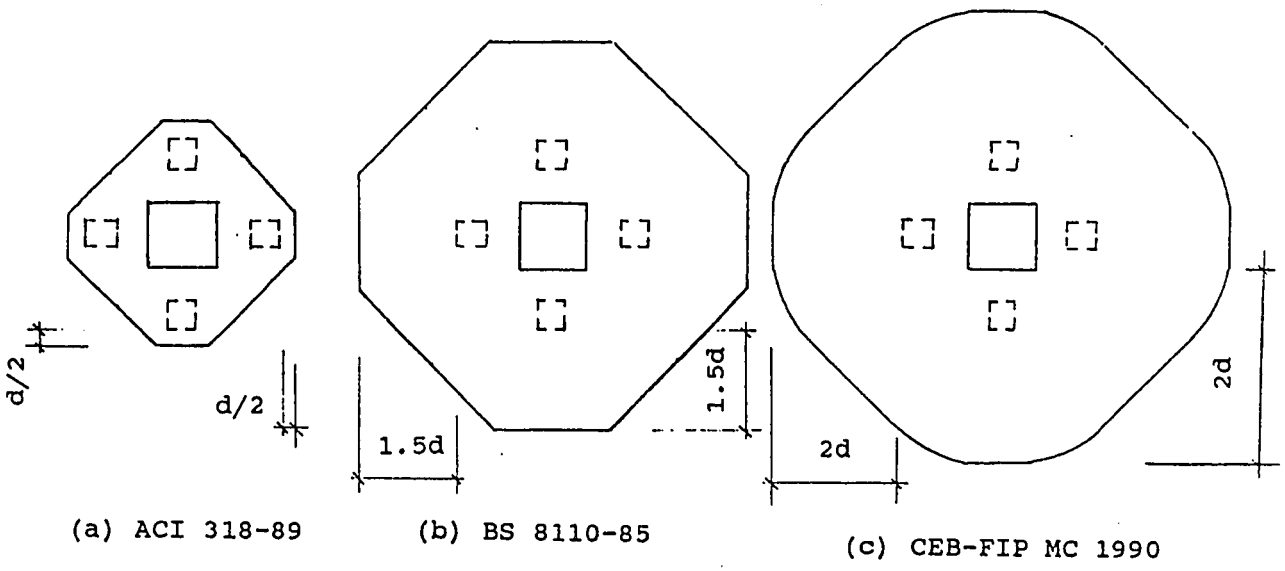

Figure 5.2 Control Perimeters with Supplementary Supports

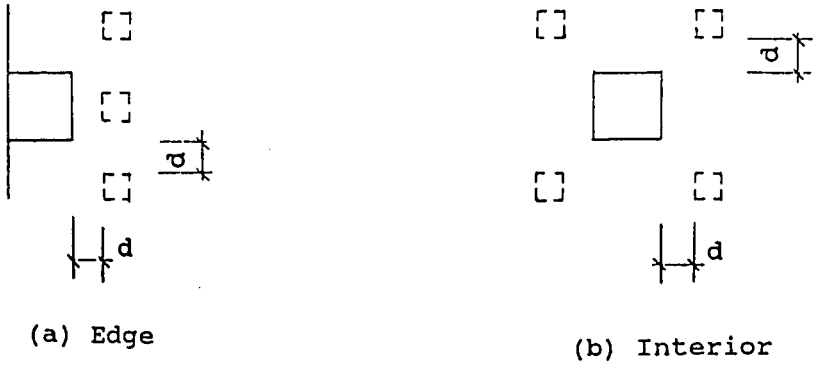

Figure 5.3 The Suggested Shoring Arrangement

CHAPTER 6

CONCLUSIONS

The major conclusions which can be made from the experimental results obtained and the review of the literature are summarized as follows.

(1) Isolated punching tests can represent the punching shear behaviour of the slab column system when the position representative of lines of contraflexure in continuous slabs at about 0.2 times the span length from the centre of the column and circular in shape.

(2) A mean coefficient ACI 318-89 equation over-estimates the measured failure load. However, it is simple and yields reasonable results for service load. The conservatism of the provisions increases as the reinforcement ratio increases according to Hawkins, Cao and Yamazaki (1990) and their statement that "ACI 318-83 provisions are nonconservative for reinforcement values less than 0.7 percent" is in agreement with the experimental results reported in this study.

(3) The equations for a critical section at d/2 from the faces of interior columns in ACI code are adequate. The finite element study by Yamazaki and Hawkins (1980) indicates that the code equation adequately represents the shear distribution over the perimeter of the critical section. However, for edge columns when there is overhang, the ACI code gives nonconservative prediction of punching shear strength.

(4) The ACI linear shear/moment interaction is adequate to predict punching shear

of column connections with moment transfer and the equation for fraction factor γ_v (eq. 3.10) in the ACI Code is adequate for edge and corner column connections.

(5) CSA overestimates the service load. It is suggested that CSA should use the same coefficient in the equation for punching shear stress as the ACI code.

(6) BS 8110-85 is inappropriate to define the ratio of flexural reinforcement in relation to a width only equal to that of the loaded area plus 1.5d to either side of it. It would be more appropriate to calculate the steel ratio over the column strip.

(7) BS 8110 is correct to take account of a size or depth effect over a relatively large range of slab depths, and the failure of the ACI Code to include a size effect term makes its prediction rather inconsistent for many tests results.

(8) In the British Codes and CEB-FIP, the use of the cube root of the concrete's compressive strength in expressions for v_{ck} is appropriate.

(9) The BS 8110 prediction is reasonable for the interior column connection, but for the edge and corner column connection the results are not consistent. The equations for edge and corner connection are too simple and should be improved.

(10) Using same area equivalent rectangular column to calculate shear strength of slab circular column connection is reasonably accurate and simplifies the calculations.

(11) The predicted results by CEB-FIP 1990 are consistent and close to the experimental results but the service load is too conservative.

(12) To obtain a 95% confidence level the code equations for punching shear stress should be changed to:

$$v_{cACI}=v_{cCSA}=0.27\sqrt{f_{ck}} \tag{6.1}$$

$$v_{cBS8110}=0.72(100\rho\frac{f_{cm}}{25})^{1/3}(\frac{400}{d})^{1/4} \tag{6.2}$$

$$v_{cCEB}=0.148\xi(100\rho f_{ck})^{1/3} \tag{6.3}$$

(13) Supplementary supports can increase punching shear capacity by about 30% at an edge column connection provided that the supports are located at a distance d (effective slab thickness) from the column faces and have enough strength and stiffness to take part of ultimate load.

(14) Supplementary supports placed at the corner of the perimeter, which is loaded area plus *d* on each side of it, may be better than placed on the column centre line because in the former case the supports can reduce stress concentration at corner of the column.

REFERENCES:

ACI Committee 318, 1989. Building Code Requirements for Reinforced Concrete and Commentary ACI 318 R-89, American Concrete Institute.

Alexander, Scott D. B. and Simmonds, Sidney H., May-June 1987. Ultimate Strength of Slab-Column Connections, ACI Structural Journal, V. 84, No. 3, pp 255-261.

Andersson J. L., 1963. Punching of Concrete Slabs with Shear Reinforcement, Meddelande Nr 47, Institutionen for Byggnadsstatik, Kungliga Tekniska Högskolan Stockholm.

Anis N. N., 1970. Shear Strength of Reinforced Concrete Flat Slabs without Shear Reinforcement, PhD thesis, Imperial College, London.

Base G. D., July 1959. Some Tests on The Punching Shear Strength of Reinforced Concrete Slabs, Technical Report TRA 321, Cement and Concrete Association, London.

Bazant Z. P. and Zhiping C., Jan. - Feb. 1987, Size Effect in Punching Shear Failure of Slabs, ACI Structural Journal, pp 44-53.

British Standard Institution, 1985. Structural Use of Concrete: Part 1, Code of Practice for Design and Construction, (BS 8110: Part 1: 1985), London, 126 pp.

CEB-FIP 1990. Model Code for Concrete, Comite Euro-International du Beton/Federation International de la Precontrainte, Paris.

CEB-FIP, 1978. Model Code for Concrete Structures, Bulletin d'Information, No 124/125-E, CEB Paris.

Cleland D. J., Franklin Y. and Long A. E., Apr 1979. The Punching Strength of Unbonded Post-tensioned Slabs at Columns, Advances in Concrete Slab Technology. Proceedings of the International Conference on Concrete Slabs at Dundee University, Pergamon Press, pp 197-207.

Criswell M. E., 1974. Static and Dynamic Response of Reinforced Concrete Slab-Column Connections, Publication SP-42 Vol 2, ACI, pp 721-746.

Dilger W. H., Elmasri M. Z. and Ghali A., Oct 1978. Flat Plates with Special Shear Reinforcement Subjected to Static and Dynamic Moment Transfer, ACI Journal, Vol 75 No 10, pp 534-549.

Dilger W. H. and Ghali A., Dec 1981. Shear Reinforcement for Concrete Slabs proceedings ASCE, Vol 107 No ST12, pp 2403-2420.

Elstner R. C. and Hognestad E., July 1956. Shearing Strength of Reinforced Concrete Slabs, ACI Journal Vol 28 No 1, pp 29-57.

Engineering News Record, July 15, 1971. Building Collapse Blamed on Design Construction, p19.

Engineering News Record, March 8, 1973. Collapse Kills Five and Destroys Large Portion of 26-story Building under Way, and March 15, 1973. Crane may not have caused collapse; probe continues.

Feld. J., 1964. Lessons from Failures of Concrete Structures, American Concrete Institute, Monograph series. Monograph No 1. pp 30-32.

* Forsell C. and Holmberg Å, Feb 1946. Stämpellast på plattor av betong, Betong Vol 31 Nr 2, Stockholm, pp 95-123.

Franklin S. O., Cleland D. F. and Long A. E., June 1982. A Flexural Method for The Prediction of The Punching Capacity of Unbonded Post-tensioned Flat Slabs at Internal Columns, Proceedings Part 2 Vol 73, Institution of Civil Engineers, London, pp 277-298.

Ghali A. and Elgabry A.A., 1990, Moment and Shear Transfer Between Columns and Concrete Slabs, Canadian Journal for Civil Engineering, Vol 17, pp 621-628.

Gardner N. J., Jan.-Feb. 1990. Punching Shear Capacity-Concrete Strength, ACI Structural Journal, V. 87, No. 1, pp 66-71.

González-Vidosa, Fernando; Kotsovos, Michael D. and Pavlovic, Milija N., May-June 1988. Symmetrical Punching of Reinforced Concrete Slabs; An Analytical Investigation Based on Nonlinear Finite Element Modelling, ACI Structural Journal, V. 85, No. 3, pp 241-250.

* Graf O., 1933. Versuche über die Widerstandsfähigkeit von Eisenbetonplatten unter Konzentrierter Last nahe einem Auflager, Deutscher Ausschuss für Eisenbeton, Heft 73, Berlin, pp 1-16.

Grossman, Jacob S., Robert Rosenwassor Associates, March 1986. Two-day Construction Cycle for High-rise Structures Based on Use of Preshores, Concrete Construction Journal.

Hadjichristou C. and Papastavrou C., 1980. Influence of Concrete Strength on Punching Shear, unpublished report, Polytechnic of Central London.

Hawkins N. M. and Corley W. G., 1971. Transfer of Unbalanced Moment and Shear from Flat Plates to Columns, Publication SP-30, ACI, Detroit, pp 147-176.

Hawkins N. M., 1980. Lateral Load Design Considerations for Flat Plate Structures, Proceedings, CSCE-ASCE-ACI-CEB International Symposium on Non-linear Design of Concrete Structures, study No. 14, Solid Mechanics Division, University of Waterloo, pp 581-614.

Hawkins N. M., Aibin Cao and Jun Yamazaki. Nov - dec 1989. Moment Transfer from Concrete Slabs to Columns, ACI Structural Journal, V. 86, No. 6, pp 705-716.

Hognestad E., Elstner R. C. and Hanson J. A., June 1964. Shear Strength of Lightweight Aggregate Concrete Slabs, ACI Journal, Vol 61 No 6, pp 643-655.

* Ingvarsson H., Betongplattors hållfasthet och armeringsurformning vid hörnpelare, Meddelande Nr 122, Institutionen för Byggnadsstatik, Kungliga Tekniska Högskolan, Stockholm, 1977.

Jirsa. J. O., Sozen M. A. and Siess C. P., June 1966. Test of a Flat Slab Reinforced with Welded Wire Fabric, Journal of the Structural Division. ASCE, Vol 92, No ST3, pp 199-224.

* Kinnunen S., 1971. FÖrsok med betongplattor understÖdda av pelare vid frikant, Rapport R2:, Statens Institut för Byggnadsforskining, Stockholm.

Kinnunen S. and Nylander H., 1960. Punching of Concrete Slabs without Shear Reinforcement, Meddelande Nr 38, Institutionen for Byggnadsstatik, Kungliga Tekniska Högskolan, Stockholm.

* Kinnunen S., Nylander H. and Tolf P., 1978: 3. UndersÖkningarrÖrande genomstansning vid Institutionen för Byggnadsstatik KTH, Nordisk Betong, pp 25-27.

* Kinnunen S., Nylander H. and Tolf P., 1983. Plattjocklekens inverkan på betong plattors hållfasthet vid genomstansning, Försök med rektangulära plattor, Meddelande Nr 137, Institutionen för Byggnadsstatik, Kungliga Tekniska Högskolan, Stockholm.

Long A. E., Feb 1975. Two Phase Approach to The Prediction of The Punching Strength, ACI Journal, pp 37-45.

* Marti P., Pralong J. and Thürlimann B., Sept 1977. Schubversuche an Stahlbeton-platten, Bericht Nr. 7305-2, Institut für Baustatik und Konstruktion, ETH, Zurich.

Mast P. E., Oct 1970. Stresses in Flat Plates near Columns, ACI Journal, Vol 67 No 10, pp 761-768.

Moe J., 1961. Shearing Strength of Reinforced Concrete Slabs and Footings under Concentrated Load, Bulletin D47, Portland Cement Association, Research and Development Laboratories, Skokie, Illinois.

Narasimhan N., 1971. Shear Reinforcement in Reinforced Concrete Column Heads, PhD thesis, Imperial College, London.

Neth V.W., de Paiva H.A.R. and Long A.E., July-Aug. 1981, Behaviour of Models of a Reinforced Concrete Flat Plate Edge-Column Connection, ACI Journal, Detroit, Michigan.

* Nölting D., 1984. Des Durchstanzen von Platten aus Stahlbeton-Tragverhalten, Berechnung, Bemessung, Heft 62, Institut für Baustoffe Massivbau und Brandschutz, Technischen Universität Braunschweig.

* Pöllet L., Dec 1983. Untersuchung von Flachdecken auf Durchstanzen im Bereich von Eck-und Randstützen, Dr Ing dissertation, Technischen Hochschule Aachen.

* Pralong J., Brändli W. and Thürlimann B., Dec 1979. Durchstanzversuche an Stahlbeton-und Spannbeton-platten, Bericht Nr 7305-3, Institut für Baustatik und Konstruktion, ETH zürich.

Regan P. E., 1981. Behaviour of Reinforced Concrete Flat Slabs, CIRIA Report 89, Construction Industry Research and Information Association, London.

Regan P. E., 1983. Punching Shear in Prestressed Concrete Slab Bridges, Structures Research Group, Polytechnic of Central London.

Regan P. E., 1984. The Dependence of Punching Resistance upon The Geometry of The Failure Surface, Magazine of Concrete Research, Vol 36 No 126, pp 3-8.

Regan P. E. and Breastrup M. W., 1985. Punching Shear in Reinforced Concrete, A-State-of-Art Report, Bulletin d'Information No 168, Comite Eurointernational du Beton, Lausanne.

Regan, P. E., Sep 1986. Symmetric Punching of Reinforced Concrete Slabs, Magazine of Concrete Research: Vol. 38, No. 136, pp 115-128.

Richart R. E., Nov. 1948, Reinforced Concrete Wall and Column Footings, ACI Journal, Vol 20 No 22 & 3, pp 97-127 and 237-260 (proceedings V45).

Shehata I. A., 1982. Punching of Prestressed and Non-prestressed Reinforced Concrete Flat Slabs, M Phil thesis, Polytechnic of Central London.

Stamenkovic A. and Chapman J. C., 1972. Local Strength of Flat Slabs at Column Heads, Report 39, Construction Industry Research and Information Association, London.

Taylor R. and Hayes B., Mar 1965. Some Tests on The Effect of Edge Restraint on Punching Shear in Reinforced Concrete Stabs, Magazine of Concrete Research Vol 17 No 50, pp 39-44.

Vanderbilt M. D., May 1972. Shear Strength of Continuous Plates, Proceedings ASCE, Vol 98 No ST5, pp 961-973.

Walker P. R., 1980, Flat Reinforced Concrete Slabs, An Investigation into The Strength and Behaviour of Corner Column-slab Connections, PhD thesis, Polytechnic of Central London.

Yamazaki J., 1975. Shear and Moment Transfer Between Reinforced Concrete Flat Plates and Columns, PhD thesis, University of Washington, Seattle.

Yamazaki, Jun and Hawkins, Neil M., 1980. Finite Element Predictions of The Behaviour of Slab-column Connections Transferring Moment, Reinforced concrete structures subjected to wind and earthquake forces, SP-63, American Concrete Institute, Detroit, pp 49-78.

Yitzhaki R., May 1966. Punching Strength of Reinforced Concrete Slabs, ACI Journal, Vol. 63, No 5, pp 527-542.

Zaghlool E. R. F., De Paiva H. A. R. and Glockner P. G., March 1970, Tests of Reinforced Concrete Flat Plate Floors, Proceedings ASCE, Vol 96 No ST3, pp 487-507.

Zaghlool E. R. F., Rawdon dePaiva H. A. and Glockner P. G., Match 1970. Tests of Reinforced Concrete Flat Plate Floors, S. D. Journal, pp 487-507.

"*" Indicates indirect references.

Appendix A

Table A.1

w	0	2.59	5.18	7.76	10.4	12.9	15.5	18.1	20.7
D_1	0	0.04	0.09	0.13	0.18	0.24	0.39	0.52	0.89
D_2	0	0.08	0.2	0.3	0.44	0.59	1.03	1.51	2.57
D_3	0	0.08	0.25	0.39	0.55	0.76	1.32	2.19	2.95
D_4	0	0.01	0.11	0.16	0.25	0.34	0.49	0.94	1.50
D_5	0	0.10	0.21	0.31	0.44	0.59	0.98	1.38	2.26
D_6	0	0.11	0.25	0.40	0.56	0.74	1.28	1.97	3.26
D_7	0	0.10	0.26	0.43	0.63	1.08	1.72	3.20	4.27
D_8	0	0.06	0.19	0.34	0.52	0.70	1.31	2.82	3.88
D_9	0	0.03	0.12	0.23	0.37	0.53	0.83	1.79	2.77
D_{10}	0	0.12	0.26	0.44	0.64	0.78	1.45	3.29	4.65
D_{11}	0	0.01	0.08	0.21	0.38	0.82	1.15	2.38	3.55
D_{12}	0	0.02	0.05	0.07	0.11	0.14	0.30	0.55	0.73
D_{13}	0	0.06	0.18	0.30	0.45	0.59	1.04	1.85	2.76
D_{14}	0	0.02	0.11	0.20	0.30	0.44	0.82	1.61	2.40
D_{15}	0	0.00	0.03	0.07	0.11	0.98	1.10	1.40	1.67
D_{16}	0	0.11	0.22	0.31	0.43	0.55	0.92	1.64	2.28
D_{17}	0	0.15	0.32	0.52	0.68	0.82	1.19	2.31	3.41
D_{18}	0	0.18	0.38	0.58	0.82	0.97	1.64	3.24	4.49
D_{19}	0	0.16	0.31	0.46	0.64	0.92	1.38	1.98	2.66
D_{20}	0	0.12	0.24	0.34	0.47	0.64	1.06	1.51	2.31
D_{21}	0	0.07	0.16	0.27	0.40	0.49	0.66	1.18	1.85
D_{22}	0	0.10	0.18	0.30	0.45	0.87	1.30	2.07	2.77

w in KN/m^2

D_1 - D_{22} in mm

Table A.2

w	0	4.14	8.28	12.4	15.5	18.6	20.7
D_1	0	0.13	0.28	0.45	0.55	0.69	0.85
D_2	0	0.31	0.73	1.24	1.48	1.88	2.37
D_3	0	0.45	1.06	1.81	2.18	2.76	3.51
D_4	0	0.19	0.43	0.71	0.83	1.04	1.34
D_5	0	0.30	0.69	1.16	1.41	1.81	2.35
D_6	0	0.39	1.00	1.73	2.10	2.73	3.51
D_7	0	0.47	1 19	2.07	2.50	3.25	4.11
D_8	0	0.45	1.20	2.02	2.38	3.13	3.93
D_9	0	0.39	1.00	1.58	1.83	2.46	3.05
D_{10}	0	0.78	1.71	2.65	3.12	4.06	5.03
D_{11}	0	0.54	1.33	1.87	2.24	2.93	3.62
D_{12}	0	0.08	0.15	0.40	0.48	0.61	0.81
D_{13}	0	0.32	0.91	1.52	1.80	2.39	3.07
D_{14}	0	0.28	0.76	1.24	1.45	1.89	2.36
D_{15}	0	0.15	0.42	0.61	0.69	0.91	1.07
D_{16}	0	0.28	0.64	1.03	1.24	1.61	2.08
D_{17}	0	0.38	1.00	1.66	1.98	2.64	3.33
D_{18}	0	0.64	1.47	2.39	2.87	3.69	4.52
D_{19}	0	0.57	1.03	1.65	1.97	2.47	3.00
D_{20}	0	0.27	0.59	0.95	1.15	1.51	1.97
D_{21}	0	0.22	0.71	1.12	1.32	1.83	2.22
D_{22}	0	0.40	0.85	1.38	1.62	1.99	2.46

w in KN/m^2

$D_1 - D_{22}$ in mm

Table A.3

w	0	5.18	10.4	15.5	20.7	23.3	25.9
D_1	0	0.19	0.39	0.57	0.77	1.06	1.54
D_2	0	0.51	1.12	1.77	2.28	3.51	5.24
D_3	0	0.75	1.64	2.57	3.40	4.90	6.98
D_4	0	0.34	0.64	1.08	1.35	1.75	2.20
D_5	0	0.38	0.94	1.48	2.09	3.26	4.56
D_6	0	0.73	1.64	2.40	3.33	5.04	7.19
D_7	0	0.91	1.96	2.87	3.94	6.17	8.84
D_8	0	0.91	1.92	2.79	3.78	5.60	6.87
D_9	0	0.73	1.45	2.12	2.89	4.12	5.68
D_{10}	0	1.27	2.43	3.48	4.74	6.15	8.52
D_{11}	0	0.86	1.75	2.48	3.38	4.20	5.84
D_{12}	0	0.15	0.35	0.52	0.72	1.06	1.37
D_{13}	0	0.67	1.45	2.10	2.89	4.30	6.20
D_{14}	0	0.54	1.15	1.70	2.28	3.23	4.63
D_{15}	0	0.29	0.58	0.84	1.07	1.47	2.01
D_{16}	0	0.44	0.96	1.37	1.86	2.47	4.09
D_{17}	0	0.74	1.56	2.27	3.05	4.17	6.86
D_{18}	0	1.10	2.19	3.15	4.18	5.20	7.34
D_{19}	0	0.74	1.47	2.06	2.74	3.32	4.54
D_{20}	0	0.41	0.85	1.27	1.75	2.40	3.58
D_{21}	0	0.53	1.08	1.59	2.12	3.08	4.50
D_{22}	0	0.48	1.09	1.60	2.26	3.23	4.62

w in KN/m^2

$D_1 - D_{22}$ in mm

Table A.4

w	0	5.18	10.4	15.5	20.7	23.3	25.9
D_1	0	0.26	0.56	0.87	1.11	1.29	2.04
D_2	0	0.69	1.59	2.47	3.38	3.95	5.04
D_3	0	0.97	2.17	3.39	4.62	5.38	6.25
D_4	0	0.33	0.81	1.13	1.55	1.79	1.95
D_5	0	0.66	1.46	2.36	3.02	3.56	4.36
D_6	0	1.02	2.21	3.53	4.65	5.48	6.83
D_7	0	1.30	2.73	4.29	5.61	6.57	8.21
D_8	0	1.22	2.55	3.92	5.21	6.11	7.60
D_9	0	1.04	2.04	3.02	3.94	4.59	5.61
D_{10}	0	1.49	3.08	4.57	6.01	6.97	8.30
D_{11}	0	1.05	2.21	3.30	4.31	4.89	5.79
D_{12}	0	0.18	0.43	0.73	0.93	1.07	1.35
D_{13}	0	0.93	1.98	3.08	4.10	4.78	6.05
D_{14}	0	0.74	1.54	2.37	3.16	3.68	4.68
D_{15}	0	0.34	0.71	1.05	1.44	1.59	2.06
D_{16}	0	0.60	1.30	2.02	2.57	3.09	3.84
D_{17}	0	1.03	2.17	3.36	4.43	5.26	6.53
D_{18}	0	1.35	2.70	4.03	5.22	6.09	7.21
D_{19}	0	0.89	1.74	2.54	3.34	3.83	4.56
D_{20}	0	0.61	1.24	1.93	2.44	2.92	3.53
D_{21}	0	0.65	1.43	2.22	2.99	3.46	4.38
D_{22}	0	0.71	1.51	2.40	3.30	3.85	4.91

w in KN/m^2

$D_1 - D_{22}$ in mm

Table A.5

w	0	7.78	15.5	20.7	25.9	28.5	31.1
D_1	0	0.34	0.71	0.94	1.19	1.32	1.61
D_2	0	1.21	2.61	3.41	4.36	5.00	6.26
D_3	0	1.69	3.66	4.85	6.20	7.12	8.87
D_4	0	0.47	1.10	1.43	1.82	2.05	2.54
D_5	0	1.15	2.42	3.11	4.00	4.61	5.64
D_6	0	1.78	3.71	4.86	6.27	7.27	9.12
D_7	0	2.23	3.65	4.97	6.83	7.93	10.1
D_8	0	2.05	4.22	5.44	7.18	8.10	9.95
D_9	0	1.52	3.14	4.00	5.28	5.87	6.98
D_{10}	0	2.49	4.94	6.27	8.06	9.03	10.6
D_{11}	0	1.51	3.26	4.19	5.28	6.00	7.03
D_{12}	0	0.31	0.68	0.87	1.14	1.28	1.58
D_{13}	0	1.60	3.33	4.29	5.68	6.48	8.08
D_{14}	0	1.25	2.57	3.32	4.46	5.07	6.22
D_{15}	0	0.60	1.14	1.46	2.00	2.19	2.64
D_{16}	0	1.02	2.20	2.82	3.71	4.22	5.22
D_{17}	0	1.80	3.74	4.75	6.31	7.32	9.18
D_{18}	0	2.24	4.34	6.16	7.99	8.88	10.3
D_{19}	0	1.40	2.68	3.42	4.31	4.98	5.79
D_{20}	0	1.00	2.07	2.61	3.29	3.80	4.72
D_{21}	0	1.14	2.41	3.07	4.17	4.72	5.87
D_{22}	0	1.24	2.59	3.40	4.40	5.07	6.25

w in KN/m^2

D_1 - D_{22} in mm

Table A.6

w	0	7.78	15.5	20.7	25.9	28.5	31.1
D_1	0	0.44	0.96	1.24	1.55	1.84	1.95
D_2	0	1.46	3.26	4.36	5.40	6.06	7.02
D_3	0	2.04	4.45	5.94	7.28	8.18	9.69
D_4	0	0.69	1.48	1.93	2.29	2.64	4.44
D_5	0	1.31	2.90	3.78	4.78	5.35	5.80
D_6	0	2.06	4.61	5.97	7.47	8.33	9.44
D_7	0	2.56	5.49	7.16	8.87	9.89	11.8
D_8	0	2.37	5.04	6.50	7.97	8.93	14.0
D_9	0	1.77	3.70	4.68	5.66	6.36	12.4
D_{10}	0	2.79	5.66	7.24	8.61	9.71	13.2
D_{11}	0	1.79	3.73	4.88	5.81	6.57	7.56
D_{12}	0	0.40	0.87	1.12	1.42	1.57	2.70
D_{13}	0	1.94	3.11	4.28	5.43	6.18	11.4
D_{14}	0	1.46	3.12	4.05	4.87	5.45	13.8
D_{15}	0	0.69	1.35	1.75	2.08	2.36	9.64
D_{16}	0	1.22	2.67	3.48	4.32	4.80	5.04
D_{17}	0	2.07	4.55	5.84	7.22	8.15	10.3
D_{18}	0	2.43	4.95	6.29	7.61	8.50	11.1
D_{19}	0	1.54	3.00	3.91	4.70	5.26	5.67
D_{20}	0	1.17	2.55	3.31	4.05	4.52	5.05
D_{21}	0	1.38	3.03	3.84	4.64	5.20	11.1
D_{22}	0	1.44	3.20	4.29	5.25	5.81	6.23

w in KN/m^2

$D_1 \sim D_{22}$ in mm

Appedix B

Calculation of 95 Percent Confidence Constant

		ACI 318-89		BS 8110-85		CEB-FIP 1990	
Data	No	Mean	Std. Dev.	Mean	Std. Dev.	Mean	Std. Dev.
Gardner	18	0.567	0.128	1.20	0.149	0.74	0.097
Elstner	21	0.433	0.072	1.28	0.185	0.738	0.106
Mowrer	19	0.448	0.099	1.37	0.168	0.755	0.090
Moe	13	0.427	0.044	1.53	0.135	0.88	0.077
Mean		0.47		1.33		0.77	
Std. Dev.		0.088		0.162		0.094	
C. of V.%		18.7		12.3		12.4	